Dissertation zur Erlangung des Doktorgrades

der Fakultät für Chemie und Pharmazie

der Ludwig-Maximilians-Universität München

Epigenetic modifications in vascular disease and regenerative medicine

Mihaela Culmes

aus

Racari, Rumänien

2012

Erklärung

Diese Dissertation wurde im Sinne von § 7 der Promotionsordnung vom 28. November 2011 von Herrn PD Dr. Jaroslav Pelisek betreut und von Herrn Prof. Dr. Ernst Wagner von der Fakultät für Chemie und Pharmazie vertreten.

Eidesstattliche Versicherung

Diese Dissertation wurde eigenständig und ohne unerlaubte Hilfe erarbeitet.

München, 22.09.2012

.

.....

Mihaela Culmes

Dissertation eingereicht am 22.09.2012

1. Gutachter: Prof. Dr. Ernst Wagner

2. Gutachter: PD Dr. Jaroslav Pelisek

Mündliche Prüfung am 05.12.2012

From far away to us you came
to improve your ken and knowledge
it was your dream and inner aim
to graduate and end the college

foreign country, different manner
the start wasn't easy, not at all
but still faithful under your banner
you always followed your own call

persistent and beyond the doubt
you went on with lifted head
in hope of fortune looking out
high spirits around did you spread

scientist with heart and soul
all the time you have been
challenging the others goal
to see more beyond the scene

always open, ready to aid
to explain, improve the others
never mind the price you paid
as you'd help your own brothers

So I esteemed to work with you
and helped you to find your fate
'cause you're the one to have a clue.
And now here you stand to pass the gate

dedicated
by
J.P.

TABLE OF CONTENTS

1 INTRODUCTION

1.1 Epigenetics

An epigenetic trait is a stable inheritable phenotype resulting from a changing of chromosome structure without alterations in the DNA sequence [1]. Main epigenetic mechanisms include DNA methylation and various histone modifications, such as e.g. methylation, acetylation or phosphorylation (*Figure 1*).

Epigenetic regulation of gene activity is a fundamental mechanism that occurs in all eukaryotic cells – in animals, humans, plants – and is important for development, tissue regeneration, and maintaining of cell phenotype. Defects in epigenetic modulation of gene activity have already been connected to cancer and other serious diseases [2-5]. Thus, understanding of epigenetics may lead to new diagnostic methods and discovery of novel therapeutic targets. This knowledge can be also useful in regenerative medicine by e.g. targeted cell reprogramming.

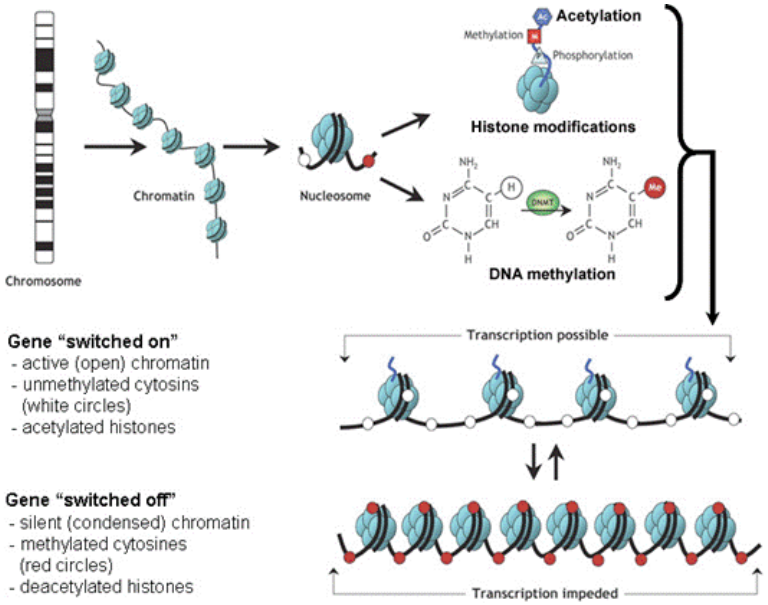

Figure 1. *Schematic overview of epigenetic mechanisms according to Rodenhiser et al. [6]. Condensation of the chromatin plays an important role in regulation of gene transcription. Open chromatin together with unmethylation of the cytosine leads to "switching on" the gene transcription; the "switching off" of the transcription is therefore associated with a condensed/folded chromatin and methylated cytosines.*

1.1.1 DNA methylation and DNMTs

DNA methylation consists of the addition of a methyl group to the 5th position of the cytosine pyrimidine ring by DNA methyltransferase (DNMT) enzymes (*Figure 2*) [7]. This

unique pyrimidine “5-methylcytosine” continues to pair with guanine. In humans and other mammals, DNA methylation is exclusively restricted to CpG dinucleotides. It is catalyzed by three different DNMTs encoded by different genes on distinct chromosomes: *DNMT1*, *DNMT3A*, and *DNMT3B. DNMT1* maintains DNA methylation and is responsible for the propagation of DNA methylation pattern during replication (mitotic cell division). It is present at the replication fork and is very specific for the hemi-methylated DNA. DNMT1 guides the methylation of CpG dinucleotides on the new DNA strand according to the methylation status of the complementary template strand. DNMT3A and DNMT3B are catalyzing *de novo* methylation and are important in the establishment of the methylation patterns in the early embryo state and also during development.

DNMT3A and DNMT3B were shown not only to correlate with changes in histone modifications [8], but also, more importantly, to play essential roles in *de novo* methylation. In mice, deletion of DNMT3B reduces the methylation of CpG islands on repetitive sequences such as LINE1 and Satα and activates gene expression on inactive X chromosome [8, 9].

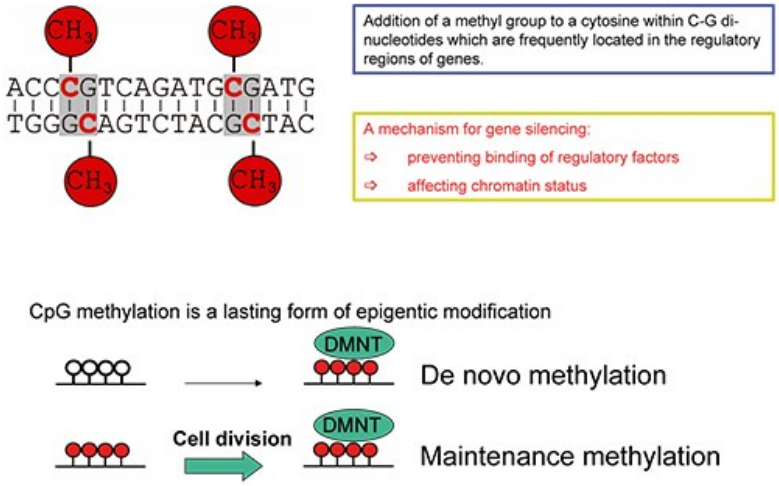

Figure 2. *Mechanism of DNA methylation [10]. DNA methylation has a specific pattern for cells in different stages of development and differentiation. This process is supported by three main enzymes: DNMT1, DNMT3A, and DNMT3B. Maintenance of the established methylation is provided in part by DNMT1 and DNMT3B. De novo methylation is supported by DNMT3A and DNMT3B.*

Approximately 70% to 90% of CpG dinucleotides, representing 3% to 6% of all cytosine, are methylated in healthy somatic cells [11]. Regarding gene regulation, DNA methylation is a repressive mark associated with transcriptional silencing. It has been shown to be involved in different cellular functions, including repetitive sequences, X chromosome inactivation, mammalian embryonic development, and lineage specification. It is also linked to a number of human diseases, mostly cancer [12]. More and more studies are emphasizing the importance of DNA methylation in other diseases such as atherosclerosis or diabetes [13, 14].

DNA methylation can affect gene expression in two general ways. First, DNA methylation itself can inhibit the binding of transcription factors to the methylated DNA sequence. This mechanism is relevant for many transcription regulators, for example *MYC* [15], activator protein-2 [16], or HIF-1α (hypoxia-inducible factor-1α) [17]. The second mechanism involves a family of methyl-CpG-binding proteins that have been described as being able to recognize methyl residues in the DNA of mammals. This family includes four proteins containing a homologous methyl-binding domain (MBD1, MBD2, MBD3, MBD4, and MeCP2) and a non-homologous methyl binding protein named KAISO [18]. These proteins can directly repress transcription, prevent the binding of activating transfactors, or recruit enzymes that catalyze histone posttranslational modifications and chromatin remodeling complexes, which in turn alter the structure of chromatin and promote transcriptional repression [11, 12]. The study of Chan *et al.* [19] demonstrated an important role in DNA methylation during transcriptional silencing of the human iNOS promoter in non-responsive human endothelial cells. In addition, another study showed that DNA methylation is not only responsible for *iNOS* transcription silencing, but also for posttranslational modifications of histones [20] Thus, DNA and histone methylation were found to be important in the transcriptional silencing of *iNOS* in cultured human endothelial cells. Hence, deregulation of these epigenetic modifications may lead to aberrant *iNOS* expression and consequently to atherosclerosis.

1.1.2 Hydroxymethylation, TET1

Recently, TET1 was found to be involved in the oxidation process of 5-azacytidine into 5-hidroxymethylcytosine (5hmC) [21]. Other studies have detected 5hmc in embryonic stem cells (ESCs) and in mouse cerebellum. This led to the hypothesis that 5hmc is a short-lived intermediate in the removal of 5-methylcytosine (5mC) [21, 22] and is involved in the epigenetic network with an important role in epigenetic reprogramming and regulation of tissue specific gene expression [23]. Moreover it has been suggested that high levels of *Tet1* are associated with a pluripotent state of the cells [24].

The further steps leading to demethylation include oxidation of 5mC to 5-formylcytosine and 5-carboxylcytosine.The ten-eleven translocation (TET) enzyme family was shown to have three members: TET1, TET2, and TET3. All three have been shown *in vitro* and *in vivo* to oxidize 5mC to 5hmC [25, 26] and also that the presence of 5hmC is depending on the presence of 5mC (*Figure 3*). This suggests that this is the only way for the synthesis of genomic 5hmC [27, 28]. TET1 depletion in mouse ESCs e.g. led to the accumulation of 5mC both globally [29] and at specific genomic regions, such as LINE1 retrotransposons and transcription factor binding sites [19].

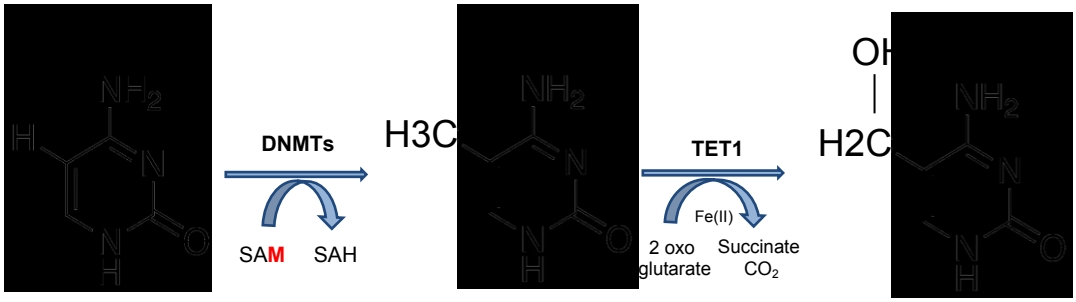

Figure 3. *Cytosine methylation and demethylation. Methylation is catalyzed by DNMT enzymes. The recently discovered TET1 protein is a 2-oxoglutarate and Fe II – dependent- dioxigenase that catalyzes the formation of 5hmC, which may represent a critical step in active oxidative DNA demethylation or may itself comprise a new epigenetic mark.*

Regarding the binding domain and the exact mechanism of TETs, there are couple of contradictory studies, and it is not yet clear whether they share the same binding domain with DNMT1 [29-31] or whether this mechanism is preventing the DNMT1 activity during replication.

1.1.3 Histone modifications – methylation and acetylation

Nucleosomes, the main components of chromatin, consist of histones. These proteins have positively charged amino-terminal tails that are exposed on the outside of nucleosomes. Histones are modified at many sites, with more than 60 different residues detected by mass spectrometry or with the help of specific antibodies [32]. Modifications of the histone tails include methylation, acetylation, phosphorylation, ubiquitination, SUMOylation, citrullination, and ADP-ribosylation. Acethylation of the lysine at the N terminal end of the histone H3 (like K9, K14, K18, and K23) and H4 (such as K5, K8, K12, and K16) as well as methylation of lysine residues in H3 (K4, K9, K27, K36, and K79) and H4 (K20) are the most relevant epigenetic modifications that have been identified until now (*Table 1*) [33]. They are carried out by specific enzymes, methyltransferases and acetyltransferases. The adding of an acetyl group has a major effect on lysine as it neutralizes the positive charge. This reduces electrostatic attraction between the histone and the negatively charged DNA backbone, loosening the chromatin structure; highly acetylated histones form more accessible chromatin and tend to be associated with active transcription. Histones that are methylated at certain residues can act epigenetically to repress or activate gene expression. Methylation of histones is catalyzed by histone methyltransferases (HMTs), which use S-adenosylmethionine (SAM) as a cofactor in nearly the same way as histone acethylases (HATs) utilize acetyl-coenzyme A as their cofactor [34]. Eukaryotic genomes are conveniently described as transcriptionally active (euchromatin) or transcriptionally silent (heterochromatin). Due to the fact that only very few demethylases were identified so far, it is believed that methylation is a process that is more stable than acetylation. Furthermore,

lysine residues in H3 and H4 tails appear to be targets for either acetylation or methylation, but not both at the same time [34].

An additional complexity of the histone modification processes comes from the fact that methylation at lysine or arginine may be mono-, di-, or tri-methyl for lysine and mono-, or di- (symmetric or asymmetric) for arginine [32].

It is to mention that the plethora of histone modifications cannot happen at the same time and on the same histone. The exact timing depends on the signaling conditions within the cell. Furthermore, acethylation of histones is associated with euchromatin, in contrast histone methylation can have opposite roles depending on the site and degree of methylation. As an example, H3K4 methylation was shown to be responsible for active transcription, while the methylation of H3K9 is involved in gene silencing.

Table 1. *Relevant methylation of the histone H3, their corresponding methyltransferases and proposed functions..*

	Histone-modifying Enzymes	Proposed Function	Reference
H3Lys4	Set1 (S. cerevisiae)	permissive euchromatin (di-Me)	[35]
	Set7/9 (vertebrates)	transcriptional activation (tri-Me)	[36]
	MLL	transcriptional activation	[37]
H3Lys9	Suv39h,Clr4	transcriptional silencing (tri-Me)	[38, 39]
	G9a	transcriptional repression genomic imprinting	[40]
	SETDB1	transcriptional repression (tri-Me)	[41]
H3Lys27	Ezh2	transcriptional silencing X inactivation (tri-Me)	[42]
	G9a	transcriptional silencing	[40]
H3Lys36	Set2	transcriptional activation (elongation)	[43]
H3Lys79	Dot1	euchromatin transcriptional activation (elongation) checkpoint response	[44-46]

In summary, gene function and cell phenotype can be influenced not only by variation in the gene sequence but also by the epigenetic programming of gene expression. Epigenetic changes can be modified by pharmacological factors [47]. Several epigenetic drugs are already in different stages of clinical trials for cancer treatment [48, 49] and psychiatric disease [50].

1.1.4 Histone methyltransferases and their role

Histone methyltransferases are enzymes that are facilitating the transfer of the methyl group (–CH3) to a specific site of proteins or nucleic acids. Theses enzymes catalyze the transfer of the methyl group from SAM on the side-chain nitrogen of lysine or arginine to histones, resulting in a methylated biomolecule and S-adenosyl-L-homocysteine (SAH) – as a byproduct.

Protein methyltransferases (PMTs) can be classified into two families – protein lysine methyltransferases (PKMTs) and protein arginine methyltransferases (PRMTs). Mono-, di- or tri - methylation of the lysine can occur (*Figure 4*). They are distinguished by the amino acid that accepts the methyl group and by the conserved sequences of their respective catalytic domains. Among the many PKMTs that have been identified so far, some of them have been validated for their methyltransferase activity [51].

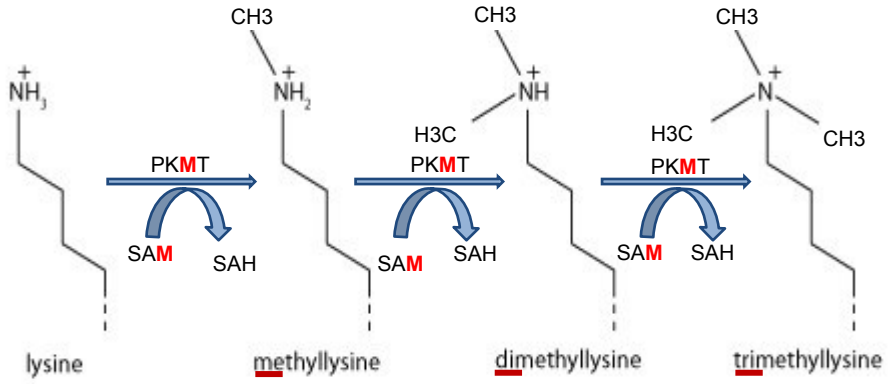

Figure 4. *Schematic view of methylation at lysine residue by protein lysine methyltransferases (PKMTs). Some PKMTs add just a single methyl group, resulting in a mono-methylated product, whereas some others produce di- or tri-methylated lysine modifications.*

Several proteins responsible for methylation have been characterized and all but one of these enzymes contains a SET domain. The exception is the ***DOT1*** family of methyltransferases, members of which methylate K79 in the globular region of histone H3 [52]. The SET domain was first recognized as a conserved sequence in three *Drosophila melanogaster* proteins: a modifier of position-effect variegation, suppressor of variegation 3-9 (Su(var)3-9), the polycomb-group (Pc-G) gene enhancer of zeste [E(z)], and the trithorax-group chromatin regulator trithorax (Trx). The SET domain, which is approximately 130 amino acids long, was characterized in 1998 and SET-domain proteins have been found in all eukaryotic organisms studied so far [52]. Seven main families of the SET-domain proteins are known: SUV39, SET1, SET2, EZ, RIZ, SMYD, and SUV4-20 families. *Table 2* summarizes the most relevant histone methyltransferases of the SET domain PKMTs.

The **SUV39** family has been characterized very thoroughly. Members of this family, human SUV39H1, were the first SET-domain protein lysine methyltransferases identified. These proteins are specifically involved in the methylation of H3K9 [38]. SUV39H1 is similar to SUV39H2 with up to 55%, depending on species [52]. The members of the SUV39 family discussed above (H1 and H2) are involved in the methylation of histone residues within both, euchromatin and heterochromatin. In contrast, another member of the same family, G9a, is the predominant histone H3K9 methyltransferase in mammalian euchromatin [52, 53]. G9a and SUV39H1 belong to the same family of SET-domain proteins and both have pre-SET and post-SET domains surrounding the SET domain.

Table 2. *Selected histone methyltransferases and their targets according to Albert et al. [54].*

Name	Histone target	Transcriptional activity	Transcriptional repression
MLL	H3K4**me1/2/3**	H3K4**me2/3**	-
MLL2			-
SETD1A	H3K4**me1/2/3**	H3K4**me2/3**	-
SETD1B			-
SUV39H1	H3K9**me2/3**	-	H3K9**me2/3**
SUV39H2		-	
EHMT2 (G9a)	H3K9**me1/2**	H3K9**me1**	H3K9**me2**
EZH1	H3K27**me2/3**	-	H3K27**me2/3**
EZH2		-	
DOT1L	H3K79**me1/2**	H3K79**me1/2**	-
SET2[55]	H3K36**me2**	H3K36**me2**	-

ESET (also called **SETDB1**), which predominantly methylates H3K9 in transcriptionally silent euchromatin [56], has been also found to play a crucial role in post-implantation development and in methylation of H3K36 and H4K20 [57]. This protein was also found to be structurally similar with **SETD1A** [52].

MLL1, also member of the SET1 family, is often implicated in leukemia as a result of aberrant *Hox* gene activation mediated by histone H3K4 methylation [58]. **EZH2** acts mainly as a gene silencer; it performs this role by the addition of three methyl groups to Lysine 27 of histone 3, a modification leading to chromatin condensation [42]. EZH2 is frequently overexpressed in a wide variety of tumors and its up-regulation correlates with advanced stages of disease and poor prognosis. Knockdown of *EZH2* inhibits growth of myeloma and prostate cancer cells [59, 60], whereas *EZH2* overexpression promotes colony formation, anchorage-independent growth and cell invasion [60-62] as well as xenograft tumor growth. This methyltransferase interacts also with HDAC1 and HDAC2 in order to repress transcription during embryonic ectodermal development [63]. Taken together, these results suggest that EZH2 could be a driving oncogene. Important is to underline that the H3K27 methyltransferase EZH2 is essential for normal embryonic development [64] It has been found highly expressed in a large number of primary tumors and several data suggest that tumors invasion is dependent on its expression, as reviewed by Albert *et al.* [54].

Histone acetylation was first reported in 1964 by Allfrey *et al.* [65]. Since then it was shown that acetylation of lysine is reversible and highly dynamic through the opposing actions of two families of enzymes, histone acetyltransferases (HAT) and histone deacethylases (HDACs) [66]. The HATs utilize acetyl CoA as cofactor and catalyse the transfer of an acetyl group to the ε-amino group of lysine side chains. The result is neutralization of the positive charge of the lysine, action that has the potential of weakening the interactions between histones and DNA. These enzymes modify multiple sites within the histone N-terminal tails [66]. HDAC enzymes have opposite effects of HATs and reverse

lysine acetylation, an action that restores the positive charge of the lysine. This process potentially stabilizes the local chromatin architecture and is consistent with HDACs being mainly transcriptional repressors. There are four classes of HDAC [67] and the following are the most representative for each class: class I (HDAC 1, 2, 3, 8), class II (HDAC 4, 5, 6, 7, 9), class III (Sirtuins, SIRT1, 2, 3, 4, 5, 6, 7), and class IV (HDAC 11). Class III requires a specific cofactor for its activity, NAD+. Generally, HDACs have relatively low substrate specificity by themselves, a single enzyme being capable of deacetylating multiple sites within histones. The problem of enzyme recruitment and specificity is further complicated by the fact that the enzymes are typically present in multiple distinct complexes, often with other HDAC family members. For examples, HDAC1 is found together with HDAC2 within the NuRD, Sin3a, and Co-REST complexes [68]. Therefore, it is difficult to determine which activity (specific HDAC and/or combined) is responsible for a specific effect. Nevertheless, in certain cases it is possible to determine, which enzyme is required for a given process, as it has been shown that HDAC1, but not HDAC2, controls embryonic stem cell differentiation [69].

1.2 Epigenetic changes in vascular disease

Non-communicable diseases (NCDs), classified by World Health Organization (WHO) into heart disease, stroke, cancer, chronic respiratory diseases, and diabetes, are the leading cause of mortality in the world. Common, risk factors that underlie the major NCDs, include tobacco, harmful use of alcohol, unhealthy diet, insufficient physical activity, overweight/obesity, raised blood pressure, raised blood sugar, and raised cholesterol. Of the 57 million global deaths in 2008, 36 million (63%) were due to NCDs [70]. In 2011, a report published by WHO states that cardiovascular diseases (CVDs) are the primary cause of death globally; more people die annually from CVDs than from any other cause. An estimated 17.3 million people died from CVDs in 2008, representing 30% of all global deaths. Of these, an estimated 7.3 million were due to coronary heart disease and 6.2 million were due to stroke. In the year 2010, CVDs were estimated to have become the leading cause of death all countries [71]. According to WHO, by 2030 almost 23.6 million people will die from CVDs annually, mainly from heart disease or stroke, both having as common cause the atherosclerotic plaque, diseases that are supposed to remain the single leading causes of death [70].

1.2.1 Atherosclerosis is the leading cause of stroke and heart attack

Atherosclerosis (AS, also known as arteriosclerotic vascular disease, ASVD) is characterized by a gradual thickening and hardening of the vessel wall as a result of the accumulation of fatty acids and cholesterol (*Figure 5*). Inflammation, together with endothelial dysfunction, is a key event in the formation of lipid-laden foam cells, the initiation and development of AS.

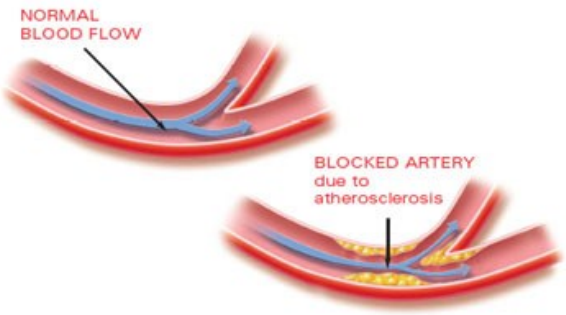

Figure 5. *Occlusion of the artery due to atherosclerotic plaque building up.*

Sudden arterial plaque rupture causes the formation of a thrombus that rapidly slow or stop blood flow, thus leading to death of the tissues supplied by the artery (infarction) in approximately 5 min. One of the usual infarctions is the heart attack and it involves the occlusion of the coronary artery by plaque, leading to infarction of the myocardium (*Figure 6*).

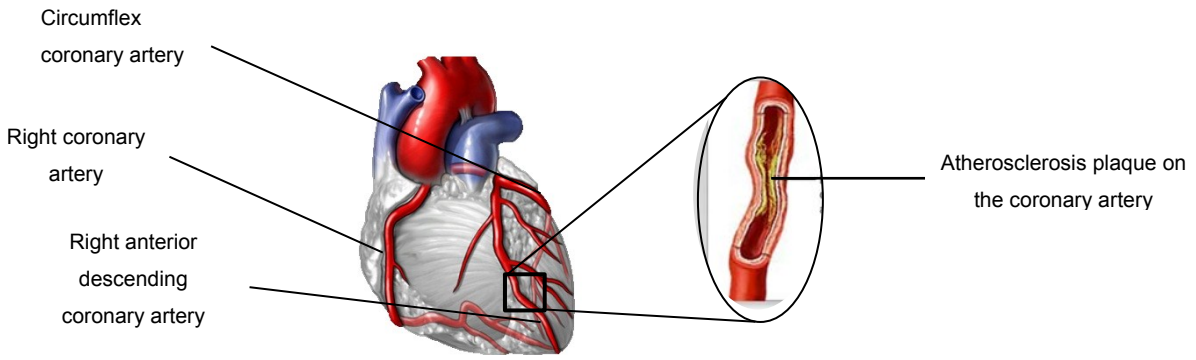

Figure 6. *Heart attack. Insufficient blood flow to the heart muscle from narrowing of coronary artery due to atherosclerotic plaque leads to heart attack.*

Atherosclerosis changes within the vessel wall of the carotid artery can lead to plaque vulnerability, which constitutes the main reason for carotid-related ischemic events [72]. If this process is happening in an artery supplying the brain, the consequence is an ischemic stroke, frequently followed by decease or permanent disabilities. Due to the lack of blood flow in certain regions of the brain responsible for sensitive or motor functions, certain activities, such as walking or speaking, may be impaired (*Figure 7*).

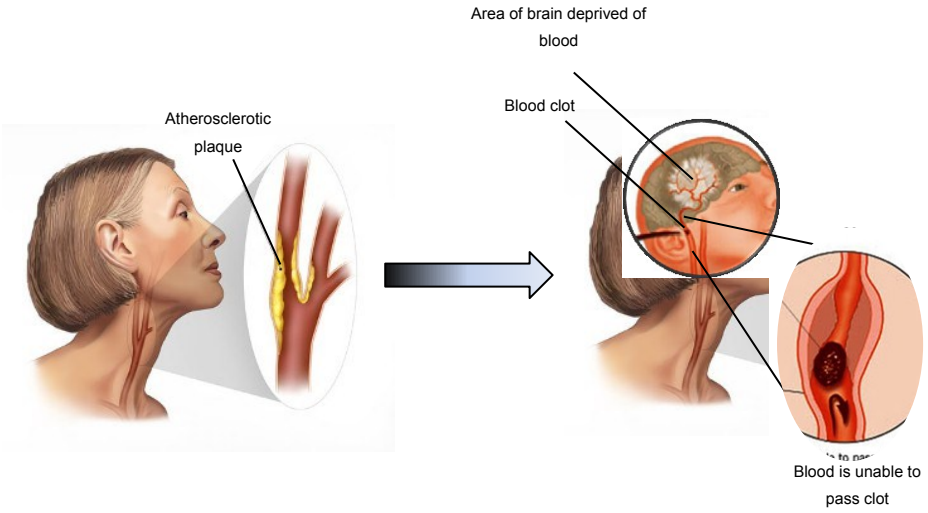

Figure 7. *Stroke. Arterial plaque rupture leads to thrombus formation that stops the blood flow. As a result the tissue supplied by a blocked artery will suffer death within minutes.*

1.2.2 Stages of atherosclerosis – histological classification

Atherosclerosis is commonly described as a chronic inflammatory disease of the vessel wall, characterized by lipid accumulation, inflammation, and extensive degradation of extracellular matrix (ECM) components [73].

The initiation step for atherosclerosis is thought to be endothelium dysfunction, possibly triggered by the oxidized low-density lipoprotein (ox-LDL) (*Figure 8*). Ox-LDL is

often associated with proteoglycans in sub-endothelium. Activation of endothelial cells triggers an increased expression of cytokines and chemokines, enhancement of the permeability of endothelial cell layer, and increased expression of adhesion molecules. Monocytes and T-lymphocytes are attracted by chemokines and connected to endothelial cells.

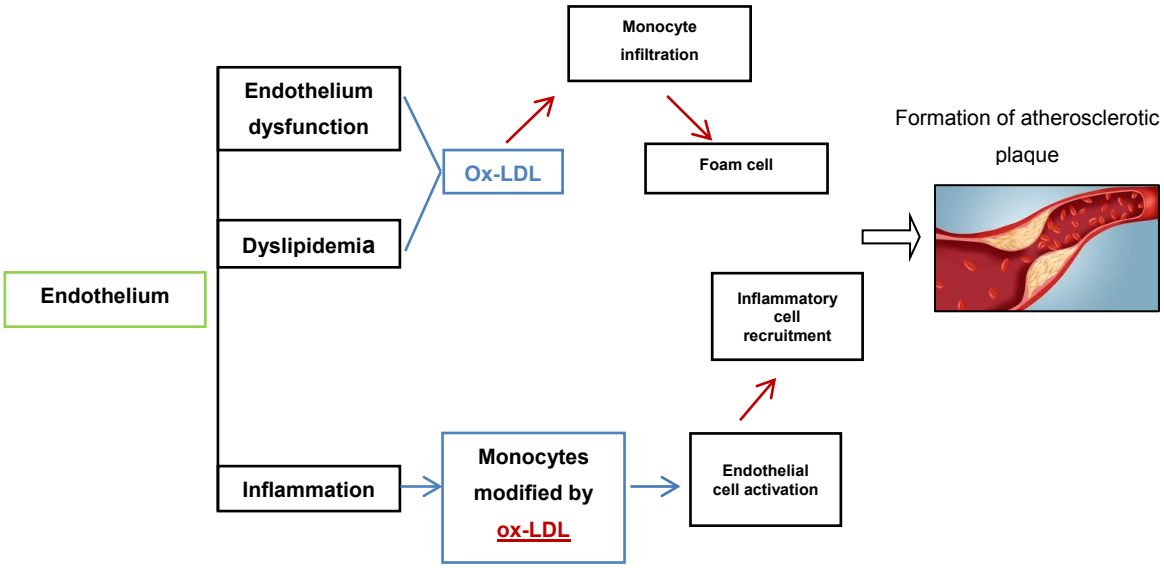

Figure 8. *Schematic view of processes leading to atherosclerosis. Inflammation together with endothelial dysfunction are key events in the formation of lipid-laden foam cells and the initiation and development of atherosclerosis.*

Subsequently, the inflammatory cells are infiltrating the sub-endothelium of the vascular wall and initiate the inflammatory reaction leading to “fatty streak” – the **type I lesion**. At this stage, there are minimal histological changes consisting in small groups (double in number compared with the normal intima) of macrophages and macrophage foam cells (macrophages containing lipid droplets).

The foam cells are cholesterol engorged monocyte-derived macrophages, and are dominant type of immune cells found within the lesions. Macrophages are taking up the ox-LDL, but are not able to digest it sufficiently, resulting in the formation of foam cells. It is still uncertain, whether the fatty streaks are the precursors of more advanced lesions [74, 75]. If the inflammatory factors are not removed, the endothelial dysfunction continues and within the **type II lesion** there are visible more lipid-laden cells than in the initial lesion; within n the smooth muscle cells (SMCs) appear lipid droplets but their number is smaller than the number of macrophage-derived foam cells. The number of intimal SMCs in fatty streaks is similar to the number of SMCs in normal intima, but an enhanced number of proliferating SMCs is observed.

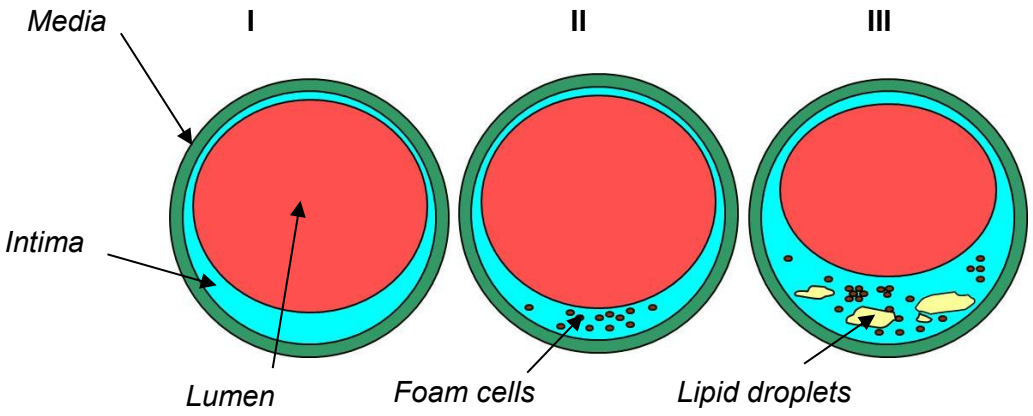

Figure 9. *Early stages of atherosclerosis.*

Intimal macrophage foam cells accumulate in the deep part of the proteoglycan layer and fill the space up to the level of the endothelial cells (ECs). Extracellular space contains small quantities of thinly dispersed lipid droplets and vesicular particles that vary in size and are visible only by electron microscopy. The inflammation at this level is characterized by the presence of few T-lymphocytes and numerous macrophages. Regarding the ECs, it has been observed their loss of orientation according to blood flow, a rounding of the cells, an increase in stigmata and stomata, an increase in stress fiber content, the formation of multinuclear cells. Activated ECs have an increased permeability of endothelium layer. With the progression to **type III lesion (preatheroma)** the lipid droplets accumulate massively in the extracellular matrix and SMCs start to become involved in intima thickening. Cholesterol starts to be rarely present in the lesion and there is a higher amount of fatty acid and fatty streaks than in the previous stages [76]. The first types are often described as early stage of atherosclerosis (*Figure 9*).

Within the advanced stages of atherosclerosis other cell types become involved. The first three types of lesions are not being considered clinically relevant. However, once started, the reaction tends to amplify itself. The first advanced lesion with a potential clinical importance is the **type IV lesion (atheroma)** (*Figure 10*) [76].

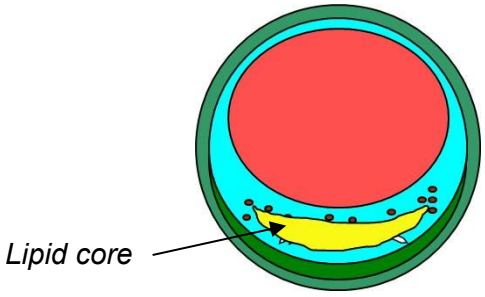

Figure 10. *Atherosclerotic lesion type IV.*

This type is characterized by a massive aggregate of extracellular lipid (a lipid core) that occupies an extensive but well defined region of intima. Smooth muscle cells (SMCs) within the lipid core are dispersed, have elongated shape and unusually thick basement membrane. Calcified areas are often found within the lipid cores. The part of the adaptive thickening between the lipid core and EC surface contains macrophages and SMCs with or without lipid droplets, T-lymphocytes and mast cells. In addition to the components of atheroma, a thick layer composed of newly formed layer of proliferating SMCs and collagen (a fibrotic cap) is located in the region between the lipid core and the endothelial cell layer at the arterial lumen, this process being specific for **type V lesion (fibro-atheroma)** [75]. Advanced stages of atherosclerosis are summarized in *Figure 11*.

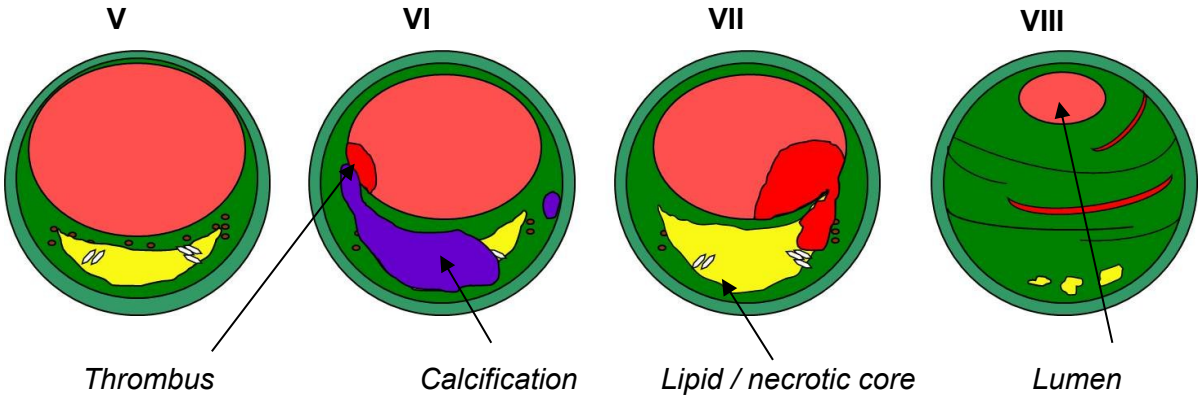

Figure 11. *Advanced stage of atherosclerosis. Type V-VIII.*

Within this lesion type, the primary proteoglycan-rich layer between lipid core and endothelial surface contains substantial more fibrotic collagenous material. Granulation tissue and capillaries at the lateral and luminal margins (shoulders) of the lipid core may be larger than in the atheroma stage. Reparative connective tissue forms in and around regions of intima with large accumulation of extracellular lipid (lipid core); new tissue consists of substantial increase of collagen and synthetic SMCs; lymphocytes, macrophages, and plasma cells are frequently associated with the capillaries, and micro-hemorrhages may be present around them. Several cores separated by fibrous connective tissue may start to form together with additional lipid cores, varying in localization, size and shape. Further progression in the atheroma will lead to the **type VI lesion (complicated atheroma)**. In the type of lesion V, thrombotic deposits and/or marked hemorrhage that accelerate growth and complexity of the lesions are visible. Erosion or ulceration of the lesion surface due to shearing fissures are main cause of the hemorrhage into lesions, thrombotic deposits, therefore this stage is perhaps the most clinically relevant. **Type VII (calcified atheroma)** of the lesion is similar with the type V but with calcium deposits that replace the accumulated remnants of dead cells and extracellular lipid. **Type VIII lesions (fibrotic lesion)** are the

lesions consisting almost entirely of scar collagen. Within this type of lesion the lipid components are no longer present [75].

1.2.3 Role of epigenetics in vascular disease

The major causes of cardiovascular disease are tobacco use, physical inactivity, an unhealthy diet, and harmful use of alcohol. Current recommendations for treatment of CVD aim to reduce risk factors [72].

The role of epigenetics in chronic diseases, such as atherosclerosis, consists in more than just acute reaction to the environmental insult (exposure) – it represents a long term change of the gene expression in the cells of the vascular wall. This means that cells are responsive and they are changed epigenetically during lifetime, suggesting that diet – gene and environment–gene interactions are among the key processes in the disease history. This hypothesis is supported by many studies that are connecting nutrition [77-79], smoking [80, 81] and environmental changes [82] with alternations in epigenetics. An interesting study of Baccarelli *et al.* showed that pollution from traffic, an environmental challenge associated with increased risk of CVD, affected DNA methylation in a study group in USA [83, 84]. The focus of these studies was on repetitive sequences LINE-1 and Alu1. A correlation has been found between the exposure to carbon dioxide and hypomethylation and a significant demethylation effect was observed for LINE-1. These data suggest that DNA might reveal a link between exposure to pollutants and the development of CVD. LINE-1 demethylation has been also detected in vascular smooth muscle cells exposed to homocysteine – a very well characterized molecule with a role in epigenetics [85].

Hyperhomocysteinemia is an accepted risk factor for CVD, supported by a large amount of studies [86, 87]. High levels of homocysteine promote the development of atherosclerotic lesions by inducing aberrant DNA methylation in both vascular smooth muscle and monocytes [85, 88]. There are several of other findings that have confounded the issue. It can be assumed that homocysteine inhibition of DNMTs would promote an overall hypomethylation. However some data suggest that hypermethylation predominates at specific loci, including extracellular superoxide dismutase, estrogen receptor α, and endothelial NO synthase [87]. Other reports, utilizing peripheral blood lymphocytes from patients with coronary artery disease, have produced conflicting results, suggesting that global methylation may be increased or decreased in different individuals [89, 90]. Collectively, the data support a role for altered DNA methylation secondary to homocysteine overload, but to date it has been difficult to specify how these alterations may correlate with disease pathogenesis.

DNA methylation is a major epigenetic modification regulating gene expression, silencing repetitive DNA elements, and maintaining chromosomal structure. Animal model experiments on mice proved the principle that DNA hypomethylation is a pre-step in the onset of atherosclerosis [91]. A recent study of Castillo-Diaz *et al.* [92] on human atherosclerotic arteries sustains the hypothesis that aberrant DNA methylation plays a role in the critical regulatory genes for induction of pro-atherogenic cellular phenotype. One of the theories that describe possible mechanisms for some cancers seem to be facilitated by so called epimutations - changes not in the DNA itself, but in the pattern of methylation, with inactivation of genes that play a role in organism defense against cancer [93]. This approach is supported by the study of Hiltunen *et al.* [13], who describes that hypomethylation in atherosclerotic lesions is present at the same level as in malignant tumors, process which affects the smooth muscle cell proliferation and gene expression in arthrosclerosis. Portions of DNA can be inactivated by covalently attaching methyl groups, which can interfere with the binding of transcriptional enzymes, and can also be signals to recruit enzymes that modify associated histones. DNA methylation is not maintained during replication, but methyl groups are added after each cycle of cell replication [94, 95].

The methylation of DNA is sustained by a family of methyltransferases (DNMT1, DNMT3A, and DNMT3B). A study on mouse embryonic fibroblasts deficient in DNMT1 were reported to have a decrease in the global DNA methylation status correlated with cell type-specific changes in gene expression that disturb several pathways, including expression of imprinted genes, cell-cycle control, growth factor/receptor signal transduction, and mobilization of retro elements [96]. The role of DNA methylation and DNMTs in cancer and developmental studies has been extensively examined. However the functions of DNMTs in cardiovascular diseases and atherosclerosis are not yet understood.

It is currently recognized that the epigenetic modifications of the genome play a major role in disease development, linking the environmental insults with gene regulation. Recent research has focused on how modification of DNA by methylation, and histone modification by acetylation, methylation, phosphorylation and/or SUMOylation may be targeted therapeutically [97]. Mouse models of hypercholesterolemia have demonstrated that HDAC7 plays a role in disease progression through repression of the cholesterol-metabolizing enzyme CYP27A1. Importantly, treatment of these animals with HDAC inhibitors significantly lowered serum cholesterol through enhanced expression of CYP27A1 and subsequently increased production of bile acids [98]. Statins, which are commonly employed as anti-cholesterol pharmaceuticals, have also been implicated in HDAC regulation, though there is doubt about how they interact with gene expression. In order to prove the complex relationship between HDAC regulation and atherosclerosis, Dje N'Guessan *et al.* [99]

demonstrated that ox-LDL reduces HDAC levels and modulates signaling pathways that are partially rescued with statin treatment. This result brings forward the utility of HDAC inhibition in CVD and highlights a portion of complex communication between metabolic and epigenetic pathways that takes place in CVD.

There is significant evidence supporting complex regulatory networks spanning metabolic and epigenetic processes in CVD. While many of the specific interactions remain to be identified, the data are so far promising. Continued research in this field is critically important given the large number of patients who are affected by CVD. Epigenetic - based therapies to target the underlying mechanisms of CVD will hopefully prove to be valuable treatments in the future [100].

1.2.4 Aim of the study – epigenetic changes in vascular disease

Chromatin is a flexible structure experiencing dynamic epigenetic changes through the whole life. The most interesting feature of epigenetics is that it can be affected by environmental interactions, giving the organism a feedback from surrounding conditions. Emerging evidences implicate a spectrum of epigenetic changes in the pathophysiology of atherosclerosis [13, 87, 94]. Genetic and epigenetic studies must be integrated to find new targets for atherosclerosis therapy and to completely understand the cause of this vascular disease. Since epigenetic modifications are potentially reversible, there is a possibility directed therapies targeted at specific modifications of the epigenome may have favorable effects on cardiovascular system of the patients suffering from atherosclerosis.

The aim of the current study was to evaluate possible alterations in DNA and histone modifications in carotid artery in concordance with the progression of atherosclerosis. In the present work several points should be addressed with regard to the above mention topic in an attempt to answer following questions:

1. Are there any changes in global DNA methylation in concordance with the progression of atherosclerosis in carotid artery?
2. Are there any changes in the genome wide methylation in DNA found in serum between patients with high grade carotid artery stenosis and healthy subjects?
3. What molecular mechanism is involved in the changes of DNA methylation? In this context, the expression of DNA-methyltransferases is examined.
4. Are there any changes in histone methylation in carotid atherosclerotic lesions compared to healthy individuals? In this case the study concentrate on two methylations in histone H3 and H4 at lysine K4 and K9, which possess opposite effect on gene activity. Methylation of H3K4 increases gene activity, in contrast methylation of H3K9 leads to gene silencing.

5. What molecular mechanisms are responsible for changes in histone H3K4 and H3K9 in atherosclerotic plaques? In this context, the expression of histone methyltransferases is evaluated.
6. Can the modification of H3K4 and H3K9 be associated with certain type of cells, important in AS, such as SMCs or inflammatory cells?

1.3 Epigenetic changes in regenerative medicine

One of the main efforts in medical treatment is the regeneration of organ function caused by injuries or diseases. Nowadays, this medical field has become a separate entity and it carries the name of “regenerative medicine”. Regenerative medicine is formed of more subdomains, all having the same purpose, namely the repair of dysfunctional cells, tissues or organs. These subdomains of regenerative medicine are reconstructive surgery, transplantation surgery, tissue engineering, and gene and cell therapy.

The 20th century has brought notable medical developments such as blood transfusion and organ transplantation. Organs were at first transplanted only between twins thanks to the immunological compatibility. Later, due to the discovery of immunosuppressive medication, allogeneic organ transplantation became a widespread surgical technique. Beginning with the 1990s, triggered by the pressing need for transplant organs, research has taken a great interest in tissue engineering. By using biocompatible materials with or without biological component, tissue engineered constructs can be used to repair and accelerate the healing of various injuries. Tissue engineering uses mostly biodegradable scaffolds that are slowly resorbed after implantation and replaced by the extracellular matrix (ECM) of the body for the purpose of building tissue grafts. The biological parts of the construct are generally cells. They contribute to the biocompatibility and integration into the host. The ideal cells applicable to the clinical setting are likely to possess the following characteristics:

1. Unlimited ability to renew symmetrically to provide abundant numbers of cells;
2. Ability to form all functional tissue of the body;
3. Compatibility with patient’s immune system.

Embryonic stem cells appear to have the characteristics 1 and 2 but not 3. Somatic stem cells can be harvested from the patient (satisfying the 3rd characteristic), but are developmentally restricted and therefore do not possess the characteristics 1 and 2 [101].

Different strategies have been developed to reprogram somatic cells. The most remarkable studies are from Takahashi *et al.* [102] and Yu *et al.* [103]. These research groups were able to reprogram fibroblasts into cells with the characteristics of embryonic stem cells through viral transfection of a combination defined factors, which have been acknowledged to be key “stemness” factors for achieving pluripotency: OCT4, KLF4, CMYC, NANOG, and SOX2. In this way, all three characteristics for an ideal regenerative cell, called induced pluripotent stem cells (iPSCs), as described above, can be fulfilled: the compatibility with the patient.

Induced pluripotent stem cells have, however, a major limitation for their use in clinical applications due to their oncogenic potential. The OCT4, KLF4, CMYC, NANOG, and SOX2 markers have been intensely studied and are known to be critically involved in self-renewal of undifferentiated embryonic stem cells. OCT4, also known as POU5F, is a transcription factor (TF) used for identification of stem cells, as well as cancer stem cells. KLF4, Kruppel-like factor 4, is a part of the KLF family that has been mainly studied for its involvement in cell proliferation, differentiation and survival, both in cancer and iPSCs. KLF4 is known to act as a transcriptional activator or repressor depending on the promoter and/or cooperation with other TFs. CMYC, whose persistent overexpression is associated with cancer, is also a TF. It has been suggested that the expression of CMYC regulated the expression of 15% of all genes [104]. It acts also by recruitment of HATs, proving its role in regulation of chromatin structure [105]. NANOG is believed to be a key TF in maintaining pluripotency, although Yamanaka *et al.* [106] proved that it is also possible to induce embryonic stem cells without this marker, making NANOG dispensable. NANOG expression is also associated with tumors and is used for diagnostic of germinoma (a type of germ cell tumor). SOX2, a TF that promotes the differentiation of ECs into neuronal ectoderm germ layer, has been shown to inhibit the differentiation into mesoderm and to have a key role in development of mammalian embryos [107]. However, its overexpression in lung carcinoma classified this TF as a key oncogene in lung squamous cell carcinoma with a role epithelial differentiation in tumor progression [108].

Adult mesenchymal stem cells have been used in many tissue engineering studies involving repair of various tissues, such as blood vessels, bone, cartilage, or skin [109-111] . These cells can be isolated from different organs of the patient himself and grown *in vitro* until a sufficient number of cells is obtain, after which they can be seeded onto the scaffold and implanted *in vivo*. In this way, the immune reactions to the construct are minimal and there are no ethical issues like those caused by the use of embryonic stem cells. Inside the body, the cells will proliferate and produce ECM that would lead to the incorporation of the construct into the host.

1.3.1 Reprogramming of mesenchymal stem cells (MSCs) through epigenetics

There have been studies concerning the differentiation of adult stem cells into cells of other phenotypes, e.g. endothelial features, mostly using mesenchymal stem cells (MSCs) [111, 112]. Bone marrow-derived MSCs (BM-MSCs) are able to differentiate into various cell lineages of bone, cartilage, adipose, myocardial, and even neuronal tissue [113-115] and into endothelial cells [115]. The disadvantages of BM-MSCs are, however, the invasive

harvesting procedure, which carries a high risk for the donor and the differentiation process lasts a long period of time. Therefore, other possible sources of such cells with less traumatizing intervention are necessary.

Adipose tissue represents an abundant and accessible source of adult stem cells, the adipose-derived mesenchymal stem cells (adMSCs). These cells can differentiate into a number of mesodermal lineages of ostogenic, chondrogenic, or adipogenic origin [116]. They have already been shown to have many characteristics in common with the BM-MSCs, including their proliferation potential and their capacity of differentiation.

Recently, Colazzo *et al.* studied the ability of adMSCs to differentiate into ECs [111]. Furthermore, Fischer and colleagues have shown that autologous adMSCs are able to support a vascular graft *in vivo* and that further work should be done to improve the differentiation process [117]. So, finding a possibility to increase the differentiation capacity of this type of cells is desired.

During development of the human body a process of differentiation of the embryonic stem cells occurs [118]. During differentiation adult cells arise, which constitute the tissues and organs of the adult organism, through a gradual inhibition of genes, until those only specific for a certain type of tissue are being expressed and transcribed. Consequently, all cells in one organism have the same genotype, but different phenotypes, according to which genes are active in each tissue. Phenotype differences are given by distinct epigenetic patterns, which involve the degree of chromatin folding and DNA methylation [119, 120]. Thus, targeted epigenetic changes, can make silenced genes available for transcription and facilitate desired reprogramming of the cell [121].

1.3.2 Epigenetic modifying drugs and cell reprogramming

During the last decades, studies of chromatin modifications have revealed their essential role in regulation of gene expression [122-124]. Epigenetic reprogramming may also allow re-establishment of the pluripotency state in already differentiated cells. Some studies have already shown that it is possible to use endogenously expressed pluripotency genes to generate stem-cell-like phenotype [125]. However, to achieve a successful reprogramming, DNA methylation status, histone modification, and chromatin structure need to be transferred into a state similar to that of the embryonic state (*Figure 12*) [126]. Expression of specific genes such as *POU5F1a*, *KLF4*, *NANOG*, and *CMYC* induces a sequence of epigenetic events, which trigger chromatin modifications and changes in the DNA methylation. If a somatic cell is induced with all these factors, its phenotype transforms to a partially reprogrammed state [127]. Thus, appropriate changes in the chromatin of

somatic cells may consequently lead to the induction of pluripotency or, better said, to the de-differentiation state of the cells. At this point, a proper protocol is necessary to increase gene expression specific for the desired cell type.

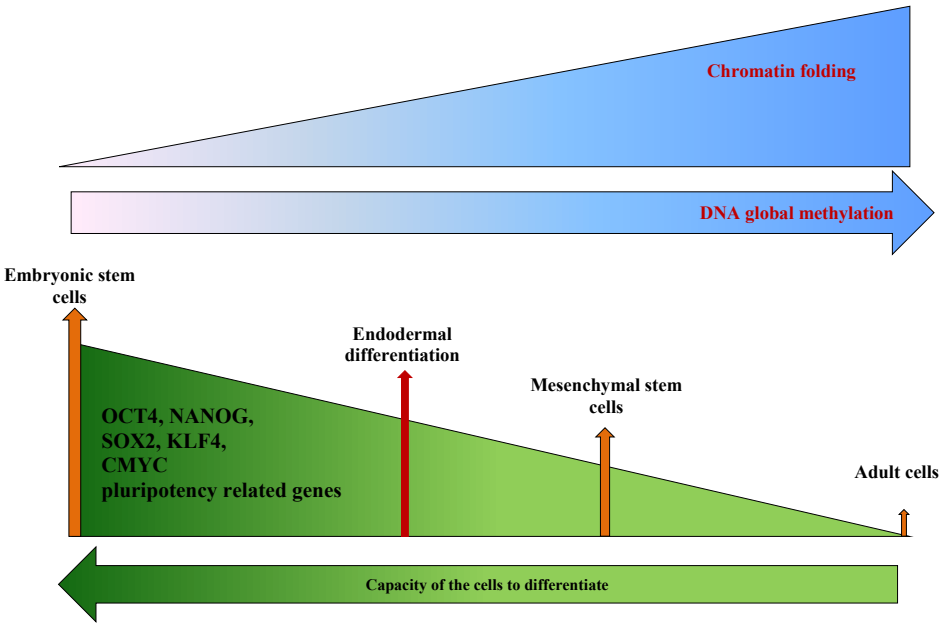

***Figure 12**. A schematic diagram of epigenetic modifications affecting cell reprogramming. The degree of DNA methylation inversely correlates with the ability of cells to regain their potential to differentiate. An appropriate alteration of epigenetics in somatic cells consequently leads to the increase in the expression of pluripotency related genes. Expression of these genes correlates with a higher reprogramming capability.*

Genes normally expressed during embryogenesis (e.g. pluripotency related genes) are silent in somatic donor cells. For gaining the reprogramming capacity, these genes must be turned on again. A possible approach might be the use of chemical modifying drugs that are able to interfere with epigenetic pattern of the treated cells, to inhibit either DNA methylation or different histone methyltransferases or deacethylases. For this purpose, DNA methylation pattern and chromatin structure must be reorganized accordingly, to resemble that of undifferentiated nuclei [128].

Several drugs such as 5-azacytidine (AZA), BIX-01294(BIX), and valproic acid (VPA) are known to have an effect on DNA methylation and/or histone modification.

1.3.2.1 5-azacytidine, inhibitor of global DNA methylation

Global inhibitors of DNA methylation are already used as research tools. Among these are demethylating agents as procainamide [129], zebularine [130], tea polyphenol (-)-epigallocatechin-3-gallate [131], and RG108 [130]. One of the most potent demethylating agents is 5-azacytidine (*Figure 13*) [132].

Azacitidine or 5-azacytidine, commercially also known as Vidaza, is a chemical analogue of cytosine, used in the treatment of myelodysplastic syndrome. It is known as a strong demethylating agent, an effect that has an important role in cellular reprogramming. 5-azacytidine-5-monophosphate inhibits orotidine-5-phosphate decarboxylase, thus blocking the de novo pyrimidine synthesis [133]. Azacytidine appears to restore normal growth and differentiation of bone marrow cells by causing hypomethylation of DNA and directing cytotoxicity on abnormal hematopoietic cells in the bone marrow. Hypomethylation may trigger the normal function of genes that regulate differentiation and proliferation [134].

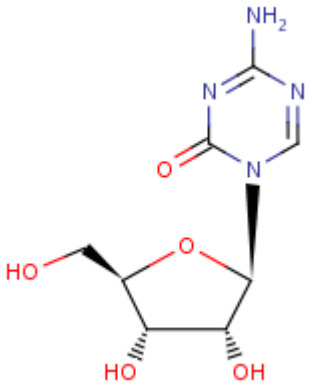

Figure 13. *Chemical structure of 5-azacytidine - (4-amino-1-beta-d-ribofuranosyl-1,3,5-triazin-2(1h)-one).The DNA methyltransferase inhibitor 5–azacytidine impedes the DNA methylation and may therefore confer gene activation [122, 123].*

The incorporation of AZA into DNA *in vitro* prevents DNA methylation [135]. Due to its inhibition effects on the DNA methylation, it has already been used in differentiation protocols of adMSCs or embryonic stem cells into hepatic lineage [136-138]. Furthermore, it has been reported that exposure of bone marrow-derived MSCs to AZA induced a myocyte-resembling phenotype with enhanced response of calcium channels, which has potential applications in ameliorating muscle loss after myocardial ischemia [139]. AZA is unstable in aqueous solutions, with a 10% loss of the product in 2-3 h at RT in lactated Ringer's solution [140]. In addition, in the presence of AZA the cytosine methylation is reduced already after one replication cycle and a part of DNA becomes only hemi-methylated. Full double stranded demethylation requires two replication cycles and occurs in 50% of the dividing cells [141]. Therefore, the use of this substance must be adapted to the intended type of cell population.

1.3.2.2 BIX-01294, a small molecule able to inhibit the G9a methyltransferase

Acetylation of lysine at the N-tail of histone H3 (K9, K14, K18, and K23) and H4 (K5, K8, K12, and K16) and methylation of lysine residue in H3 (as K4, K9, K27, K36, and K79) and H4 (K2) are the most relevant histone modifications that have been identified until now [33].

Many studies have been performed in order to understand the involvement of H3K4 and H4K9 methylation in cancer, embryogenesis, and cell reprogramming. One of the best described modifications is the methylation of lysine 9 of histone H3 (H3K9) [142].

After Jackson *et al.* showed that H3K9me2 histone modification is most likely the sign of gene silencing in *Arabidopsis thaliana* [143], it has been proposed and later confirmed that there is a crosstalk between DNA methylation, absence of H3K4 methylation, and the presence of H3K9 methylation, although the exact mechanism is still unclear [144, 145]. This correlation may be caused in part by DNA methyltransferases specifically recognizing histone modifications. For instance, the *de novo* DNA methyltransferase, Dnmt3A and its cofactor Dnmt3L recognize unmethylated H3K4 via an ADD domain [146, 147]. Moreover, G9a Suv39h1/2 and Setdb1 (all H3K9 methyltransferases), Ezh2 (H3K27 methyltransferase), and heterochromatin protein 1 (HP1), have been implicated to recruit DNA methyltransferases in cancer cells and therefore to modify the DNA methylation pattern [148].

Recently, Kubicek *et al*. showed that BIX-01294 is a specific inhibitor of histone methyltransferase G9a, which is responsible for methylation of H3K9 (*Figure 14*) [124]. By using this chemical compound the epigenetic repression status of several genes could be altered. Furthermore, BIX-01294 seems to compensate the lack of *Oct4a* expression in mouse cells, which are not able to express it natively [125].

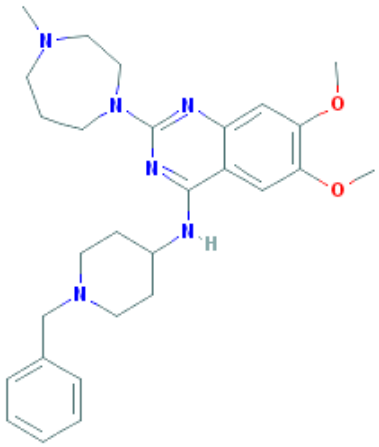

Figure 14. *Chemical structure of BIX-1294 - (N-(1-benzylpiperidin-4-yl)-6, 7-dimethoxy-2-(4-methyl-1, 4-diazepan-1-yl) quinazolin-4-amine) [149]. BIX is a small molecule with the capacity to specifically inhibit the G9a methyltransferase.*

BIX modulates H3K9me2 levels in mammalian cells and potentiates induction of pluripotent stem cells from somatic cells *in vitro* [125]. BIX-01294 occupies the histone peptide binding site and in this way inhibiting the action of G9a [150]. The study of Feldman

et al. [151] confirmed that H3K9 methylation promotes by the SET-containing protein G9a is inhibiting the *Oct3/4* re-expression, preventing the reprogramming of the mouse cells. Therefore, using this chemical compound, the epigenetic repression status of several genes, including *POU5F1*, could be altered and cellular reprogramming might be achieved.

1.3.2.3 Valproic acid as a histone deacethylase inhibitor

Acetyltrasferases (HATs) are enzymes responsible for the transfer of acetyl group to lysine residues and histone deacetylases (HDACs) coordinate their removal. Acetylation neutralizes the positive amino acid charge decreasing the affinity for DNA. The histone tail dislodges from the nucleosome increasing accessibility of transcription factors, which leads to gene expression [152].

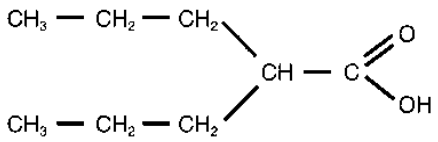

Figure 15. *Chemical structure of valproic acid (2-propylpentanoic acid).*

Valproic acid (VPA) is a simple fatty acid (2-propylpentanoic acid) that has a clinical use as anti-convulsive and mood stabilizing drug used in epilepsy and bipolar disorders (*Figure 15*). The mechanism of VPA includes the neurotransmitter GABA. By inhibiting the GABA-transaminase, it is increasing GABA concentration, therefore enhancing neurotransmission of GABA [153]. In addition, VPA has an inhibiting effect on voltage-gated Na+ channels. The mechanisms of action of VPA in neuropsychiatric disorders are far from fully understood. Moreover, it has been shown that VPA (and its metabolites) can bind covalently and irreversibly to various tissue proteins [13], resulting in alternation of their conformation [154]. VPA also induced changes in the expression of multiple genes, mediated at least partially through the direct inhibition of HDAC [155-157].

Valproic acid, in addition to selectively inhibiting the catalytic activity of class I HDACs, induces proteasomal degradation of HDAC2, in contrast to other inhibitors such as trichostatin A (TSA) [158]. As an inhibitor of histone deacetylases, VPA plays also an important role in the regulation of gene expression [124] and might be thus a promising effector molecule for epigenetic reprogramming.

1.3.3 Adipose tissue more than a fat storage

Adipose tissue is a loose connective tissue located in different places of the body. It is found beneath the skin (subcutaneous fat), around internal organs (visceral fat), in bone marrow (yellow bone marrow), and in breast tissue. The majority of the adipose tissue is

found directly underneath the dermis, but is also found intra-abdominally, as omental fat pads and surrounding several organs of the body.

Humans and other mammals have two main adipose tissue types: white adipose tissue (WAT) and brown adipose tissue (BAT) [159]. The distinction between them is given by the color and the appearance of the adipose cells. The cells from the WAT contains only one fat vacuole, whereas the BAT adipose cells contain multiple vacuoles of fat and many mitochondria [160], with its brown color presumably coming from the relatively high cytochrome *c* content and better vascularization [159].

WAT is mainly considered to be storage for excess energy acquired from food intake [161]. It makes up as much as 20% of the body weight in men and 30% in women [162]. It is mostly found subcutaneously and intra-abdominally between the abdominal muscles and the visceral organs, where it is forming fat deposits, such as the *Omentum majus*. Recently, research has shown that WAT has also important endocrine functions and is releasing the so-called “adipokines”, which regulate the immune response, blood pressure, angiogenesis, hemostasis, bone metabolism, and thyroid function [163].

1.3.4 Cellular components of adipose tissue and relevant CD markers expression pattern

Adipocytes are found in both types of adipose tissues, brown and white, but they have different functions and even different phenotypes (*Figure 16*). The cells originating from BAT have the main function in thermogenesis and present several smaller adipose droplets together with multiple mitochondria. By contrast, WAT cells are mainly regulating the energy balance and possess one large lipid vacuole [164]. These cells belong to a completely independent cell lineage and recent reports suggest that at least some precursors for white fat cells are derived from mural cells associated with blood vessels [165, 166]. White adipose tissue also contains progenitors of multiple mesodermal cell lineages and is an attractive source of autologous cells for transplantation [116]. An MSC population was found in human WAT, which can be driven to differentiate into adipocytes, osteoblasts, and chondrocytes. Whether all mesenchymal stem cells found in adipose tissue are adult mesenchymal stem cells or only a subpopulation, it is a matter of further investigation. There have been studies that are showing differences in the cell population with a regard not only to the tissue type – brown or white, but also to age, gender or body mass index (BMI) of the patients [167-172]. Similarities were shown between human WAT stroma vascular cells and bone marrow stromal cells [173]. There are studies that define, confirm, establish, and validate both the *in*

situ and *in vitro* links between adult human mesenchymal stem cells (MSCs) and perivascular cells, referred to as pericytes [174, 175].

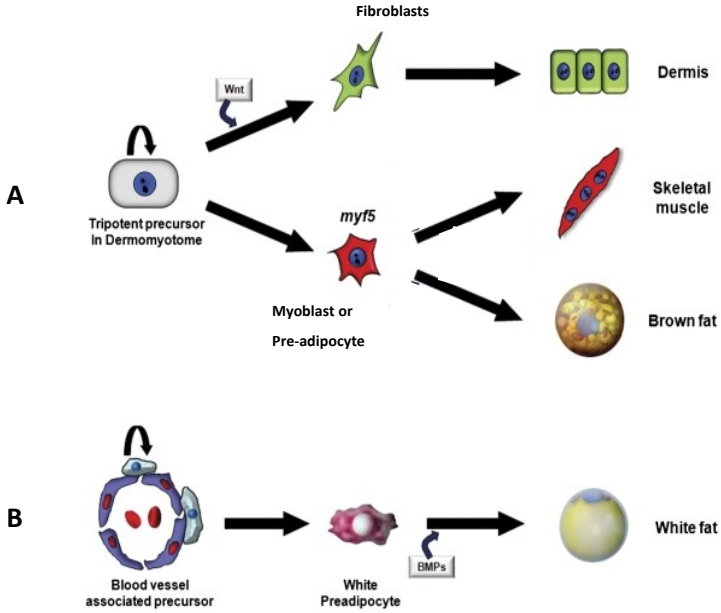

Figure 16. *Different origins and properties of brown and white adipose tissue adipocytes. (A) Brown adipose tissue originating from myoblasts positive precursors; (B) White adipose tissue with origins from pericytes. Modified from Seale et al. [166].*

Overall yield of cells from adipose tissue is influenced by donor age, obesity and/or anatomical site of the sampling [169-171]. Although intensive research work has been performed on progenitor cells from adipose tissue, the mesenchymal stem cells population remains a cell population difficult to characterize. Mostly, this cell population mixture is named “adipose-derived mesenchymal stem cells” [176], but are often called adipose tissue mesenchymal stem cells [177], multi-lineage cells from adipose tissue [178], or adipose tissue derived stromal cells [179].

There are two main procedures to harvest adipose tissue, namely liposuction and plain excision during procedures like abdominoplasty or breast reduction. It is still controversial, which of these cell sources provide a better cell population. Some studies state that liposuction aspirates represent a better source compared with the excised one [180] and others claim the contrary [181].

It also has been shown that, *in vitro,* markers of MSCs are progressively decreased in their expression at higher passages and in this context also their osteogenic potential [182]. For reliable experiments it is recommendable to characterize the cell population, to establish a standard isolation procedure and to work with a homogenous cell population.

Tissue regeneration and recovery in the adult body depend on self-renewal and differentiation of stem and progenitor cells. MSCs have the ability to differentiate into various

cell types and have already been isolated from the stromal fraction of bone marrow, dental tissue or adipose tissue [183]. Studies that are comparing the different types of cell populations have found many similarities regarding their differentiation repertoire, their adherence on the plastic property, or cell phenotype and morphology. Further similarities have been found concerning growth kinetics, expansion capacity, and expression of surface proteins. A basic characterization of mesenchymal stem cell populations points out the presence of CD105, CD90, CD73 [184], and absence of C14, CD34 or CD45 [185].

1.3.5 Source of mesenchymal stem cells and their differentiation potential

Adipose tissue is considered an alternative source of MSCs compared to bone, BM-MSCs, since it can be obtained by a less invasive method and in larger quantities. Isolation of MSCs from adipose tissue has a high success rate with a considerably high yield via a quick and simple liposuction procedure with minimal down time and without the need for prolonged cell culturing.

Adipose tissue is derived from the mesoderm and is one of the tissues that contain high fraction of mesenchymal stem cells [186]. AdMSCs are being increasingly considered as a readily available source of adult stem cells. It has been suggested that from 5 g of adipose tissue up to 35 million cells can be generated [136]. Therefore, this tissue can be regarded as a suitable source of potential stem cells for autologous cell therapies and regenerative medicine. It was recently shown that adMSC can undergo a process of differentiation towards the endothelial cell lineage [117].

1.3.6 Regenerative medicine and vascular disease

The surgical treatment of CVD often requires interventions, such as coronary artery or peripheral bypass, procedures that involve placement of vascular grafts usually originating from the patient's own blood vessels. These grafts are currently the most successful types of implants [187], but their availability is limited due to their utilization in other procedures or because they are often diseased.

For replacement of blood vessels over 6 mm in diameter, synthetic grafts can be used, produced for example from polytetrafluoroethylene (PTFE) [188]. This synthetic implant is able to replace vessel function and to improve the life expectancy of the patient but has also plenty of drawbacks. There is a high risk of infection, stenosis of the anastomosis, propensity for occlusion due to thrombosis, and calcification [189]. The artificial vascular

grafts cannot fully reproduce the biologically sophisticated functions of native vessels. Additionally, they require anticoagulants to control the risk of thromboembolism, while the allograft and bio-prosthetics undergo calcification, and structure deterioration [190]. The undeniable advantages of natural vessels are the capability of growth and adaptation to various physiologic conditions [191]. The ideal properties of a tissue engineered vascular graft would be, among others, resistance to infections, cellular components that would allow the vessel to grow and renew, and non-trombogenicity. In the case of smaller diameter conduits (<6 mm), the use of the PTFE grafts is highly limited due to the currently very low patency rates of less than 25% after 3 years and the obligatory anticoagulant medication [192].

Given the high and increasing number of surgical interventions that require prosthetic transplants and the limited availability of autologous vessels to which there can be added, the poor performance of the synthetic alternatives, it is a big challenge for vascular surgeons and scientists to develop a new generation of biocompatible blood vessel substitutes [193].

1.3.7 Biological grafts

Biological vascular grafts can originate from different sources. The most successful vascular grafts are the ones harvested from the patient himself, named autografts, because risks of incompatibility are eliminated. Because of the very little availability of autografting material, alternatives have been investigated, and these efforts were materialized by the introduction of allografts (grafts from human donors) or xenografts (grafts from other species). Nevertheless, these methods present the great disadvantage of triggering the immune response of the host and the patient has to stay under immunosuppressive medication the whole life.

The concept of tissue engineering has been successfully applied in the production of vascular grafts. The aim is to create fully biocompatible grafts by completely eliminating the synthetic component of the constructs, combined with their repopulation with cells, either *in vivo* or *in vitro*. Strategies to achieve this goal include the use of biodegradable scaffolds or of naturally-derived scaffolds. The biodegradable scaffolds are based on cells seeded on polymers that can be resorbed by the body after implantation [194]. The idea behind this approach is to provide support for cells until the scaffold is replaced by newly-formed tissue. Examples of biodegradable polymers are polyglycolic acid (PGA), poly-L-lactic acid (PLLA), or poly-ε-caprolactone (PCL). This type of scaffolds can be completely degraded through hydrolysis and have a very good resistance to physiologic blood pressure. Scaffolds for vascular grafts can be derived from naturally-occurring polymers, with collagen being one of

the most abundant structural proteins in the human body [195] and a major component of the extracellular matrix of tissues, including that of blood vessels. Tubular constructs can be produced from collagen gels, which can be seeded with cells and implanted at the injured site [196]. Despite their potential and subsequent improvements, these constructs have low mechanical strength [197]. In 1998, L'Heureux introduced the sheet-based tissue engineering [198]. This method comprised of rolling sheets of smooth muscle cells grown *in vitro* onto a cylindrical support and culturing them until the sheets combine to each other. The construct is then devitalized by dehydration and the remaining ECM secreted by the cells is reseeded with endothelial cells. These scaffolds have good mechanical resistance but they were shown to be prone to intimal hyperplasia and aneurysm formation [199].

Another promising technique of obtaining biological scaffolds is decellularization [200]. Cells are being removed from xenogenic or allogenic blood vessels with the use of chemical, physical, or enzymatic agents. What remains is the ECM of the vessel, composed of collagen, fibronectin and glycoproteins, free of cellular antigens and cannot cause an immune response [201]. Onto this scaffold, similar to the above mentioned procedures, autologous cells are being seeded in order to coat the inner surface of the vessel [202]. A recent study has shown promising results, after this method was applied *in vivo* in a porcine model [189]. BM-MSCs and endothelial-like cells were seeded onto acellular arterial grafts, and implanted. The grafts showed lack of immune reaction, synthesis of autologous ECM, and *in* vivo remodeling of the construct.

1.3.8 Aim of the study - epigenetics in regenerative medicine

The need for biological tissue grafts is growing all over the world due to the obvious shortage of donors and the currently inadequate characteristics and limited applicability of the synthetic tissue substitutes. These issues have encouraged the research of autologous cells tissue engineering applications that could elude the above mentioned limitations.

This study focused on the possibility to epigenetically reprogram adult mesenchymal stem cells (MSCs), derived from adipose tissue (adMSCs) into cells with endothelial features. Autologous endothelial cells would be the best cell type used in coating artificial scaffolds prior to implantation, in order to reduce the risk of thrombosis and consequently the risk of cardiovascular events. The limitation of using native endothelial cells comes from their very limited availability. By contrast, adMSCs can be found in higher numbers in the patient's own adipose tissue, and have already been shown to possess high replication potential and so, to be available in a sufficient number to be used in tissue engineering.

AdMSCs themselves do not possess any endothelial characteristics. However former studies have shown that it is possible to induce non-typical gene expression by means of viral transduction. But this approach has been challenged due to ethical reasons and its limited success rate. On the other hand, epigenetic reprogramming induces gene expression without manipulating of the genome. Therefore, treatment of adMSCs with epigenetic modifying drugs such as AZA, BIX or VPA could facilitate de-differentiation towards progenitor stem cells by increased expression of pluripotency-related genes. This step would be followed by triggering the expression of endothelial-specific genes, which could improve the differentiation of adMSCs into endothelial cells that would make them suitable for applications in e.g vascular surgery.

The aim of the current study was therefore to evaluate the ability of adMSCs to increase their differentiation potential and consequently to differentiate into cells of endothelial characteristics. In this regard following items were to address:

1. Isolation and characterization of adMSCs from human adipose tissue to achieve homogenous cell population.
2. Treatment of adMSCs with epigenetic modifying drugs to induce an increase in the expression of pluripotency-related genes
3. To evaluate, whether epigenetic modifications have a positive effect on differentiation of adMSCs towards endothelial lineage.

2 MATERIALS AND METHODS

Collection of human tissue for research purposes was conducted according to the ethical guidelines of Technische Universität München, Klinikum rechts der Isar. The local ethics committee approved the study and written informed consent was given by all donors.

2.1 Cell culture experiments

2.1.1 Isolation of primary adipose derived mesenchymal stem cells (adMSCs)

Human adMSCs were isolated from abdominal subcutaneous adipose tissue obtained from the Department of Plastic Surgery (n = 68). Cell isolation was performed by modification of the method described previously *(Figure 17)* [203]. Briefly, the adipose tissue was cut into small pieces, placed into a 50 ml falcon tube, washed two times with Dulbecco's phosphate buffered saline (PBS, PAA Laboratories GmbH, Cölbe, Germany) and centrifuged at 430 x g for 10 min w/o brakes. Then, the tissue was transferred into a new falcon tube and mixed with sterile collagenase solution (4 mg collagenase II in 5.5 ml PBS). Subsequently, the mixture was shaken at 37°C for 30 min until an emulsion was formed. Warm growth cell culture medium (DMEM with high glucose 4.5 g/l (Biochrom AG, Berlin, Germany) with 10% fetal bovine serum (FBS, PAA Laboratories GmbH), 1% L-glutamine (PAA Laboratories GmbH), 1% penicillin/streptomycin (PAA Laboratories GmbH)) was added to the suspension and centrifuged at 600 x g for 10 min. The remaining adipose tissue was removed, the cell pellet was re-suspended in culture medium, and the cells were plated in 175 cm^2 culture flasks. Growth medium was first changed after 24 h and then regularly every 3 days.

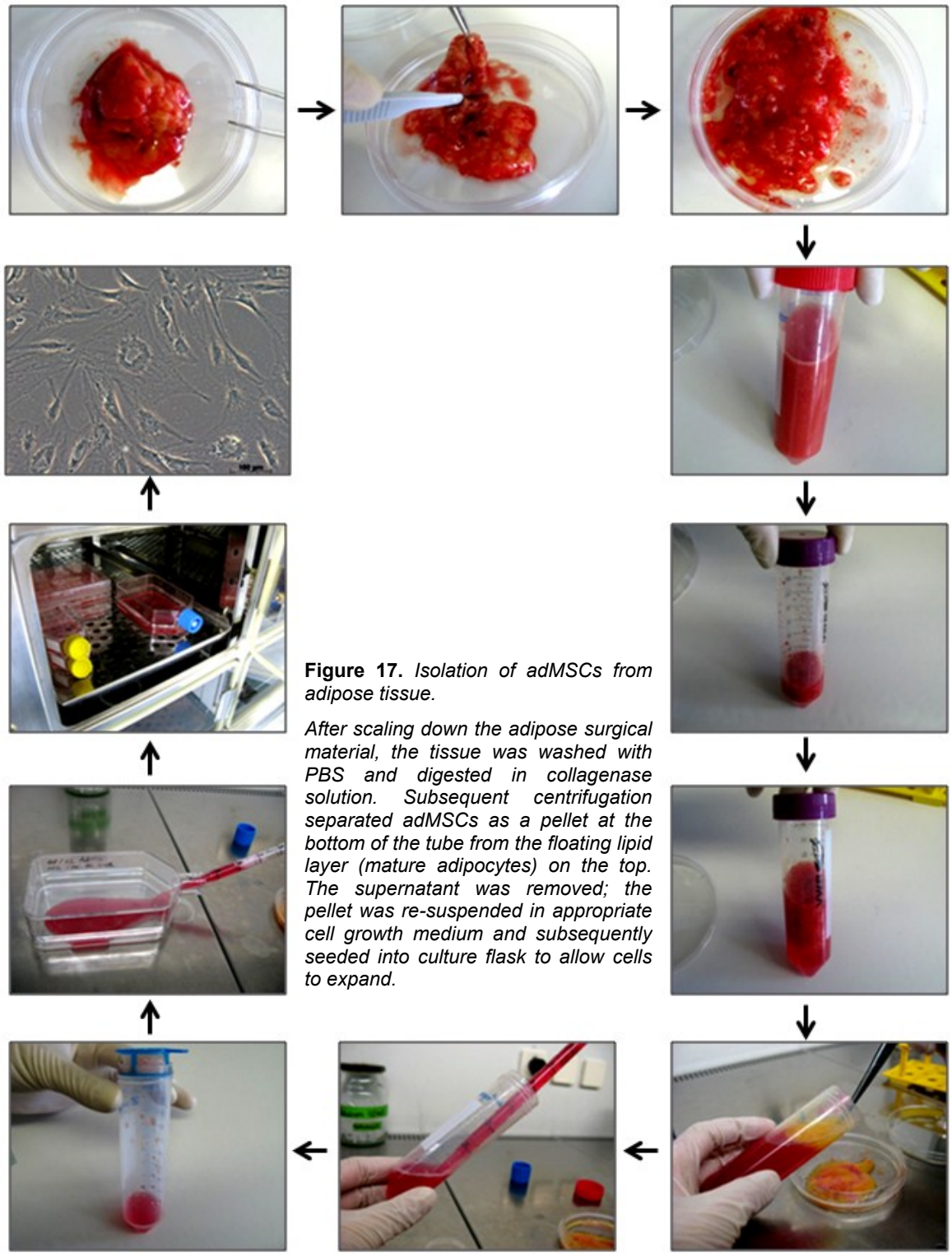

Figure 17. *Isolation of adMSCs from adipose tissue.*

After scaling down the adipose surgical material, the tissue was washed with PBS and digested in collagenase solution. Subsequent centrifugation separated adMSCs as a pellet at the bottom of the tube from the floating lipid layer (mature adipocytes) on the top. The supernatant was removed; the pellet was re-suspended in appropriate cell growth medium and subsequently seeded into culture flask to allow cells to expand.

2.1.2 Cell culture

2.1.2.1 Culture of adipose-derived mesenchymal stem cells

The cells were cultured in Dulbecco's modified Eagle's medium: DMEM with high glucose 4.5 g/l (Biochrom AG) supplemented with 10% FBS (PAA Laboratories GmbH), 5 ml penicillin/streptomycin (PAA Laboratories GmbH), and 2 mM L-glutamine (PAA Laboratories GmbH), and incubated at 37°C in 5% CO_2 atmosphere. To maintain the cells in culture, medium was changed every three days. AdMSCs were sub-cultured when they reached a confluence of 80%. Cell number and viability were determined by trypan blue exclusion method. For all experiments adMSCs were used in the third passage, except for the flow cytometry (fluorescence activated cell sorter - FACS analysis), where the cells were analyzed in each passage until the passage 3.

2.1.2.2 Osteogenic differentiation

The osteogenic differentiation was induced by cultivation of adMSCs in osteogenic differentiation medium. The medium was changed every 3 days. The potential of adMSCs to differentiate in osteoblast-like cells was evaluated at different time points, 7, 14, and 21 days. As positive control osteogenic progenitor cells were used. The human osteogenic progenitors were isolated from tubercular bone specimen of patients operated for hip joint replacement orthopaedic surgery. None of the donors had any disease with effect on the bone metabolism. Osteogenic differentiation media content was: 500 ml Alpha Medium (Biochrom AG), 50ml FBS (PAA Laboratories GmbH), 10 ml HEPES (Biochrom AG), 5 ml penicillin/streptomycin (PAA Laboratories GmbH), 5 ml L-Glutamine, 5 ml MEM Vitamins (Biochrom AG), dexamethasone 100 nM (Sigma-Aldrich, Munich, Germany), L-ascorbic acid 0.25mM (Sigma-Aldrich), Beta-Gliycerophosphate 10 mM (Sigma-Aldrich).

2.1.2.3 Adipogenic differentiation

Adipogenic differentiation was induced with appropriate adipogenic differentiation medium, as mentioned by Kern [204]. Medium was changed every 3 days. The potential of adMSCs to differentiate in adipocytes was evaluated 14 and 21 days after the start of the recommended protocol. Adipogenic differentiation medium comprised of 500 ml DMEM High Glucose (Biochrom AG), 50 ml FBS (PAA Laboratories GmbH), 5 ml penicillin/streptomycin (PAA Laboratories GmbH), 5 ml L-glutamine (PAA Laboratories GmbH), 5 ml Amphotericin B (PAA Laboratories GmbH), 1 mM dexamethasone (Sigma-Aldrich), 0.5 mM 3-isobutyl-1-methyl-xanthine (Sigma-Aldrich), 10 µg/ml recombinant human insulin (Sigma-Aldrich), and 100mM indomethacin (Sigma-Aldrich).

2.1.2.4 Endothelial differentiation

Endothelial differentiation medium (EM) was prepared by adding 5 ml penicillin/streptomycin (PAA Laboratories GmbH), 5 ml L-glutamine (PAA Laboratories GmbH), and 5 ml Amphotericin B (PAA Laboratories GmbH) in 500 ml endothelial medium (PAA Laboratories GmbH). The medium was changed every 3 days. The endothelial differentiation was evaluated after 7 and 14 days of cell cultivation under these differentiation conditions.

2.1.2.5 Cell line used as positive control

NTERA-2 (ACC DSMZ no. CRL-527) cell line were purchased from Leibniz-Institut DSMZ-Deutsche Sammlung von Mikroorganismen und Zellkuturen GmbH (Braunschweig, Germany) and cultivated under the recommended conditions [205].

HUVEC cells (C12200, Promocell GmbH, Heidelberg, Germany) used endothelial culture conditions, mentioned above.

Osteoblast progenitor cells have been isolated from trabecular bone specimens and cultures as previously described [206].

2.1.2.6 Cell propagation

Cells were seeded and cultivated in plastic culture flasks (175 cm^2), Petri dishes (10 cm^2), 6 well plates, 96-well plates, or 4-well chamber slides (all purchased from BD Bioscience, Heidelberg, Germany) depending on the experiments intended, as shown in *Table 3*.

Table 3. *Cell cultivation condition used in the current study.*

Type of the seeding surface	Cell number at 70% confluence/well(flask)	Cells at full confluence/well(flask)	Trypsin / EDTA	Volume of the medium	Type of experiments
T-175	$1.5x10^6$	$2.5x10^6$	5 ml	25 ml	Cell propagation
T-75	$0.75x10^6$	$1.2x10^6$	3 ml	15 ml	Cell propagation
Petri dish	$0.75x10^6$	$1.2x10^6$	2 ml	10 ml	RNA, DNA, protein extraction
6well plate	$0.10x10^6$	$0.20x10^6$	-	3 ml	Von Kossa ALP, and Oil RedO stain, cells for FACS analysis, ac-LDL uptake assay
96-well plate	$0.005x10^6$	$0.01x10^6$	-	0.100 ml	ALP assay, Oil Red O assay, MTT assay
4-well chamber slide	$0.015x10^6$	$0.020x10^6$	-	1 ml	ICC

2.1.2.7 Cell counting

The cell number was determined by using the Fuchs-Rosenthal counting chamber as shown in *Figure 18*. The Fuchs-Rosenthal consists of a thick glass slide with an H-shaped central area that is subdivided in two square counting areas. Each counting area is again divided in 16 areas of 1 mm^2 each, which are sub-divided into 16 squares. It is generally recommended to count 16 areas of 1 mm^2 each, preferably 8 in each chamber.

Procedure: a mixture of 10 µl Trypan Blue solution (Sigma-Aldrich) and 10 µl cell suspension was prepared in a 1.5 ml reaction tube. After 5 min of incubation, 10 µl of mixture was pipetted into the counting chambers of the haemocytometer and the cells visible in the 1 mm^2 squares were counted in both counting areas after microscopic visualization in phase contrast field.

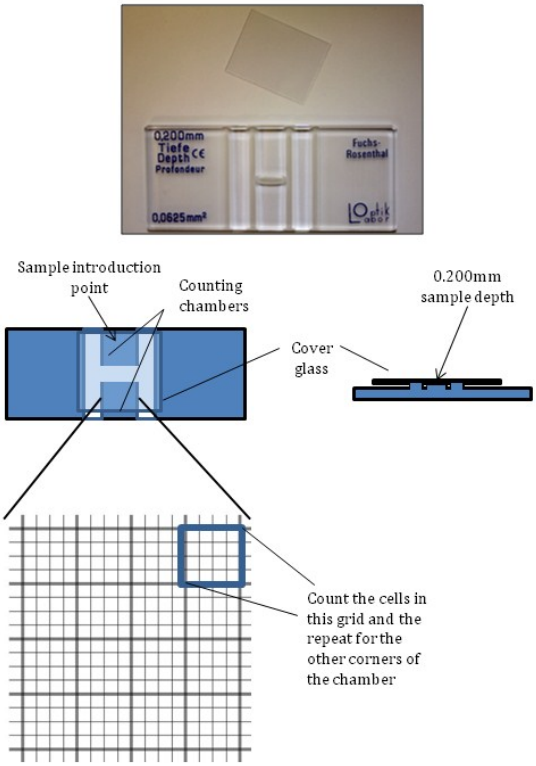

Figure 18. *Schematic view of the Fuchs-Rosenthal counting chamber. Each large square has a surface area of 1.0 mm^2, and the depth of the chamber is 0.2 mm. As there are 1000 mm^3 per ml, each large square represents a volume of 0.0002 ml, so that it is equal to 1/ 0.0002 ml = 5000. The volume factor is 5000.*

The cell number was calculated by using the following formula:

$$Cells\ per\ mL\ = average\ count\ per\ square \times 5000 \times dilution\ factor$$

2.1.3 Cell culture analysis

2.1.3.1 Cytochemistry

2.1.3.1.1 Von Kossa staining

This method uses a precipitation reaction in which silver ions react with phosphate, a component of hydroxyapatite (bone mineral) in the presence of acidic material. Photochemical degradation of silver phosphate occurs when exposed to light, and metallic silver is visualized as a dark-colored material. This technique is used for demonstrating deposits of calcium or calcium salt, so it is not specific for the calcium ions itself.

Procedure: Cells were fixed for 10 min with 4% formaldehyde (Apotheke des Klinikum rechts der Isar der TU München, Germany) at RT, washed for 10 min with distilled water, and then incubated with 1% silver nitrate solution (Sigma-Aldrich). The solution was added on the chamber slides and incubated under light exposure for 40 min at RT. Cells were then

carefully washed with distilled water (B. Braun Melsungen AG, Melsungen, Germany) and incubated for 5 min at RT in a solution of 5% sodium thiosulphate (Sigma-Aldrich) to remove the unreacted silver nitrate. Once the staining was finished the calcification of the matrix was evaluated microscopically and digitalized.

2.1.3.1.2 Alkaline phosphatase staining

5-bromo-4-chloro-3-indolyl-phosphate (BCIP) reaction produces a dark blue, precisely localized precipitate in the presence of alkaline phosphatase (ALP) and with the help of nitroblue tetrazolium (NBT) that is the most commonly used electron-transfer agent and co-precipitant for this reaction (*Figure 19*). BCIP is the ALP-substrate that reacts further after the dephosphorylating to give a dark-blue indigo-dye as an oxidation product. NBT serves herein as the oxidant and gives also a dark-blue dye. It intensifies thereby the color and makes the detection more sensitive.

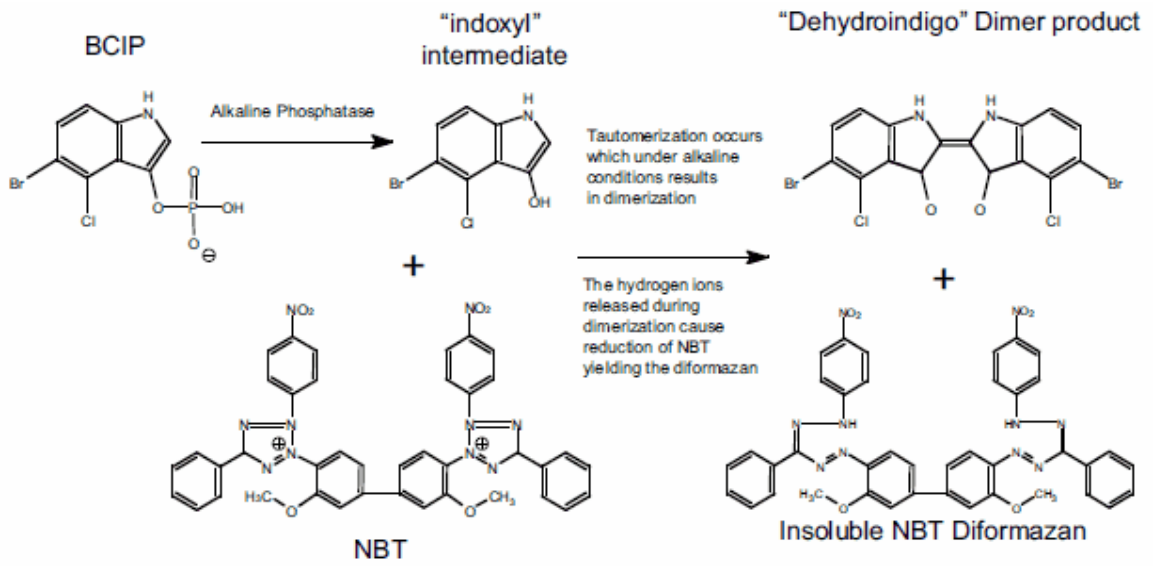

Figure 19. *Diagram of the NBT/BCIP reaction. When alkaline phosphatase removes the phosphate group of BCIP (5-bromo-4-chloro-3-indolyl-phosphate), the resulting molecules dimerize under oxidation conditions to give the blue precipitate (5, 5'-dibromo-4,4'-di dichloro-indigo). During the reaction with BCIP, NBT (nitroblue tetrazolium) is reduced to its colored form [207].*

Procedure: Cells were fixed for 10 min with a fixation buffer (acetone- methanol ratio 1:1). Each time one tablet of NBT/BCIP (Roche, Mannheim, Germany) was dissolved in 10 ml distilled water. The cells were then covered with the solution for 5 min until a color became visible. Kaiser's mounting medium (Merck, Darmstadt, Germany) was applied and the stain was visualized under microscope.

2.1.3.1.3 Oil red O staining

Oil Red O staining is an assay performed to detect oil droplets produced by adipocytes. The mechanism of the staining of lipids is a function of the physical properties of the dye being more soluble in the lipid to be demonstrated than in the vehicular solvent. The Oil Red O is a polyazo dye (*Figure 20*).

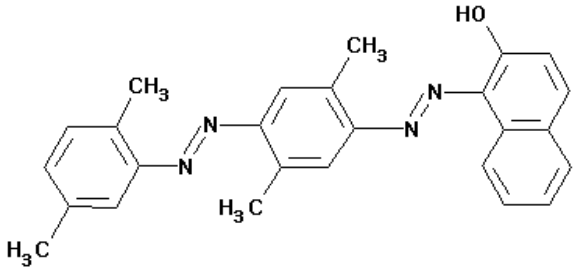

Figure 20. *Oil Red O chemical structure (1-([4-(Xylylazo) xylyl] azo)-2-naphthol 1-[2,5-Dimethyl-4-(2,5-dimethylphenylazo) phenylazo]-2-naphthol).*

Procedure: After fixing of the cells for 10 min with 4% formaldehyde, they were washed with tap water for 10 min and rinsed very briefly in 40% isopropanol (Apotheke MRI). On the cells, 0.5% Oil Red O solution in isopropanol was then added and incubated for 15 min at RT, after which the cells were washed briefly in 40% isopropanol. Following this procedure the nuclei were counterstained with haematoxylin (Apotheke MRI) for 2 min. The cells were washed with tap water, covered with mounting medium consisting of Kaiser's (hydrophilic mounting medium) (Merck) and glass cover slides. The staining was then analyzed under the microscope.

2.1.3.2 Assays

2.1.3.2.1 Viability assay

The viability assay is based on a colorimetric assay that measures cell viability and involves the reduction of yellow 3-(4, 5-dimethythiazol-2-yl)-2, 5-diphenyl tetrazolium bromide (MTT) by the mitochondrial succinate dehydrogenase. The MTT enters the cells and passes into the mitochondria where it is reduced to an insoluble, dark purple formazan salt. This product is solubilized and measured spectrophotometrically at a wavelength of 570 nm. Since reduction of MTT can only occur in metabolically active cells, this assay is measuring the cell viability not their toxicity.

Procedure: AdMSCs were harvested by trypsinization, resuspended in culture medium, and plated in a 96-well plate. After 24 h, the cells were treated either with 5-azacytidine (Sigma-Aldrich), BIX-01294 (Sigma-Aldrich), or VPA (Sigma-Aldrich) for 24, 48 or 72 h. Following treatment, the medium was replaced by 0.5 mg/ml MTT in a water solution and the plate was incubated for 2 h at 37°C, in 5% CO_2. The MTT solubilization solution was prepared from 5 g sodium dodecyl sulphate (SDS) (Sigma-Aldrich), 49.7 ml dimethyl sulfoxide (DMSO) (Sigma-Aldrich), and 0.3 ml acetic acid (Merck). Solubilization solution (100 µl/well) was used to dissolve the formazan crystals. Absorbance was measured at 570 nm / 690 nm using a FLUOstar Omega fluorometer (BMG Labtech, Ortenberg, Germany).

2.1.3.2.2 Alkaline phosphatase activity assay

Alkaline phosphatase (ALP) is a hydrolytic enzyme acting optimally at alkaline pH. The activity of this enzyme can be quantified photometrically by measuring the p-nitrophenol amount produced in the reaction of p-nitrophenolphosphate substrate with ALP at alkaline pH (*Figure 21*).

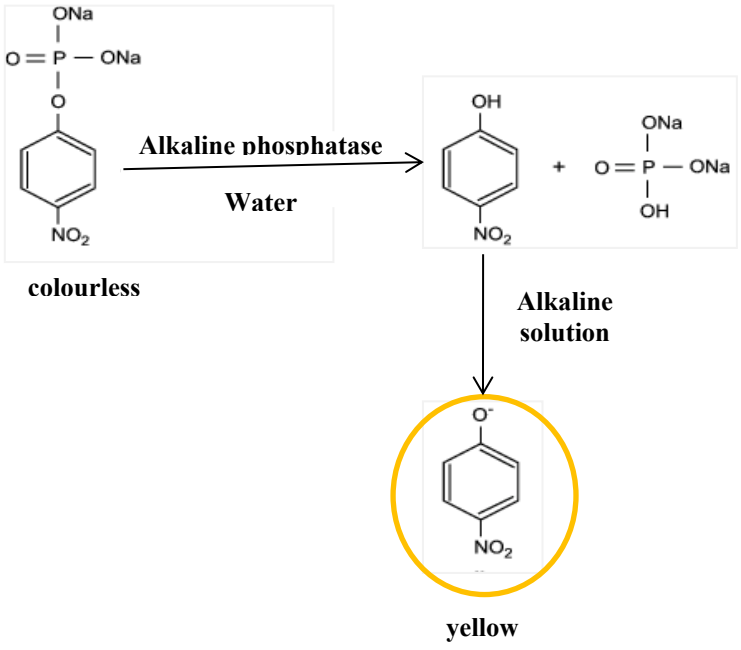

Figure 21. *Reaction of p-nitrophenol with alkaline phosphatase in alkaline solution.*

Procedure: AdMSCs were plated in 96-well plates (5000 cells per well) and were culture in osteogenic differentiation medium. As a negative control, adMSCs were cultivated in normal growth medium. As a positive control, osteoblast progenitor cells were cultivated in osteogenic differentiation medium. At selected time points (7, 14, and 21 days), ALP activity was measured. A standard curve with different concentration of p-nitrophenol (4-nitrophenol solution 10 mM, Sigma-Aldrich) was plotted. A substrate solution was prepared by adding 1.3

mg 4-nitrophenyl phosphate disodium salt hexahydrate (Sigma-Aldrich) in an alkaline solution. The alkaline solution was prepared from 0.375 g glycine (Sigma-Aldrich), 1.211 g 2-Amino-2-(hydroxymethyl)-1,3-propanediol (or Trizma base, Sigma-Aldrich), 0.203 mg $MgCl_2$ (Sigma-Aldrich) in distilled water and adjusted to pH=10.5 with NaOH (Merck). After discarding and washing the cells with PBS, 100 µl substrate solution were added in each well and incubated at 37˚C for 30 min. ASys Expert Plus plate reader (Omnilab, Bremen, Germany) was warmed up to 37˚C and the kinetic measurement was performed at 405 nm in 5-minute intervals for 30 min.

2.1.3.2.3 Oil Red O quantification assay

By solubilizing the droplets stained with Oil Red O in isopropanol, this technique allows the quantification of adipogenic differentiation [208].

Procedure: For this assay, cells were seeded in 96-well plates and cultured in adipogenic differentiation medium. The cells from two study groups (elderly and young) were then stained with Oil Red O without counterstaining with haematoxylin; after washing with 40% isopropanol and distilled water, into each well was added 100 µl of 60% isopropanol and incubated for 15 min at RT on a shaker. The optical density of the solution was then measured at 520 nm with the spectrophotometer. In order to normalize the results to the protein amount, an additional assay was performed, namely Sulphorhodamine B (SRB assay).

2.1.3.2.4 Sulphorodamine B – protein measurement

The Sulforhodamine B (SRB) assay system allows the measurement of the total biomass of the cells by staining cellular proteins with the SRB [209]. The key component is the dye, Sulforhodamine B (or Acid Red 52). The cells are briefly washed, fixed, and stained with this dye. The incorporated compound is then liberated from the cells with a TRIS solution. An increase or decrease in the number of cells (total biomass) results in a concomitant change in the amount of dye incorporated by the cells.

Procedure: SRB solution was prepared in 1% acetic acid solution by adding 0.2 g Sulforhodamine B (Sigma-Aldrich) in 50 ml 1% acetic acid (Merck). After the Oil red O assay, cells were washed and into each well of a 96-well plate 50 µl SRB solution were added. After incubation for 30 min at RT on a shaker the SRB solution was removed; cells were washed carefully with 1% acetic acid five times, each time for 5 min, again on the shaker. Into each well were then added 100 µl of 10 mM TRIS aqueous solution and

incubated for 10 min at RT on the shaker. Measurement of the absorbance was performed at 595 nm (SRB solution) and 690 nm (other impurities or background absorbance) [209].

2.1.3.2.5 Ac-LDL uptake

DiI-Ac-LDL, acetylated low density lipoprotein labeled with 1,1'-Dioctadecyl-3,3,3',3'-tetramethylindocarbocyanine perchlorate, labels both vascular endothelial cells and macrophages. It can be used to identify and/or isolate these cells from mixed cells populations. When cells are labeled with DiI-Ac-LDL, the lipoprotein is degraded by lysosomal enzymes and the DiI fluorescent dye accumulates in the intracellular membranes. Labeling cell with DiI-Ac-LDL has no effect on cell viability. Non-endothelial cells (fibroblasts, smooth muscle cells, pericytes, epithelial cells) are not labeled [210].

Procedure: DiL labeled Ac-LDL was purchased from Bioquote Limited (York, UK). The cells were carefully washed with PBS and incubated with the DiI-Ac-LDL solution (10 µg/ml endothelial medium) for 4 h, at 37 ºC, in 5% CO_2. Cells were carefully washed three times with PBS and afterward fixed in 4% formaldehyde for 10 min. The formaldehyde solution was removed, cells were washed with PBS, and cell nuclei were stained with Sybrgreen I dye (Sigma-Aldrich) for 15 min at RT, protected from light. Sybrgreen I excess was removed by washing with PBS three times. Cells were then analyzed by the use of a fluorescence microscope. The positive control comprised of HUVEC cells and the negative control of adMSCs that have been cultured under normal growth conditions.

2.2 Immunohistochemistry

The immunochemical procedures carried out in the present work were performed with the LSAB kit (DAKO, Hamburg, Germany) or APAAP kit (DAKO), following the instructions of the manufacturer. Each antibody was used at an optimal dilution and with an antigen retrieval method shown in *Table 4*, *5*, and *6*. Antibodies were diluted in an antibody diluent purchased from DAKO.

2.2.1 LSAB method

Most of the immunochemical staining methods in use today are based on the high affinity that streptavidin (*Streptomyces avidinii*) and avidin (chicken egg) possess for biotin. The LSAB reagents are applied in the following order: primary antibody, biotinylated secondary antibody, streptavidin-enzyme conjugate. The color reaction is then developed with the appropriate substrate/chromogen.

Procedure: Prior to performing this staining method, TRIS buffer (1x) was prepared by diluting a stock solution (10x) in a distilled water. Stock of TRIS buffer (10x) was prepared by adding 60.5 g Trizma base (Sigma-Aldrich) and 90 g NaCl (Merck) in 1 l distilled water, and adjusting the pH to 7.6 with HCl (Apotheke MRI). Cells were fixed with acetone : methanol, ratio 1:1 (v/v), for 10 min. The fixation buffer was removed and cells were washed with 1x TRIS buffer. All following steps were performed at RT and according to the manufacturer instructions. Blocking of the peroxidase was performed with 0.3% hydrogen peroxide (Merck), followed by 1 h incubation with the appropriate antibody as presented in *Table 4*, *5*, and *6*. The samples were incubated with secondary antibody (solution A) for 25 min, followed by streptavidin-enzyme conjugate (solution B) for another 25 min. The chromogenic solution was prepared from 15 µl DAB+ (solution C) and 750 µl HRP substrate (solution D). Each step of the protocol was followed by washing in 1x TRIS buffer. After incubation for 3-5 min with the chromogen, samples were counterstained with haematoxylin for 30 seconds. Mounting medium used was Pertex (Leica Mikrosysteme Vertrieb GmbH, Wetzlar, Germany).

2.2.2 APAAP method

This method is based on an indirect reaction. The staining sequence of this technique consists of the use of an unconjugated primary antibody, a secondary antibody, the soluble enzyme-anti-enzyme complex, and substrate solution. The primary antibody and the antibody of the enzyme immune complex must be from the same species. The secondary antibody must be directed against immunoglobulins of the species producing both the primary antibody and the enzyme immune complex. Soluble enzyme-anti-enzyme immune complex techniques were named after the particular enzyme immune complex they used.

Procedure: For this procedure TRIS buffer (1x) (see LSAB method) was used for washing the samples after each step of the following protocol. Cells have been fixed with a fixation buffer (acetone: methanol ratio 1:1) for 10 min. The fixation buffer was removed and cells were washed with 1x TRIS buffer. All following steps have been performed at RT and according to the manufacturer instructions. First antibody against the target protein was incubated with the samples for 1 h using optimized dilution for each antibody as shown in *Table 4*. The incubation with the secondary antibody (sol. A) for 25 min was followed by incubation with the APAAP immunocomplex (sol. B) for another 25 min. Meanwhile, the chromogen solution was prepared from 30 µl sol. C, 30 µl sol. D, 30 µl sol. E, and 750 µl sol. F (substrate solution). The chromogenic mix was incubated for 15 min, until the red color has been observed under the microscope. Haematoxylin counterstain followed for the nuclear stain, and mounting was done with hydrophobic mounting medium, Pertex (Leica Mikrosysteme Vertrieb GmbH).

Table 4. *Antibodies used for characterization of the adMSC population for ICC.*

Name	Reacts with	Clone	Isotype	Brand &Cat. Nr.	Dilution	Detection System
Mouse anti vimentin	Human	Mouse	IgG	Dako	1:500	APAAP
Mouse anti Ki67	Human	Mouse	IgG	Chemicon International IC	1:200	APAAP
CD105 Ab-3, mouse anti-human	Human	SN6h	IgG	Neomarkers MS-1290-P0	1:500	LSAB
Monoclonal Mouse Anti-Human CD31, Endothelial Cell	Mouse	JC70A	IgG	DAKO (M0823)	1:50	LSAB

Table 5. *Antibodies used for detection of pluripotency markers.*

Name	Reacts with	Clone	Isotype	Brand &Cat. Nr.	Dilution	Detection System
OCT4A(C30A3) Rabbit mAb	Human, Mouse	Rabbit	Rabbit IgG	Cell Signaling (#2840)	1:400	LSAB
Rabbit Polyclonal to OCT4	Human, Mouse	Polyclonal	Rabbit, IgG	Abcam (ab19857)	1:500	LSAB
Rabbit polyclonal to Nanog	Human, Mouse	Polyclonal	Rabbit IgG	Abcam (ab21624)	1:500	LSAB
Negative Control Rabbit Immunoglobulin Fraction (Normal)	-	-	Rabbit	DAKO (X0903)	1:500	LSAB

Table 6. *Antibodies used for characterization of the adMSCs differentiated into ECs.*

Name	Reacts with	Clone	Isotype	Brand &Cat. Nr.	Dilution	Detection System
Flk-1/KDR/VEGFR2 Ab-1	Human	Rabbit	Rabbit	Thermo Scientific (RB-1526-P0)	1:200	LSAB
Monoclonal Mouse Anti-Human CD31, Endothelial Cell	Human	JC70A	IgG1	DAKO (M0823)	1:50	LSAB
Monoclonal Mouse Anti-Human Von Willebrand Factor	Human	F8/86	IgG1	DAKO (M0616)	1:400	LSAB
Mouse anti hVCAM-1 (CD106)	Human	Mouse IgG	IgG	R&D Systems	1:500	LSAB
Negative Control Rabbit Immunoglobulin Fraction (Normal)	-	-	Rabbit	DAKO (X0903)	1:500	LSAB
Mouse IgG1 Negative Control	-	-	-	DAKO (X0931)	1:50 1:200 1:400 1:500	APAAP and LSAB

2.3 Flow cytometry (FACS analysis)

Flow cytometry analysis allows simultaneous measuring of relative cell size (FSC), cell granularity, internal complexity (SSC), and florescence intensity. The major components comprise a fluid system, an optical system with laser, reflector, and filter device. According to the florescence staining applied, wavelengths differ between 450 and 700 nm. FITC requires a laser wavelength of about 488 nm in the green range, APC has its optimum at 633 nm in the red spectrum, and PE requires laser with wavelength at 532 nm in the yellow spectrum.

For flow cytometry, adMSCs in passages 0, 1, 2, and 3 were used. The cells were detached from their culture plates with trypsin/EDTA and labeled by incubation at 4ºC for 60 min with the following monoclonal antibodies: mouse anti-human FITC-labeled CD14, mouse anti-human FITC-labeled CD45 (Biozol Diagnostica Vertrieb GmbH, Eching, Germany), mouse anti-human PE-labeled CD105 (Biozol Diagnostica Vertrieb GmbH), and mouse anti-human APC-labeled CD90 (BioLegend, London, UK). Acquisition and analysis were performed on a FACS Canto II, BD Biosciences (San Jose, CA, USA) (*Table 7*). An isotype control was included in each experiment. Data processing and analysis were performed with the FlowJo software. All antibodies were used at a concentration of 0.5 µg/10^6 cells in a total volume of 100 µl.

Table 7. *Antibodies used for FACS analysis.*

Name	Reacts with	Clone	Isotype	Brand &Cat. Nr.	Dilution
mouse anti-human FITC-labeled CD14	Human, Mouse	mouse	mouse	Biozol, Germany	0.5 µg/10^6 cells in 100 µl.
mouse anti-human FITC-labeled CD45	Human, Mouse	mouse	mouse	Biozol, Germany	0.5 µg/10^6 cells in 100 µl.
mouse anti-human PE-labeled CD105	Human, Mouse	mouse	mouse	Biotech, USA	0.5 µg/10^6 cells in 100 µl.
mouse anti-human APC-labeled CD90	Human, Mouse	mouse	mouse	BioLegend, USA	0.5 µg/10^6 cells in 100 µl.

2.4 Tissue sampling, processing, and analysis

2.4.1 Study group, atherosclerotic plaque processing, and characterization

The study group included atherosclerotic plaque specimens from 26 patients with high grade carotid artery stenosis, who underwent carotid endarterectomy (CEA) (*Figure 22*). The specimens were taken from the biobank of the department of Vascular Surgery, selecting the entire range of atherosclerotic lesions from type II to VII (according to AHA classification [76, 211]). Control samples consisted of 10 healthy carotid vessels and were obtained from patients, who underwent trauma surgery. In addition, serum samples from 10 healthy volunteers were included as a control for blood analysis. All patients underwent neurological examination before and after the surgical intervention. The study was conducted according to the guidelines of the world medical association declaration of Helsinki [212]. All the patients gave their informed consent.

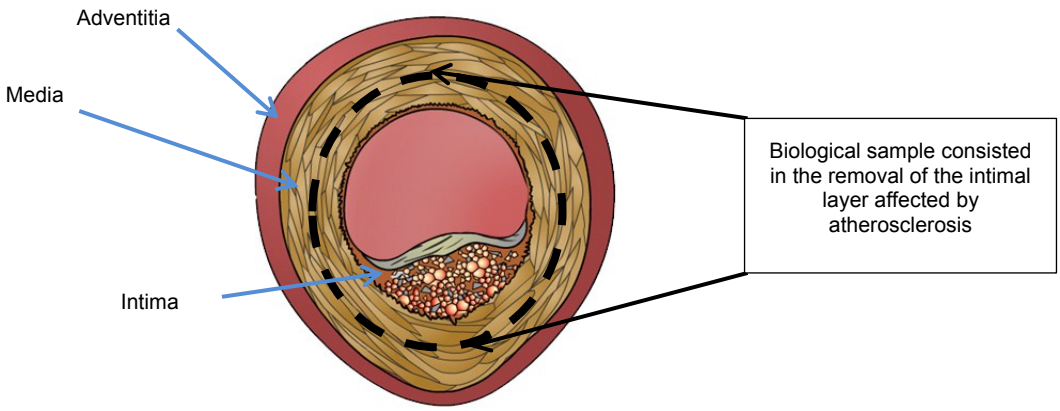

Figure 22. *Biological samples excised from patients with carotid artery stenosis consist of the following layers: Intima – affected by atherosclerosis, and a part of media. The border between these two layers can be recognized microscopically by elastica van Gieson staining of the elastin fibers and the presence of smooth muscle cells within intima layer.*

Procedure: Carotid plaque was collected during the surgical procedure, segmented in blocks of 3-4 mm, fixed in 4% formaldehyde for 24 h, dehydrated, and embedded in paraffin. Segmenting was performed in the way to receive different stages of atherosclerosis plaques between II and VII. For a proper histological characterization, 3 µm sections were prepared from each sample followed by haematoxylin-eosin and elastica van Gieson staining. Histological classification was performed under the supervision of Dr. rer. nat. J. Pelisek and the technical assistant experienced in histology Fr. R. Hegenloh. Type II and III lesions were defined as an early stage of atherosclerosis, type V, VI, and VII as an advanced stage.

2.4.2 Decellularisation and recellularization

One of the processes used for creation of bio-scaffold for autologous vessels is decellularization. Through this process, the cells can be removed from tissue by variety of treatments (chemical, physic-chemical). What remains is a bio-scaffold consisting of the component of extracellular matrix such as collagens and proteoglycans. For this purpose, sodium dodecyl sulphate (SDS) is a detergent known to solubilize cell membrane and proteins without affecting the integrity of the bio-scaffold [213].

Procedure: A sterile 0.66% aqueous solution of SDS (Sigma-Aldrich) was used. Human saphenous vein was segmented in pieces of 2 cm; each was placed in a 15 ml tube filled with 7 ml SDS solution (decellularization solution). The tubes where then placed on a rotational-shaker and the decelllularization solution was changed under sterile conditions after 30 min, 1 h, 6 h, 24 h, 48 h, and 96 h. The resulting bio-scaffolds were then washed three times under sterile conditions with PBS.

Cells were harvested with trypsin/EDTA (Biochrom AG), counted, and $0.75x10^6$ were suspended in 2 ml endothelial medium. The scaffold was placed in a 10 cm^2 Petri dish

without medium; the cell suspension was placed inside of lumen of the vessel (seeded) and incubated for 2.5 h at 37ºC, 5% CO_2. As a next, endothelial medium was added and the cells were cultivated further on for 2 and 7 days.

2.4.3 Histochemistry

In order to use the atherosclerotic plaque material for histological or immunohistological staining, fresh tissues have been fixed for 24 h in 4% formaldehyde, followed by dehydration, embedding in paraffin, and sectioning in 3 µm thin slides. As an additional step in case of calcified tissue (advanced stage atherosclerosis plaque) the specimens were incubated in an aqueous solution saturated with EDTA for up to 7 days, dependent upon the extent of calcification. Prior the staining procedure all sectioned tissue slides were deparaffinised by incubation in xylene for 20 min, followed by isopropanol for 20 min, 99.8% ethanol for 10 min, 70% ethanol for 10 min, and distilled water for 10 min. All the materials used for histochemistry were purchased from Apotheke MRI.

2.4.3.1 Haematoxylin – Eosin staining

Following deparaffinization, nuclear staining was performed by incubating the slides with Mayer's haematoxylin for 5 min at RT. The slides were then washed in tap water for 10 min, incubated with acidified eosin for 5 min, rinsed briefly in tap water and in increasing concentrations of alcohol (70% ethanol, 96% ethanol, 100% isopropanol) followed by xylene. The samples were mounted in hydrophobic mounting medium and covered with glass cover slides.

2.4.3.2 Elastica van Giesson staining

The Elastica van Gieson staining is a combination of Weigert's haematoxylin, van Gieson's picrofuchsin, and the resorcin-fuchsin solution that allows differential analysis of nuclei, connective tissue, muscle and elastic fibers.

Procedure: Weigert's haematoxylin was prepared fresh by mixing Weigert's solution A and Weigert's solution B (ratio 1:1). The slides, previously dried at 56ºC and deparaffinized, were incubated in Weigert's haematoxylin for 10 min and washed in warm tap water for another 10 min. Next step consisted of staining of the cytoplasm by incubation with van Gieson solution for 3 min. This step was followed by washing in distilled water and increasing concentrations of alcohol (70% ethanol, 96% ethanol, isopropanol) followed by xylene. The samples mounted in hydrophobic mounting medium and covered with glass cover slides.

2.4.4 Immunohistochemistry

All stainings were performed on thin slices of tissue fixed with formaldehyde and embedded in paraffin (FFPE tissues). Depending on the target antigen, an antigen epitope retrieval step was employed (see *Table 8* and *9*).

Procedure: The tissue was sectioned into slices of 3 µm, mounted on glass slides, briefly dried at 56ºC, and deparaffinized. The antigen-retrieval methods used were heat induced epitope retrieval (HIER) or proteolytic enzyme induced epitope retrieval (PIER). HIER consists of incubating the sectioned slides at 100ºC under pressure for 7 min in 10 mM aqueous sodium citrate solution (Sigma-Aldrich), at pH 6.0. PIER consists of 20 min incubation with a 5 µg/ml proteinkinase (Sigma-Aldrich). After epitope retrieval, the protocol followed the manufacturer's instructions described above.

Table 8. *Antibodies used for characterization of the atherosclerotic plaque.*

Name	Clone	Isotype	Brand &Cat. Nr.	Dilution	Detection System	Antigen Retrieval Method
Monoclonal Mouse Anti-Human CD31, Endothelial Cell	JC70A	IgG1	DAKO (M0823)	1:50	LSAB	HIER
Monoclonal Mouse Anti-Human Muscle Actin	HHF35	IgG1	DAKO (M0635)	1:200	APAAP	HIER
Monoclonal Mouse Anti-Human Von Willebrand Factor	F8/86	IgG1	DAKO (M0616)	1:400	APAAP	PIER
Monoclonal Mouse Anti-Human CD68	Kb1	IgG1	DAKO(M0184)	1:2000	LSAB	HIER
Monoclonal Mouse Anti-Human CD45, leucocyte Common Antigen	2B11+ PD7/26	IgG1	DAKO(M0701)	1:200	LSAB	HIER
Mouse IgG1 Negative Control	-	-	DAKO (X0931)	1:50; 1:200; 1:400	APAAP and LSAB	PIER and PIER

Table 9. *Antibodies used for detection of epigenetic changes at histone level.*

Name	Reacts with	Isotype	Brand & Cat. Nr.	Dilution	Detection System	Antigen Retrieval Method
Di-Methyl-Histone H3 (Lys4)(C64G9) Rabbit mAb	Human, Mouse , Rat, Monkey	Rabbit IgG	Cell Signaling (#9725)	1:3000	LSAB	PIER
Di-Methyl Histone H3(Lys9) Antibody	Human, Mouse, Rat, Monkey	Rabbit IgG	Cell Signaling (#9753)	1:200	LSAB	PIER
Negative Control Rabbit Immunoglobulin Fraction (Normal)	-	Rabbit	DAKO (X0903)	1:200 1:3000	LSAB	PIER

2.4.5 Microscopy and digitalization

Digital micrographs were captured with a Zeiss AxioCam MRc digital camera attached to a Zeiss Axio Observer Z1 microscope (Carl Zeiss Microscopy GmbH, Jena, Germany), equipped for light and fluorescence microscopy. The microscope was controlled by the AxioVision software, version 4.8.2 (Carl Zeiss Microscopy GmbH).

2.5 Gene expression analysis at mRNA level using PCR

2.5.1 RNA extraction from cells

The RNA extraction method used in the present work is based on the reversible binding properties of silica-based columns and RNA. Cells are first lysed and RNases are inactivated. The cell lysates are then applied onto the columns to which total RNA binds, while cellular debris and DNA is digested with the peqGOLD DNase I enzyme and other contaminants are effectively washed out.

Procedure: RNA isolation was performed with peqGOLD Total RNA Kit purchased from PEQLAB GmbH (Erlangen, Germany). Cells were lysed with 400 µl lysis buffer and scraped off the 10 cm^2 culture dishes. Following steps were then performed according to manufacturer's instructions. RNA was finally eluted in RNase-free water, the concentration and the quality measured with a Nanodrop 2000c spectrophotometer (PEQLAB GmbH), and stored at -80ºC until further use.

2.5.2 RNA extraction from FFPE tissue samples

RNA was extracted from FFPE tissue with the High Pure FFPE RNA Micro Kit (Roche Applied Science, Mannheim, Germany). Two tissue slices, each of 10 µm thickness, were placed into a 1.5 ml reaction tube, deparaffinized by adding 800 µl xylene, vortexed, and incubated at RT for 5 min. The xylene was then removed by 400 µl ethanol 98.6%, vortexed and centrifuged at 12000 rpm for 4 min at RT. The supernatant was carefully removed and 1000 µl ethanol 98.6% were added again and mixed through vortexing followed by centrifugation at 12000 rpm for 4 min at RT. The supernatant was carefully removed and extraction procedure was continued according to manufacturer's instructions. RNA was eluted in RNase-free water, quantified spectrophotometrically, and stored at -80ºC until further use.

2.5.3 cDNA synthesis

The cDNA synthesis was performed with the RevertAid First Strand cDNA Synthesis Kit (Fermentas GmbH, St. Leon-Rot, Germany). The kit is using the M-MuLV Reverse Transcriptase that is active in a range between 42-50ºC and oligo $(dT)_{18}$ primer.

Procedure: For each reaction up to 1 µg RNA in a total volume of 11 µl was used. To each RNA sample 1 µl oligo $(dT)_{18}$ primer was added, gently mixed, briefly centrifuged, and incubated at 65ºC for 5 min. The sample was then chilled on ice for at least 2 min; meanwhile a working mix was prepared (4 µl of 5x reaction buffer, 2 µl of 10 mM dNTPs mix, 1 µl RNase inhibitor, and 1 µl M-MuLV Reverse transcriptase). The mix was added on the sample and incubated for 1 h at 43ºC followed by 5 min at 70ºC. At the end of the reaction the samples were diluted to a final concentration of 10 ng/µl. For real time PCR, 20 ng cDNA were used for each reaction.

2.5.4 SYBR Green-based real-time PCR

In conventional PCR, the amplified product, also named amplicon, is detected by an end-point analysis, running DNA on an agarose gel after the reaction is finished. In contrast, real-time PCR allows the accumulation of amplified product to be detected and measured as the reaction progresses in “real time” after each cycle. For this purpose, data are collected throughout the PCR process rather than at the end of the PCR. Real-time detection of PCR products is possible by including in the reaction a fluorescent molecule that reports an increase in the amount of DNA with a proportional increase in fluorescent signal. For this purpose, fluorescent DNA-binding dyes or labeled sequence specific primers or probes are employed. Specialized thermal cycling devices equipped with fluorescence detection modules are used to monitor the fluorescence as amplification occurs. The measured fluorescence reflects the amount of amplified product in each cycle. The biggest advantage of real-time PCR over conventional PCR is that it allows determining the starting template copy number with high sensitivity and accuracy. The quantitative RT-PCR reaction in this work was performed by two methods: the DNA-binding dye SYBR Green I or TaqMan hydrolysis probes.

SYBR Green I dye is a highly specific, double-stranded DNA (dsDNA) binding dye used to detect PCR product as it accumulates during PCR cycles. The melt-curve analysis should be used each time to distinguish specific PCR products from the nonspecific ones. The major drawback of DNA-binding dyes is that it binds non-specifically to every dsDNA in the reaction tube. A melt-curve is generated by increasing the temperature in small increments and monitoring the fluorescent signal at each step. As the dsDNA in the reaction denatures or melts, the fluorescence decreases. A characteristic peak at the amplicon’s

melting temperature (Tm, the temperature at which 50% of the base pairs of a DNA duplex are separated) distinguishes it from other products such as primer-dimers, which melt at different temperatures than the desired amplicon; two different peaks of the same samples with two different melting points thus mean two different amplicons, one of them unspecific (*Figure 23*). If the product is transferred onto an electrophoresis gel, two different bands are observed, corresponding to the two peaks in the melt-curve graph. In general to ensure reliable results, all primers have to be optimized and proved by the melting curve and gel electrophoresis.

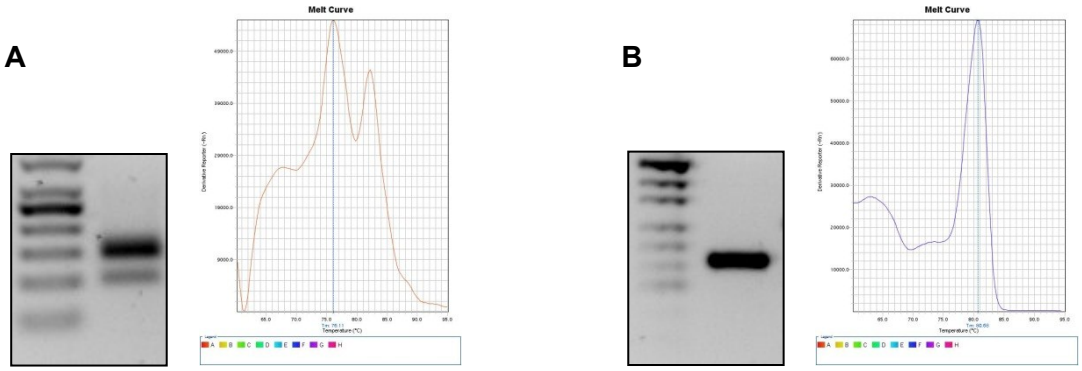

Figure 23. *Examples of melt curves. (A) Melt curve presents two peaks corresponding with the electrophorese gel with two bands; (B) one melt peak corresponds with one band on the electrophorese gel.*

Data analysis of the quantitative PCR (qPCR) consists in comparing the amplification curve in the exponential phase of different targets with the amplification curve of a housekeeping gene, which serves as internal control (*Figure 24*). The calculation method used in the present work was ΔCT using a reference gene, which is widely used and easy to understand. To compare target gene expression in two different samples, one was set as control-sample (e.g. the non-treated cells, or healthy tissue) and the following formula was used:

$$\text{Relative expression} = 2^{CT\,(GAPDH) - CT\,(target\ gene)}$$

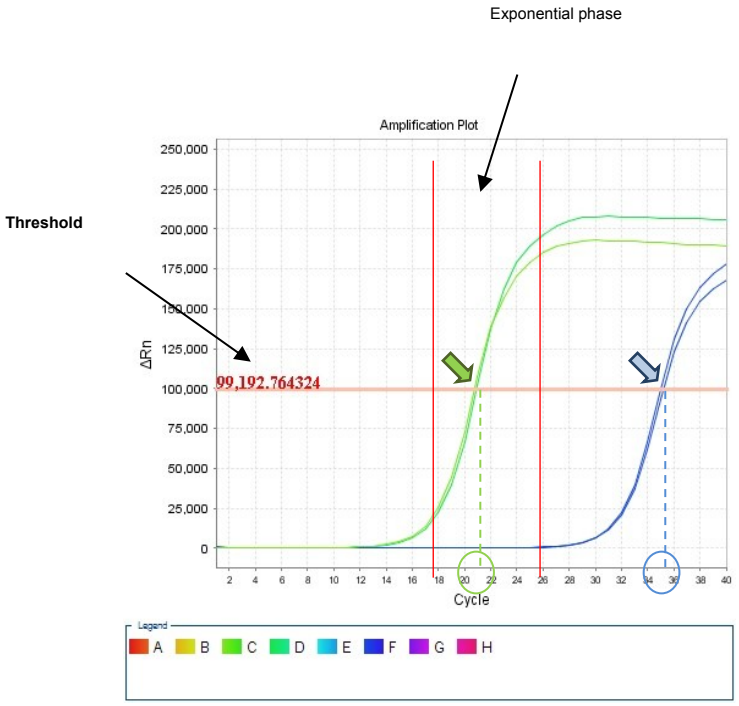

Figure 24. *Amplification plot for two different target genes; green and blue arrows indicate the CT value in the exponential phase for both targets.*

Procedure: Transcript levels of pluripotency, endothelial, and angiogenic related genes were determined using the ready to use polymerase Sybr Fast qPCR Master Mix (PEQLAB GmbH). The cDNA template was equivalent to 20 ng of total RNA for each PCR reaction. Measurements were performed in triplicates; a non-template blank served as a negative control. Amplification curves and gene expression were normalized to the housekeeping gene GAPDH. Primers for the genes *OCT4A*, *NANOG*, *KLF4*, *CMYC*, *VEGF*, *PDGF*, *VEGFR-2*, *ANG-1*, and *ANG-2* were designed by Primer3 software (version 0.4.0, Whitehead Institute for Biomedical Research, Cambridge. MA, USA), purchased from MWG Operon Eurofins (Ebersberg, Germany) and are summarized in *Table 10*. Primers for the genes *SOX2*, *VCAM-1*, *Factor VIII*, and *PECAM-1* were purchased from Qiagen GmbH (Hilden, Germany) as ready-to-use primer mix as shown in the *Table 10*. PCR amplicons were confirmed to be specific by size (gel electrophoresis) and melt-curve analysis. The PCR program was set as follows: denaturation for 5 min at 95°C, amplification for 40 cycles. Each cycle comprised of 10 seconds at 95°C, 30 seconds at 60°C, and 10 seconds at 72°C. The device used was StepOnePlus (Life Technologies GmbH, Darmstadt, Germany).

Table 10. *Primers used for the real time PCR.*

Gene	Sequence forward (5'->3')	Sequence reverse (5'->3')	Amplicon (bp)	Gene bank Locus
OCT4a	TGGAGAAGGAGAAGCTGGAGCAAAA	TATTCACCCAAACGACCATCTGCC	185	NM_002701
NANOG	ACCTTGGCTGCCGTCTCTGGCT	GCAAAGCCTCCCAATCCCAAACA	150	NM_024865
KLF4	AGTGCTGAGCAGCAGGGACTGT	GGTAATGGAGCGGCGGGACTTG	128	NM_004235
C-MYC	TGCGGTCACACCCTTCTCCCTT	TGAAGGTCTCGTCGTCCGGGTC	149	NM_002467
VEGF	ATGAGGACACCGGCTCTGACCA	AGGCTCCTGAATCTTCCAGGCA	126	NM_001025366
VEGFR-2	AGTGTGGAGGACTTCCAGGGAG	AGCTGACACATTTGCCGCTTGG	120	NM_002253
PDGF	TCAGGTGGGTTAGAGATGGAGT	GAAAGGAACCAGAGGAAGAGGT	126	NM_002607
ANG-1	GAGGCACGGAAGGAGTGTGCTG	CGGCGCTGATTGCTGCACCCTA	101	NM_139290
ANG-2	AAAAGCTGACACAGCCCTCCCA	ACTGCTGTGTTCTCTCCAGGCA	90	NM_001147
GapdH	QuiantiTect Primer Assay Hs_GAPDH_2SG		119	NM_002046
VCAM-1	QuantiTect Primer Assay Hs_VCAM1_1_SG		106	NM_001078
Factor VIII	QuantiTect Primer Assay Hs_F8_1_SG		120	NM_000132
PECAM-1	QuantiTect Primer Assay Hs_PCAM1_1_SG		144	NM_000442
SOX2	QuantiTect Primer Assay Hs_SOX2_1_SG		64	NM_003106
DNMT1	QuantiTect Primer Assay Hs_DNMT1_1_SG		93	NM_001130823
DNMT3A	QuantiTect Primer Assay Hs_DNMT3A_1_SG		144	NM_022552
DNMT3B	QuantiTect Primer Assay Hs_DNMT3B_1_SG		128	NM_001207055
MLL1	QuantiTect Primer Assay Hs_C17orf49_1_SG		99	NM_001142798
SETD1A	QuantiTect Primer Assay Hs_KIAA0339_1_SG		74	NM_014712
SETD1B	QuantiTect Primer Assay Hs_SETD1B_1_SG		110	NM_001145415
SUV39H1	QuantiTect Primer Assay Hs_ SUV39H1_1_SG		108	NM_003173
EHMT2	QuantiTect Primer Assay Hs_ EHMT2_1_SG		97	NM_006709

2.6 Epigenetic analysis of methylated DNA using PCR

In the present work, DNA methylation status of three repetitive elements (LINE1, Satα, and Alu1) was analyzed by MethyLight, TaqMan-based real-time PCR assay. DNA isolated from cells was bisulfite converted, and then the amplification of LINE1, Satα, and Alu1 was performed by real time PCR as described previously [214], using the methylated Alu1 sequence for normalization and the set of primers and probes from *Table 11*.

Table 11. *Sequences of the primers for Methylight assay according to Weisenberger et al. [214].*

Reaction ID	Sequence forward (5' to 3')	Sequence reverse (5' to 3')	Probe (5' to 3'[a])	Amplicon (bp)	Gene bank Locus
LINE- M1	GGACGTATTTGGAAAA	AATCTCGCGATACG	FAM-	80	X52235

	TCGGG	CCGTT	TCGAATATTGCGTTT TCGGATCGGTTT-BHQ1 BHQ1 = Black Hole Quencher 1		
Alu1	GGTTAGGTATAGTGGT TTATATTTGTAATTTTA GTA	ATTAACTAAACTAAT CTTAAACTCCTAACC TCA	VIC-CCTACCTTAACCTCC C-MGB MGB = Minor Groove Binding	97	Consens us seq. [214]
Satα-M1	TGATGGAGTATTTTTA AAATATACGTTTTGTA GT	AATTCTAAAAATATT CCCTTCAATTACGTA A	SybrGreen I chemistry	121	M38468

2.6.1 DNA isolation from cells

PeqGOLD Tissue DNA Mini Kit (PEQLAB GmbH), QIAamp DNA FFPE Tissue Kit (Qiagen GmbH), and QIAamp DNA Blood Mini Kit (Qiagen GmbH,) were used to extract the genomic DNA from cells, from FFPE tissue, and from serum, respectively. These kits take advantage of the reversible binding properties of a silica-based material, combined with the speed of mini-column spin technology. The buffers provided with the columns allow genomic DNA to bind to the matrix. Samples were first homogenized, lysed under denaturing conditions, and then applied to the DNA Columns, where the DNA is effectively bound to the silica membrane. Cellular debris, proteins, and other contaminants were washed away by specific buffers. The high quality DNA was finally eluted in Elution Buffer.

Procedure: DNA from cultured cells was isolated with PeqGOLD Tissue DNA Mini Kit. The cells were lysed with 400 µl lysis buffer and scraped from the 10 cm^2 dishes. The lysate was placed in 1.5 ml reaction tubes and the procedure was followed according to manufacturer's instructions. The final concentration of the isolated genomic DNA was measured with a Nanodrop 2000c spectrophotometer (PEQLAB GmbH) and the DNA solution was stored at -20ºC until bisulfite conversion was performed.

2.6.2 DNA isolation from FFPE tissue and serum

DNA was isolated with the QIAamp DNA FFPE Tissue Kit. First, 4 slices of 10 µm thickness were cut from the carotid tissue samples and placed in a 1.5 ml tubes. The protocol was followed as described in the manufacturer's instructions. DNA concentration was measured with the spectrophotometer and stored at -20ºC until bisulfite conversion was performed.

Fresh blood was collected, centrifuged and serum was stored at -80ºC until DNA was further used. DNA was isolated with the QIAamp DNA Blood Mini Kit, according to manufacturer's instructions using 200 µl of serum for each extraction procedure.

2.6.3 Bisulfite conversion

Incubation of the target DNA with sodium bisulfite results in conversion of unmethylated cytosine residues into uracil, leaving the methylated cytosines unchanged. Therefore, bisulfite treatment leads to changes in DNA sequence for methylated in contrast to unmethylated DNA as shown in *Table 12*.

Table 12. *Example of the effect of bisulfite conversion on unmethylated cytosines.*

	Original sequence	After bisulfite treatment
Unmethylated DNA	T-**C**G-T-**C**G-A-**C**G-T	T-**U**G-T-**U**G-A-**U**G-T
Methylated DNA	T-**C**G-T-**C**G-A-**C**G-T	T-**C**G-T-**C**G-A-**C**G-T

The critical step for correct determination of a methylation pattern is the complete conversion of unmethylated cytosines. For this purpose, commercially available kits were used. Sodium bisulfite conversion of DNA from cells, FFPE material, or serum was in all cases performed by using EpiTect Bisulfite Kit (48) (Qiagen GmbH).

The EpiTect Bisulfite procedure comprises of the following steps: bisulfite mediated conversion of unmethylated cytosines; binding of the converted single-stranded DNA to the membrane of an EpiTect spin column; desulfonation of membrane-bound DNA; removal of desulfonation agent; elution of the converted DNA from the spin column. The eluted DNA was used for the analysis of DNA methylation by MethyLight assay, a Taqman based real time PCR.

Procedure: DNA was diluted to 500 ng DNA in 20 µl of elution buffer for each bisulfite conversion reaction. According to the manufacturer, bisulfite mix was added to the DNA solution. To this mixture, DNA protect buffer was added, well mixed, and placed in the thermal cycler with a program shown in *Table 13*.

Table 13. *Thermal cycler conditions for bisulfite conversion reaction.*

Step	Temperature	Time
Denaturation	95°C	5 min
Incubation	60°C	25 min
Denaturation	95°C	5 min

Incubation	60°C	85 min (1 h 25 min)
Denaturation	95°C	5 min
Incubation	60°C	175 min (2 h 55 min)
Hold	20°C	Indefinite

After bisulfite conversion was completed, the tubes were briefly centrifuged, and the content transferred into a new 1.5 ml reaction tube. The next steps were performed according to instructions provided with the kit. Finally, bisulfite converted DNA was diluted to 10 ng/µl and aliquots were stored at -80ºC until the Methylight assay was performed. For each PCR reaction 20 ng bisulfite converted DNA was used.

2.6.4 TaqMan-based real time PCR

TaqMan procedure specifically detects the target gene sequence, so nonspecific products do not affect the accuracy of quantification this being the main advantage over DNA binding dyes. TaqMan assays employ a sequence-specific, fluorescently labeled oligonucleotide probe called the TaqMan probe, in addition to the sequence-specific primers. The probe contains a fluorescent reporter at the 5' end and a quencher at the 3' end. When intact, the fluorescence of the reporter is quenched due to its proximity to the quencher. During the combined annealing/extension step of the amplification reaction, the probe hybridizes to the target and the dsDNA-specific 5'→3' exonuclease activity of nuclease (thermostable polymerases) cleaves off the reporter. As a result, the reporter is separated from the quencher, and the resulting fluorescence signal is proportional to the amount of amplified product in the sample.

Procedure: For the determination of global DNA methylation a TaqMan-based methylation specific real-time PCR (Methylight) system was used. Methylation of LINE1 (Metabion International AG, Germany) and Satα (MWG Operon Eurofins) was determined using the TaqMan Universal PCR Master Mix, No Amp Erase UNG (Roche). As reference for input of bisulfite converted DNA a methylation independent ALU1 (Metabion International AG, Martinsried, Germany) TaqMan system was used. For each real time PCR amplification the template was equivalent to 10 ng of bisulfite converted DNA and measurements were performed in triplicates. Fully methylated bisulfite converted DNA from the EpiTect PCR Control DNA Set (Qiagen GmbH) was used as 100% methylated control. Primers were optimized for StepOnePlus thermocycler. Quantification was normalized to the ALU1 gene within the log-linear phase of the amplification curve obtained for each probe/primer set using the ΔCT method using a reference gene.

2.7 Expression analysis on protein level using Western blot

Western Blot, also known as immunoblotting or protein blotting, is a method used to detect specific proteins in a complex mixture extracted from cells or tissue. The Western blotting procedure relies upon three key elements (*Figure 25*): 1. sample preparation and separation of the protein mixture by size using gel electrophoresis; 2. transfer of separated proteins to a membrane; and 3. detection of a target protein by appropriate antibodies. Once detected, the target protein is visualized as a band on a blotting membrane, X-Ray film, or an imaging system.

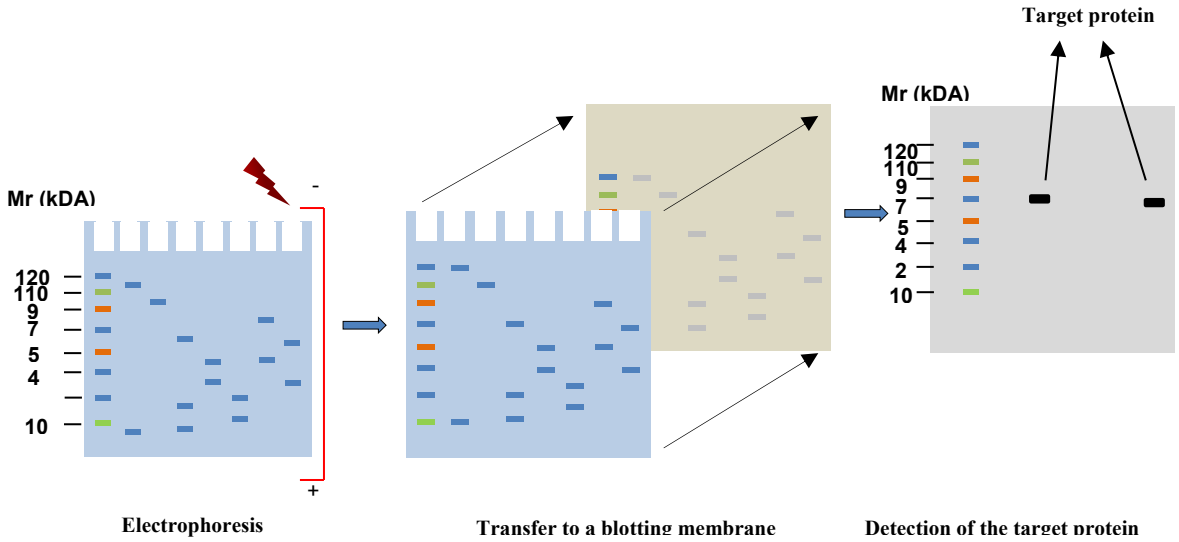

Figure 25. *Schematic overview of the Western Blot method.*

2.7.1 Sample preparation from cells

All chemical substances for this assay were purchased from Sigma-Aldrich, if not otherwise mentioned. Protein isolation from cells was made with RIPA (Radio Immuno Precipitation Assay) buffer. The content of the buffer was: 50 mM TRIS-HCl (Merk) (pH=7.5); 150 mM NaCl; 1% TRITON X-100; 0.1% SDS (w/v); 0.5% Natriumdeoxdesoxycholat (w/v) in distilled water. For optimal reproducibility all steps were carried out on ice. For protein isolation from the cells, they were cultivated in 10 cm^2 dish ($0.5x10^6$ cells). The procedure was as follows: medium was removed, cells were washed once with sterile PBS (PAA Laboratories GmbH), 1 ml of RIPA buffer was added, and incubated 10 min at -20˚C. The cell debris was collected with a cell scraper and the lysate was transferred into a 1.5 ml reaction tube, followed by centrifugation for 20 min at +4°C. After centrifugation the supernatant containing the proteins was collected in a new tube, the protein concentration was measured; aliquots were made and stored at -20˚C until further use.

2.7.2 Sample preparation from tissue

Histone isolation from fresh carotid tissue was performed with EpiSeeker Histone Extraction kit (Abcam, Cambridge, UK), according to its instructions. Briefly, samples were homogenized with a pre-lysis buffer, and centrifuged at +4°C at 10000 rpm 1 min. The supernatant was removed and the tissue pellet was resuspended in lysis buffer, incubated on ice for 30 min, followed by a centrifugation step by 12000 rpm at +4°C for 5 min. The supernatant was collected in a new tube and supplemented with Balance-DTT buffer. The protein concentration was measured with BCA assay and stored at -20˚C until further use.

Samples were diluted in RIPA buffer to a final concentration of 1 µg/µl. From each sample 20 µl were added into 1.5 ml reaction tubes, together with 5 µl Laemmli buffer 5x (6 ml 1M TRIS-HCl pH=6,8; 10 ml 99% Glycerol; 200 µl 500 mM EDTA; 2 g SDS; 10 mg Bromphenol Blue). Samples were heated for 5 min at 99ºC for denaturation of proteins and incubated on ice.

2.7.3 Protein separation by polyacrylamide gel electrophoresis (PAGE)

The electrophoresis gel is composed of 2 gel types with a different concentration in acrylamide: the stacking gel and the separation gel (*Figure 26*).

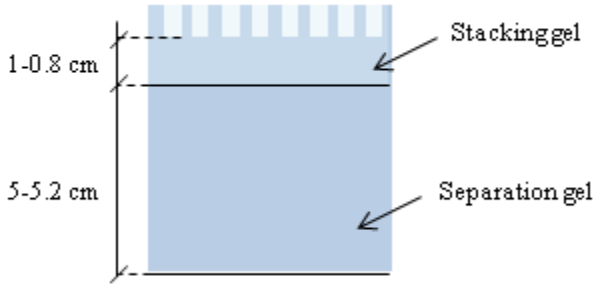

Figure 26. *Arrangement of the electrophoresis gel.*

Depending on the target protein, different acrylamide concentrations for the separation gel were used as described in *Table 14*. For the stacking gel the composition is described in *Table 15*.

Table 14. *Separation gel recipes.*

Solution	Volume (ml) for 1 gel		
	15% used for H3K4me2 and H3K9me2	10% used for OCT4A	6% used for VCAM-1 and VEGFR-2
TRIS-HCl 1.5M(pH=6.8)	2.5	2.5	2.5
Distilled water	2.3	4	5.3

Acrylamide (29:1)	5	3.3	2
SDS10%	0.1	0.1	0.1
Ammonium persulphate (APS)10%	0.1	0.1	0.1
N,N,N′,N′-Tetramethylethylenediamine (TEMED)	0.005	0.005	0.005

***Table 15**. Stacking gel recipe.*

Solution	Volume (ml) for 4ml (1 gel)
TRIS-HCl 0.5M(pH=6.8)	1.25
Distilled water	2.7
Acrylamide (29:1)	0.7
SDS 10%	0.05
APS 10%	0.05
TEMED	0.005

2.7.4 Protein transfer to PVDF membrane

After the electrophoresis was finished, the procedure was continued by protein transfer onto a PVDF membrane using semi-dry system. The scheme of this procedure is shown in *Figure 27*.

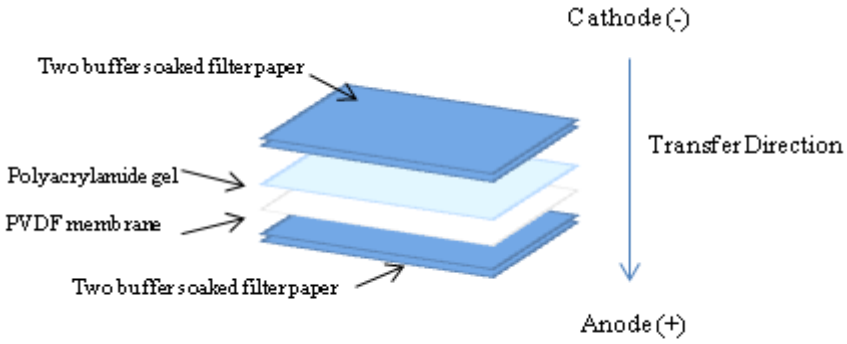

***Figure 27.** Assembling of the transfer sandwich.*

An aqueous solution of the transfer buffer was prepared by adding following substances/solutions to 900 ml distilled water (B. Braun Melsungen AG): 3.03 g Trizma base, 14.4 g glycine, and 100 ml methanol (Merck). The filter papers and acrylamide gel were soaked in transfer buffer; the PVDF membrane was shortly activated in methanol and incubated in transfer buffer for 30 min. The assembling of the system was made as described in *Figure 27*. The semi-dry transfer device was set to 10V for 30 min followed by other 5 min at 15V.

2.7.5 Protein detection

The PVDF membrane containing the proteins was then incubated in blocking buffer (5% non-fat skimmed milk powder (Biomol GmbH, Hamburg, Germany) in TBS-T) for 1 h at RT on a shaker. TBS-T was prepared from 900 ml distilled water to which following solution were added: 100 ml TBS buffer, and 1 ml Tween 20. TBS buffer was prepared by adding 24.2 g Trizma base and 80 g NaCl (Merck) to 1000 ml distilled water and adjusting the pH value to 7.6 with HCl 2N (Apotheke MRI). Each antibody was diluted in a blocking buffer and incubated over night at +4˚C as described in *Table 16*, *17* and *18.*

The next day the membrane was washed in TBS-T solution for 30 min to remove the excess of the first antibody. The secondary antibody solution was made in the same blocking buffer and added to the PVDF membrane, which was then incubated for 1 h at RT.

Table 16. *Antibodies used for characterization of the angiogenesis in adMSCs.*

Name	Reacts with	Clone/Made in	Brand &Cat. Nr.	Dilution	Size (kDa)
Mouse anti hVACM-1(CD106)	Human	Mouse IgG	R&D Systems	1:100	110
Flk-1 antibody(VEGFR-2)	Human	Mouse IgG_1	R&D Systems	1:100	170
Anti-GAPDH antibody [6C5]	Rat, Rabbit, Chicken, Human,	6C5	Abcam (ab8245)	1:1000	36
Peroxidase-Labeled Affinity Purified Antibody to Mouse IgG (H+L)(Human Adsorbed)	Mouse	Goat	KLP (074-1806)	1:5000	-
Peroxidase-Labeled Affinity Purified Antibody to Rabbit IgG (H+L)(Human Adsorbed)	Rabbit	Goat	KLP (074-1516)	1:5000	-

Table 17. *Antibodies used for detection of pluripotency markers.*

Name	Reacts with	Clone/Made in	Brand &Cat. Nr.	Dilution	Size (kDa)
OCT4A(C30A3) Rabbit mAb	Human, Mouse	C30A3	Cell Signaling (#2840)	1:500	48
Rabbit polyclonal to Nanog	Human, Mouse	rabbit	Abcam (ab21624)	1:500 - 1:50	38
Anti-GAPDH antibody [6C5]	Rat, Rabbit, Chicken, Human,	6C5	Abcam (ab8245)	1:1000	36
Peroxidase-Labeled Affinity Purified Antibody to Rabbit IgG (H+L)(Human Adsorbed)	Rabbit	Goat	KLP (074-1516)	1:5000	-

Table 18. *Antibodies used for detection of di-methylation at K4 and K9 sites of histone H3.*

Name	Reacts with	Clone/Made in	Brand & Cat. Nr.	Dilution	Size(kDa)

Di-Methyl-Histone H3 (Lys4)(C64G9) Rabbit mAb	Human, Mouse , Rat, Monkey	Rabbit IgG	Cell Signaling (#9725)	1:3000	17
Di-Methyl Histone H3(Lys9) Antibody	Human, Mouse, Rat, Monkey	Rabbit IgG	Cell Signaling (#9753)	1:200	17
Peroxidase-Labeled Affinity Purified Antibody to Rabbit IgG (H+L)(Human Adsorbed)	Rabbit	Goat	KLP (074-1516)	1:5000	-

The PVDF membrane was treated for 30 min with TBS-T then submersed in a working solution (Solution A/Solution B, ratio 1/1) of SuperSignal® West Pico Chemiluminescent Substrate (Thermo Scientific, Bonn, Germany) for 5 min. The excess reagent was drained and the blot was covered with clear plastic wrap. The membrane was placed in a film cassette with the protein side facing up. In the dark, a FUJI Medical X-Ray Film (FUJIFILM Europe GmbH, Düsseldorf, Germany) was placed on top of the membrane and various exposure times were used to achieve optimal results. The film was then developed with Medical Film Processor (Konica Minolta model, SRX-101A, Konica Minolta Medical and Graphic Imaging Europe GmbH, Munich, Germany)

2.7.6 Protein quantification

In order to quantify the amount of each targeted protein, developed films were digitized using a color image scanner (HP Scanjet 3800). The bands on the films with the same exposure time were compared to each other after a previous normalization to a housekeeping gene for GAPDH. The intensity quantification was made with ImageJ software (National Institutes of Health, Bethesda, USA).

2.8 Statistical analysis

Data are presented as mean ± SEM. Statistical analysis was performed with GraphPad Prism (GraphPad Software Inc, San Diego, USA). For single comparison Mann-Whitney U test was used. The significance of differences with more than two samples was evaluated using Kruskal-Wallis test, followed by Dunns post-test for multiple comparisons: * for $p<0.05$; ** for $p<0.01$; *** for $p<0.001$ were considered statistically significant.

3 RESULTS

3.1 Epigenetic changes in vascular disease

3.1.1 Histological characterization of specimens

The stage of atherosclerosis (AS) was classified as described in the section Materials and Methods. Tissue specimens were divided into the following groups: control (healthy carotid artery - *Figure 28*), early stage of AS (II-III, AHA classification - *Figure 29*), and advanced stage of AS (V-VII, AHA classification - *Figure 30*).

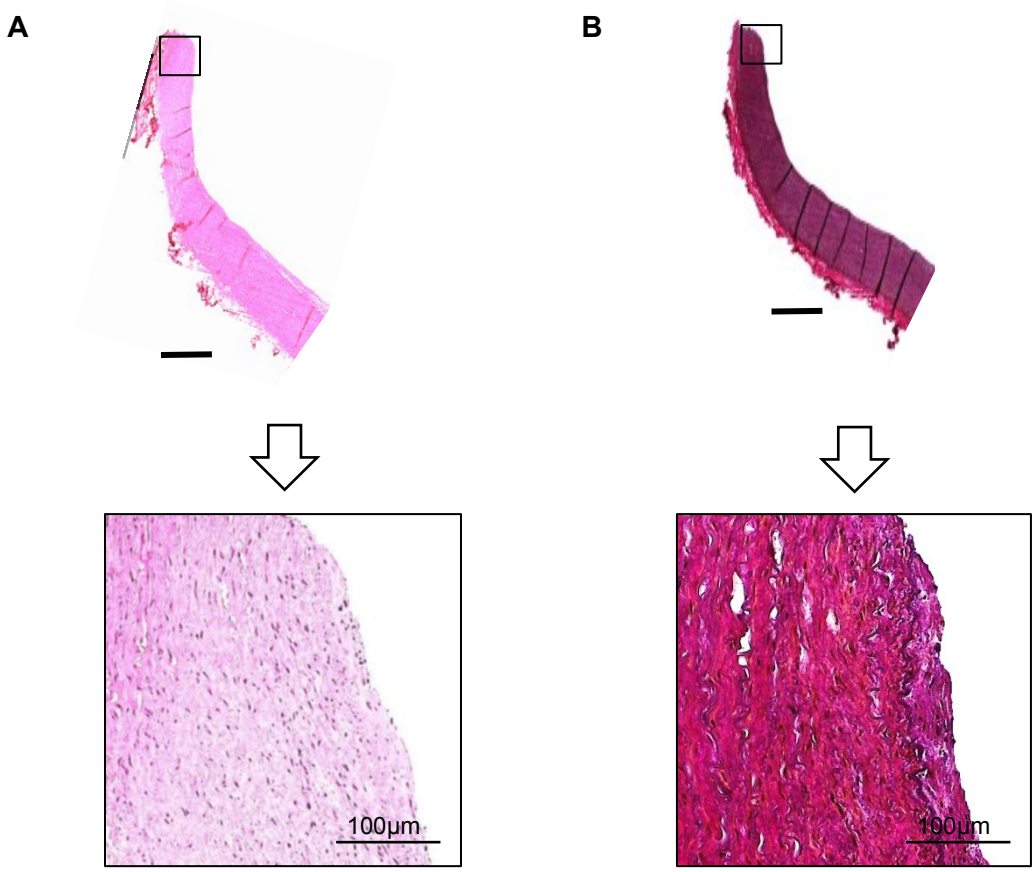

Figure 28. *Example of a control vessel. (A) H&E representative staining and (B) elastica von Gieson representative staining. Bar on the overview pictures represents 1 mm.*

The early stage of AS type II and III was recognized by markedly enlarged intima compared with control vessels, with scattered yellow-colored fatty streaks, enhanced intracellular lipid accumulation, and increased number of macrophages and macrophage-derived foam cells. Furthermore, an increased amount of collagen fibers was observed (*Figure 29*).

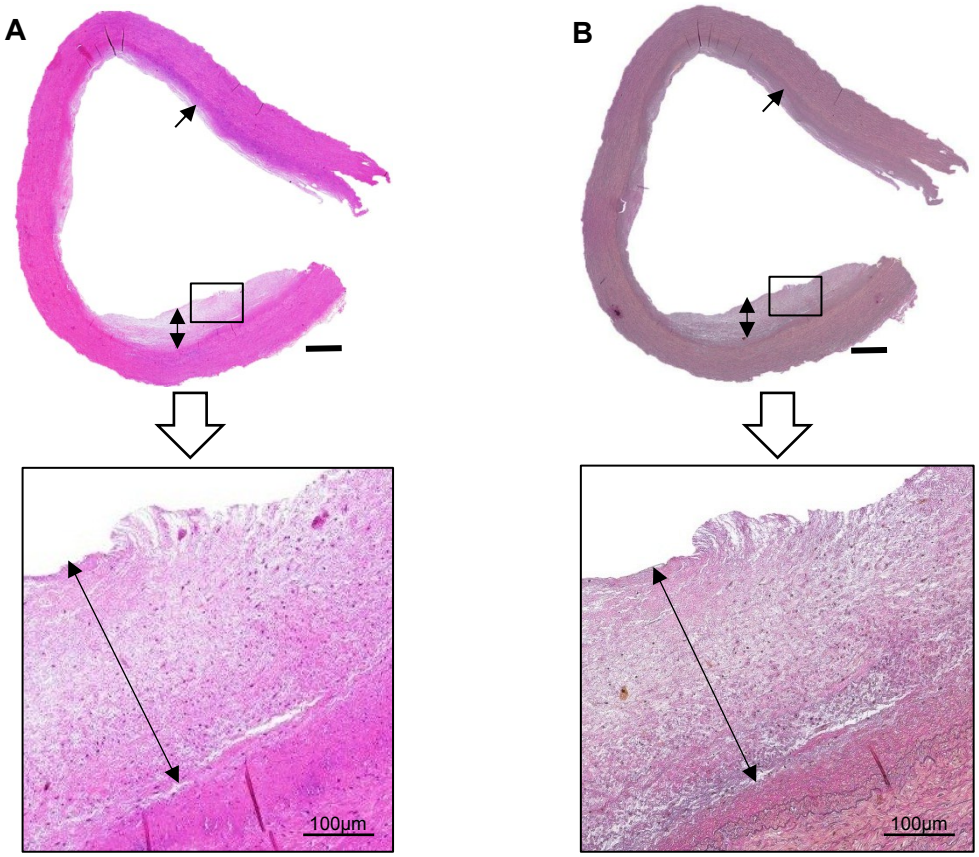

Figure 29. *Example of histopathology of the group with early stage atherosclerosis showing initial stage of atherosclerosis with enlarged fibrocellular intimal thickness. (A) H&E staining, (B) Elastica von Gieson staining. Bar on the overview pictures represents 1 mm.*

Type V lesion was characterized by massive aggregates of extracellular lipids forming necrotic or lipid core with a fibrous cap that was either thick (stable plaque) or thin (<200 µm, unstable plaque) [215]. Moreover, increased inflammation and a higher amount of leukocytes, macrophages, and thrombotic deposits and/or marked hemorrhage were visible. Type VII lesion had calcium deposits that partially replaced the Type VI lipid/necrotic core. (*Figure 30* and *Figure 31*)

In this manner 20 early and 20 advanced stage lesions were chosen, in each case early and advanced stages of atherosclerosis from the same patient and same atherosclerotic plaque.

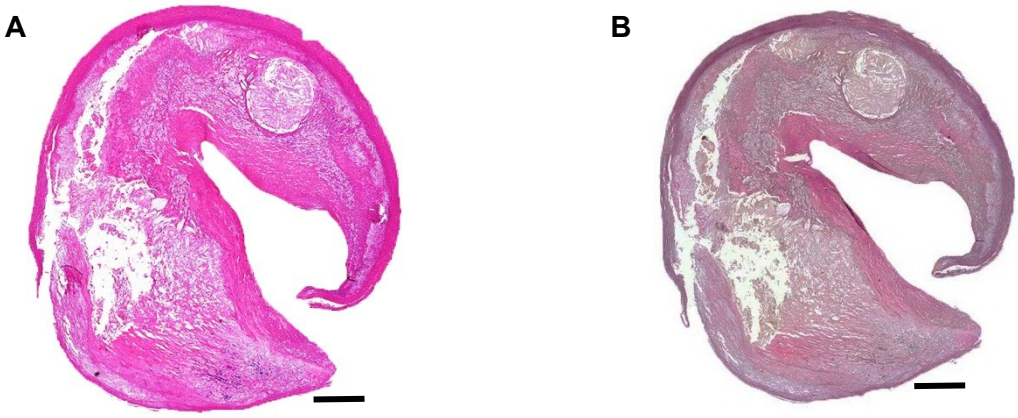

Figure 30. *Example images of advanced stage of atherosclerosis. (A) H&E staining, (B) Elastica von Gieson staining. Bar represents 1 mm.*

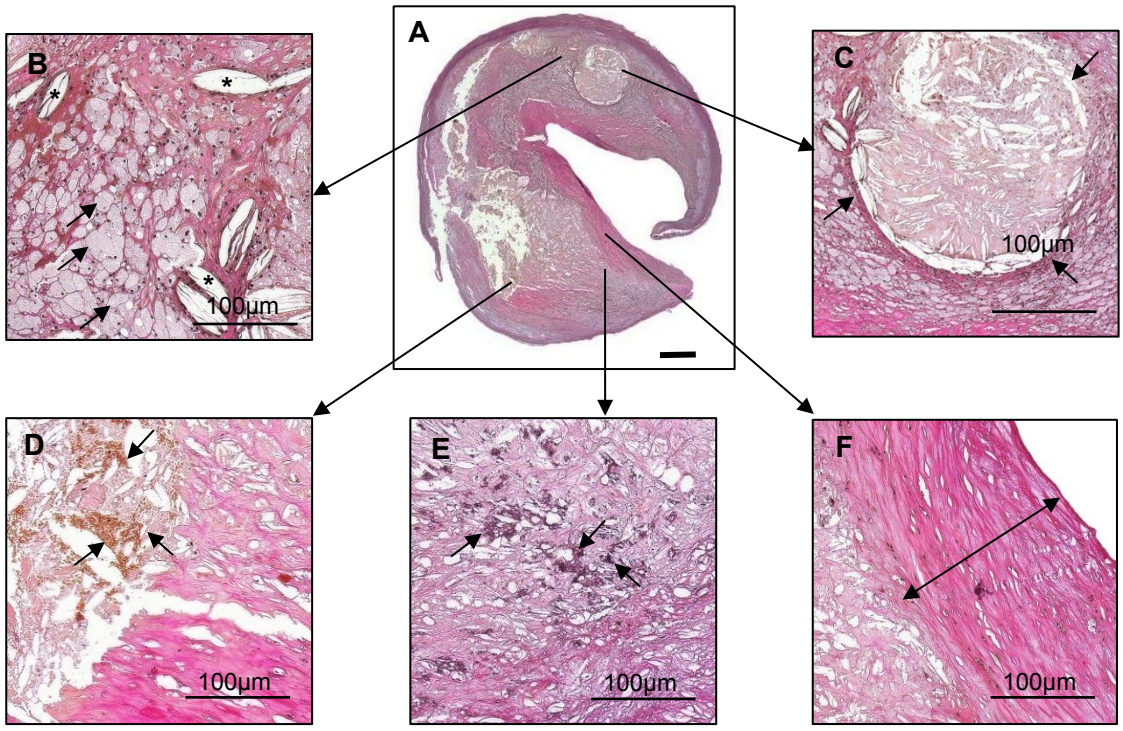

Figure 31. *Elastica van Gieson staining of advanced atherosclerosis with typical histopathologic characteristics. (A) Overview image of the whole atheroma plaque (bar represents 1 mm), (B) cholesterol crystals (asterisks) and inflammatory foam cells (arrows), (C) lipid core containing cholesterol crystals, (D) accumulation of erythrocytes within the atheroma (intraplaque bleeding), (E) calcification (F) fibrous cap of the atherosclerotic plaque.*

3.1.2 Global DNA methylation

3.1.2.1 Global DNA methylation in carotid tissue samples

The results of global DNA methylation from carotid specimens adjacent to different types of atherosclerotic lesions, determined by histology, are summarized in *Figure 32*. The extent of global DNA methylation correlated negatively with the degree of atherosclerosis. In early AS, the methylation of LINE1 decreased to 62.3% ($p<0.01$) compared with the DNA

methylation in healthy control vessels. Further decrease in DNA methylation to 32.4% ($p<0.001$) was observed in advanced stage of atherosclerosis, again compared with the healthy controls. Similar results were found also for the repetitive sequence Satα, with significant reduction in DNA methylation to 73.2% ($p<0.01$) in early stage and to 39.3% ($p<0.001$) in advanced stage of AS, compared with healthy vessels (*Figure 32*).

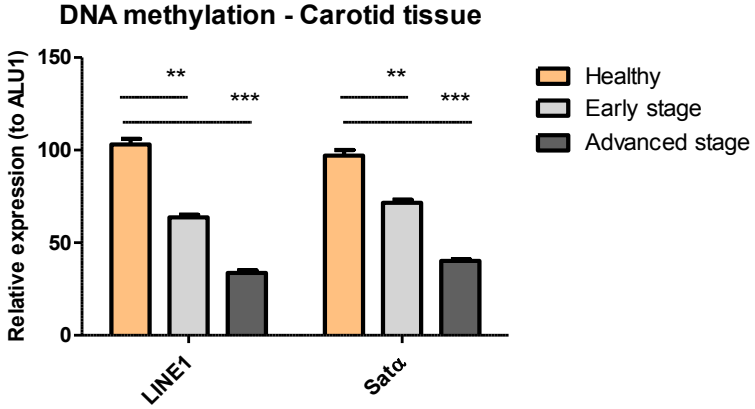

Figure 32. *Global DNA methylation status is decreased with the progression of atherosclerosis. The graphs represent the quantitative evaluation after setting the methylation in the control group as 100%.*

3.1.2.2 Global DNA methylation in serum

Interesting results were also observed following the analysis of blood serum samples. For both repetitive DNA sequences LINE1 and SATα, significant reduction in DNA methylation was found in patients with high grade carotid artery stenosis compared with healthy individuals. The global DNA methylation was reduced to 36.9% ($p<0.001$) for LINE1 and to 67.5% ($p<0.001$) for SATα, normalized to the DNA methylation in healthy volunteers (*Figure 33*).

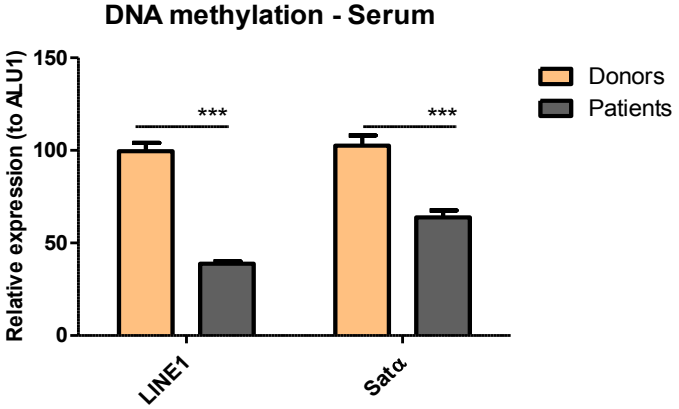

Figure 33. *Global DNA methylation of free DNA extracted from blood serum. DNA methylation is significantly decreased in patients with advanced atherosclerosis. The graphs represent the quantitative evaluation after setting the methylation in the control group as 100%.*

3.1.2.3 Expression of DNA methyltransferases and demethylase at mRNA level

At mRNA level the expression of DNA methyltransferases *DNMT1*, *DNMT3a*, *DNMT3b,* and demethylase *TET1* were determined by quantitative SYBR-Green based real time PCR. In all cases, normalization to the expression of housekeeping gene *GAPDH* was performed. *DMNT1*, a methyltransferase responsible for the maintenance of DNA methylation, showed a significant decrease in expression in AS (*Figure 34*). The differences between early and advanced stage of AS were not statistically significant (p=0.4701). *DNMT1* expression in early stage was decreased to 53.2% (p=0.0393), and in advanced stage to 27.2% (p=0.0393), in comparison with the control healthy tissue.

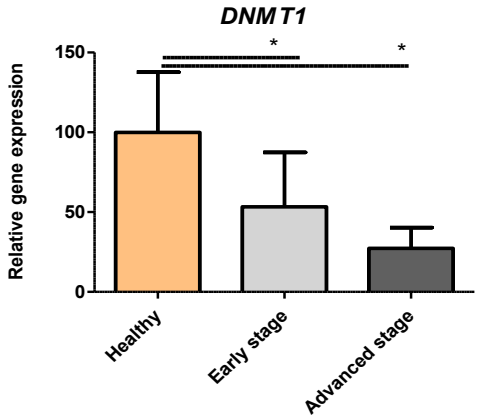

Figure 34. *Expression of DNMT1 decreased with the severity of atherosclerosis. The graphs represent the quantitative evaluation after setting the control group as 100%.*

TET1, an enzyme involved in the demethylation process, responsible for the intermediate form 5-hidroxymethylation, showed an increased expression level that corresponded with the progression of AS (*Figure 35*). An increased by 13.2-fold, (p=0.7441) was observed in the early stage of AS, and by 44.1-fold (p=0.4350) in the advanced stage. However, due to broad distribution of the values the postulated significance was not achieved, compared with the expression of *TET1* in control tissue samples.

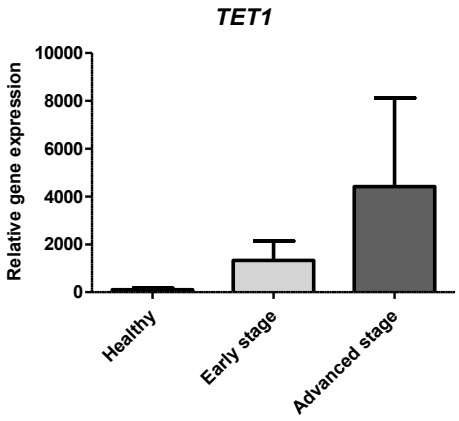

Figure 35. *Expression of TET1 at mRNA level in different stages of atherosclerosis compared to healthy tissue samples. The graphs represent the quantitative evaluation after setting the control group as 100%.*

De novo methylation process is supported by two enzymes, DNMT3A and DNMT3B, the latter having also a role in maintaining the DNA methylation pattern (*Figure 36*). The expression of *DNMT3A* was detected neither in control tissue nor in atherosclerotic lesions. In contrast, *DNMT3B* expression was found in both healthy and atherosclerotic samples. Decrease in expression of *DNMT3B* was observed in AS, compared to healthy tissue, both in early and advanced stage, with the tendency of further reduction in *DNMT3B* expression with the progression of AS. In early stage the expression decreased to 46.0% (p=0.9048), and in advanced stage to 31.0% (p=0.6095), in comparison with the healthy control tissue (*Figure 36*).

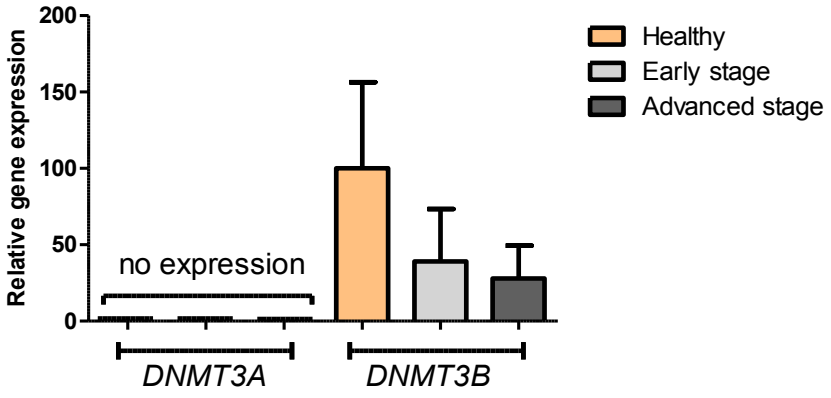

Figure 36. *Quantitative expression analysis of DNMT3A and DNMT3B in carotid tissue samples. No expression was observed for DNMT3A. Expression of DNMT3B decreased with the progression of atherosclerosis. The graphs represent the quantitative evaluation after setting the control group as 100%.*

3.1.3 Immunohistochemical analysis of histone methylation

One of the objectives of the present study was to analyze the histone, methylation, especially di-methylation on histone H3 at lysine 4 and at lysine 9 (H3K4 and H3K9), and to

evaluate, whether any changes in this epigenetic modification are associated with certain type of cells within atherosclerotic plaques in comparison with healthy vessel tissue.

3.1.3.1 Histone methylation in smooth muscle cells

The first staining was performed for smooth muscle cells (SMCs) (*Figure 37*.). Smooth muscle (SM) actin clearly identified SMCs within the control tissue as well in early and advanced atherosclerosis. Consecutive slides stained for SM-actin were used for detection of H3K4 di-methylation. In the control tissue, not all SMCs were positive for H3K4me2 staining. In contrast, both early and advanced stage of atherosclerosis showed an increase in the number of positive cells. No further differences were observed between early and advanced atherosclerosis (*Figure 37*).

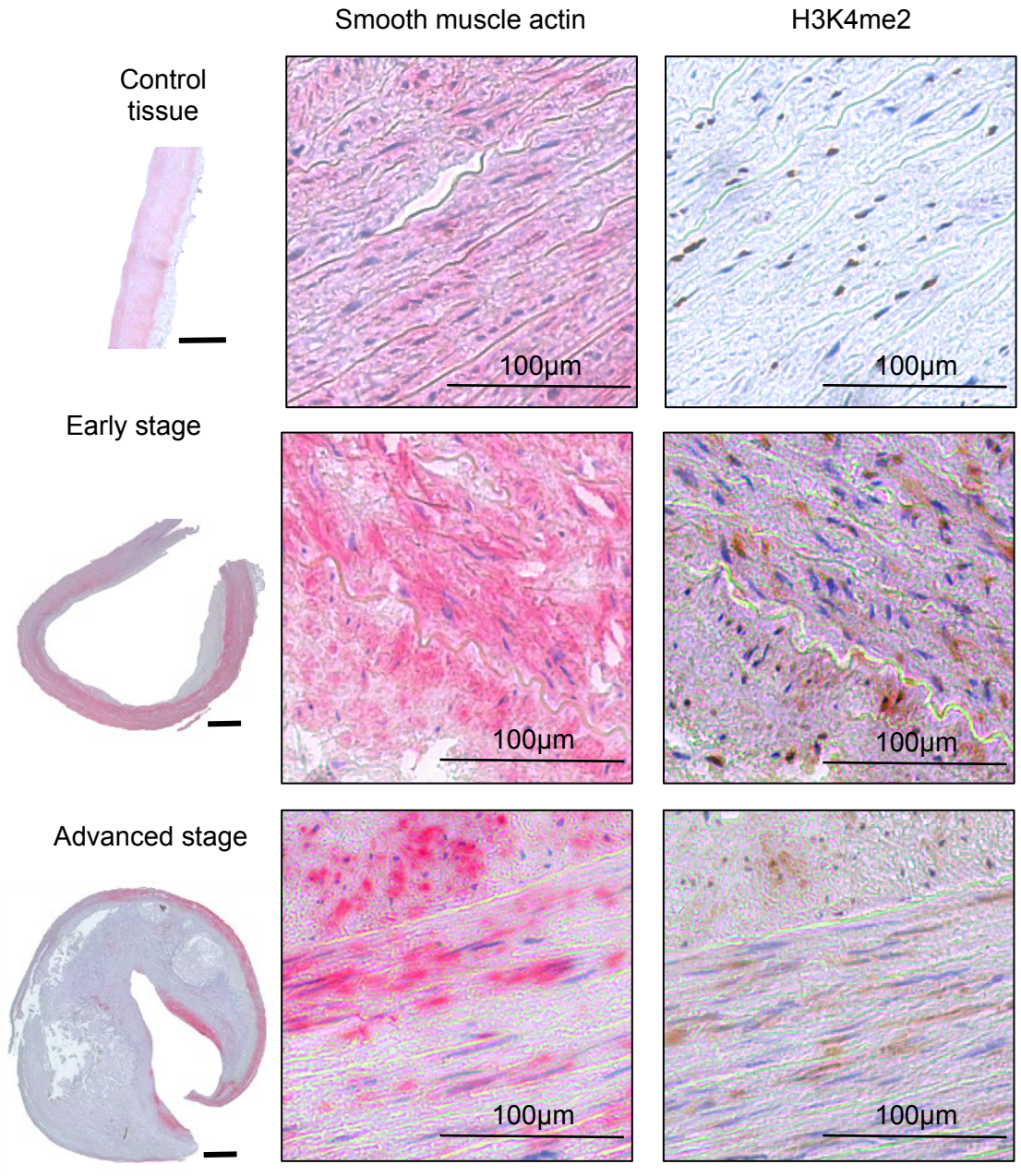

Figure 37. *Representative stainings of consecutive slides for smooth muscle cells and H3K4me2. Red color represents the positive cells for smooth muscle, whereas brown color represents cells positive for H3K4me2. Samples were counterstained with haematoxylin (blue color). The bar in the overview image represents 1 mm.*

Similar consecutive staining as described before was performed for SMCs and H3K9me2. The results revealed that only a small fraction of cells was positive for H3K9me2 and SM-actin (*Figure 38*). No differences were observed between the control vessels, early, or advanced stage of atherosclerosis.

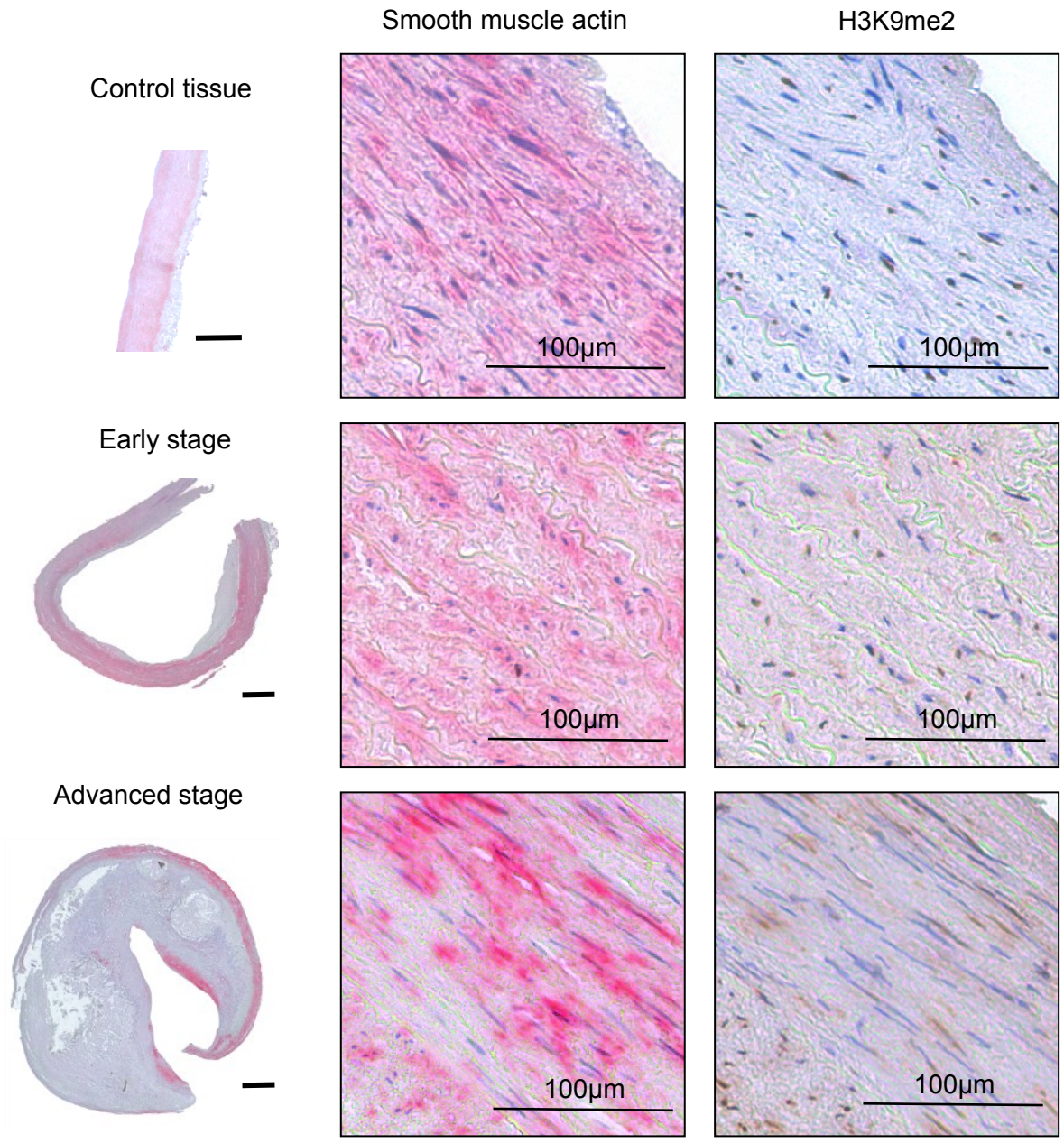

Figure 38. *Representative stainings of consecutive slides for smooth muscle cells and H3K9me2. Red color represents the positive cells for smooth muscle, whereas brown color represents the cells positive for H3K9me2. Samples were counterstained with haematoxylin (blue color). The bar in the overview image represents 1 mm.*

3.1.3.2 Histone methylation in inflammatory cells

Consecutive slices of FFPE tissue samples from each study group were stained for the inflammatory marker CD45 and for H3K4me2 (*Figure 39*). CD45 is a leucocyte common antigen present on all blood cells except erythrocytes. It is expressed especially in B- and T-lymphocytes.

In general, in a healthy vessel, no significant amount of inflammatory cells, comprising CD45 or CD68 antigens, is present. In agreement, no CD45 positive cells were found in the control tissue of the selected study group. For this reason, images of the stained control healthy vessels were omitted in *Figures 39-42*. In contrary to the control vessel, in early and especially advanced stage of atherosclerosis marked accumulation of inflammatory cells, positive for CD45, was observed. Interestingly, all these cells were negative for H3K4me2 (*Figure 39*).

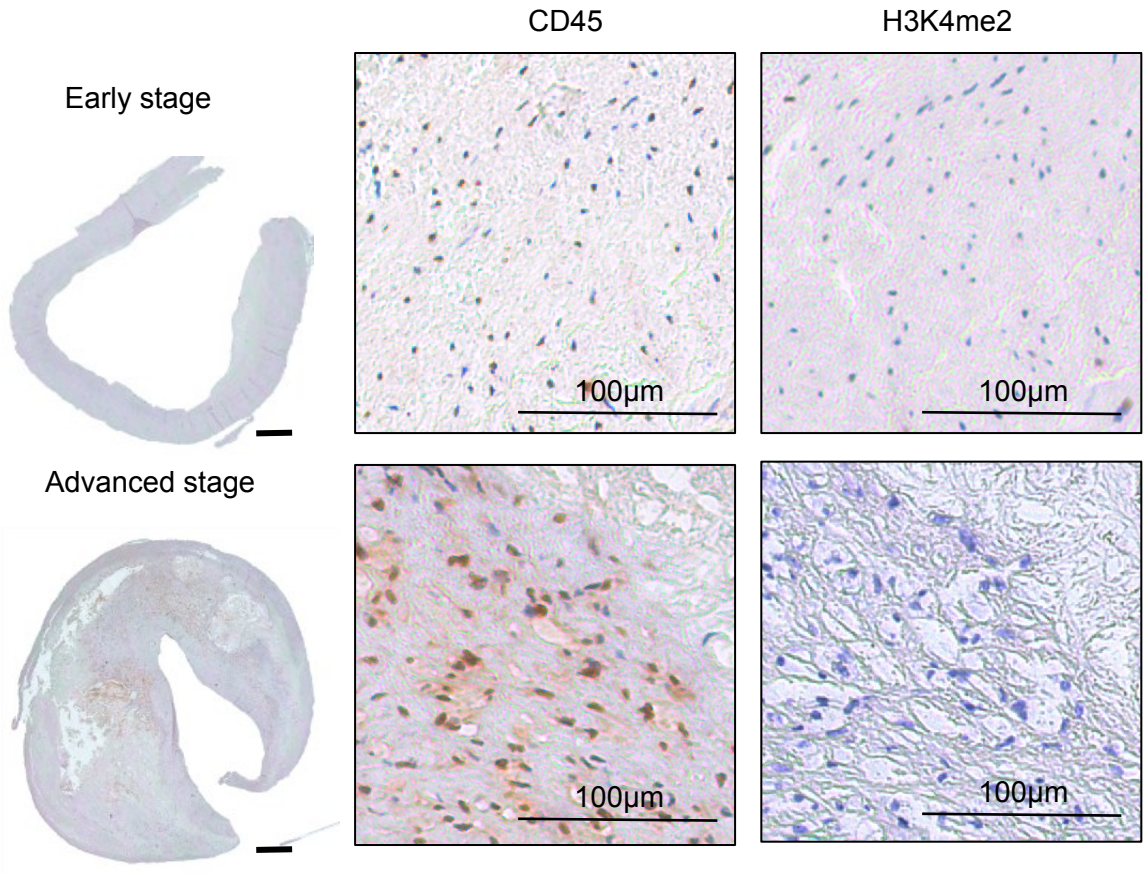

Figure 39. *Examples of consecutive staining for CD45 positive inflammatory cells and for histone H3 di-methylation of lysine K4 in early (first row) and advanced (second row) stage of atherosclerosis. Brown color represents the positive cells for different markers: CD45 – first column, H3K4me2 – second column. Blue color shows the nuclear counterstain by haematoxylin. The bar in the overview image represents 1 mm.*

The same staining procedure as for H3K4 was performed also for H3K9 (*Figure 40*). In contrast to the negative staining for H3K4me2 in inflammatory cells, CD45 positive cells were found to be positive for H3K9me2. No differences were observed between early and advanced stage of AS. Albeit, increased intensity and more cells were seen in advanced atherosclerotic plaques.

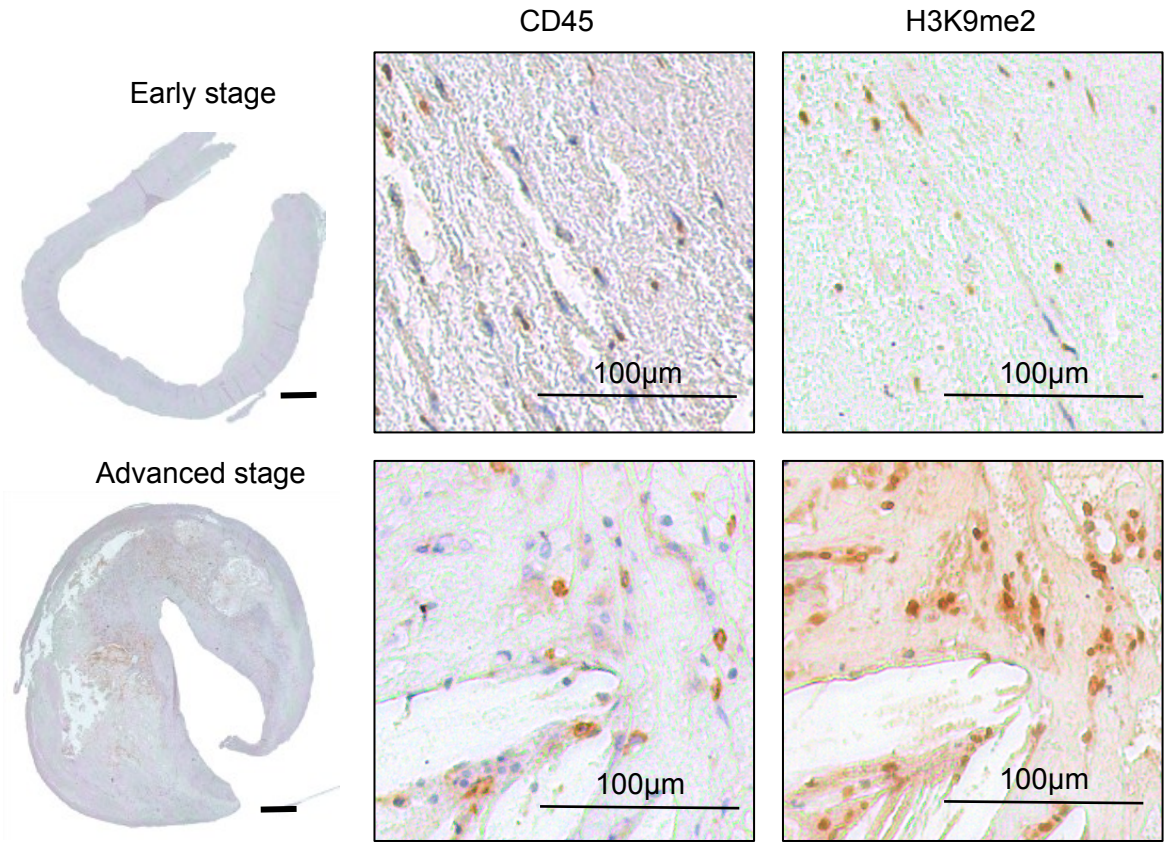

Figure 40. *Examples of consecutive staining for CD45 positive inflammatory cells and for histone H3 di-methylation of lysine K9 in early (first row) and advanced (second row) stage of atherosclerosis. Brown color represents the positive cells for different markers: CD45 – first column, H3K9me2 – second column. Blue color shows the nuclear counterstain by haematoxilin. The bar in the overview image represents 1 mm.*

Another group of inflammatory cells that markedly contribute to plaque progression are CD68 positive cells, comprising monocytes, macrophages, and macrophage-derived foam cells. Therefore, consecutive staining for CD68 and histone di-methylation of H3K4 or H3K9 was performed (*Figure 41* and *42*). Only few CD68 positive cells were observed in early stage of atherosclerosis, according to their morphology, mainly monocytes and macrophages. In contrast, advanced stage of atherosclerosis comprised predominantly lipid-laden macrophages and macrophage-derived foam cells.

After examination of the corresponding regions for CD68 and H3K4, only a small fraction of CD68 positive cells was found to be also positive for H3K4me2 in both early and advanced stage (*Figure 41*). Furthermore, no differences were observed between early and advanced atherosclerosis.

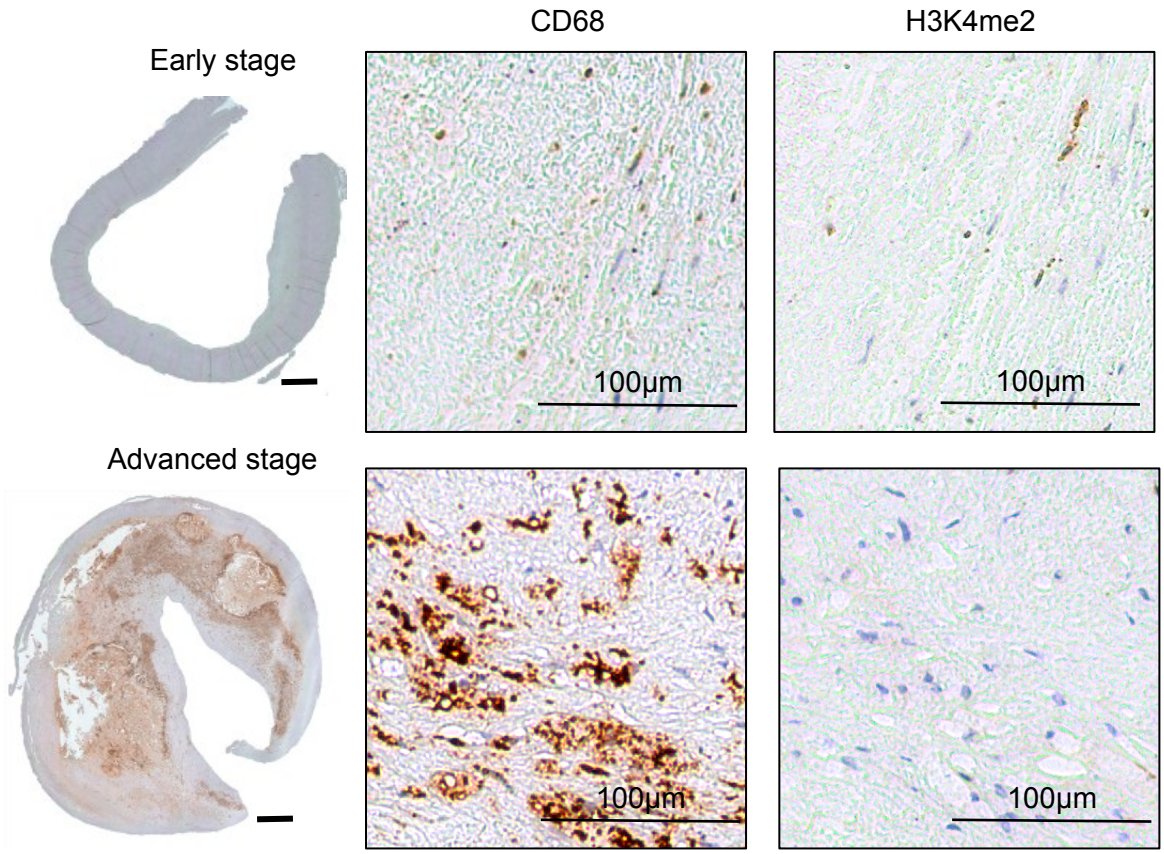

Figure 41. *Examples of consecutive staining for CD68-positive inflammatory cells (monocytes, macrophages, and macrophage-derived foam cells) and di-methylation of histone H3 at lysine K4 in early (first row) and advanced (second row) of atherosclerosis. Brown color represents positive cells for CD68 – first column, and for H3K4me2 – second column. Blue color shows the nuclear counterstain by haematoxylin. The bar in the overview image represents 1 mm.*

In contrast to the staining for H3K4me2, markedly more CD68 positive cells in atherosclerotic lesions were positive also for H3K9me2 staining (*Figure 42*). In both, early and advanced stage of atherosclerosis, almost all monocytes, macrophages, and macrophage-derived foam cells were methylated on histone H3 at the lysine K9.

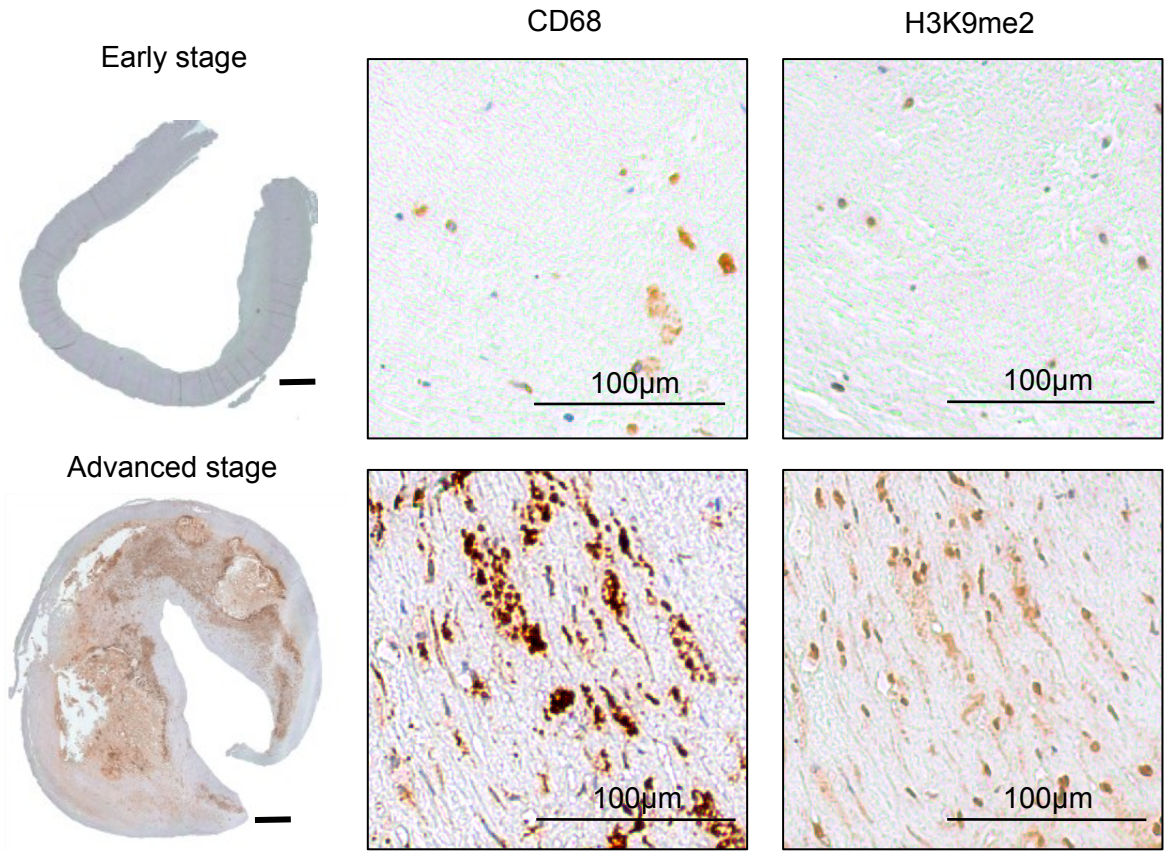

Figure 42. *Examples of consecutive staining for CD68-positive inflammatory cells (monocytes, macrophages, and macrophage-derived foam cells) and di-methylation of histone H3 at lysine K9 in early (first row) and advanced (second row) of atherosclerosis. Brown color represents positive cells for CD68 – first column, and for H3K9me2 – second column. Blue color shows the nuclear counterstain by haematoxylin. The bar in the overview image represents 1 mm.*

3.1.4 Analysis of histone methylation at protein level

For possible quantification of histone methylation at the protein level, western blot analysis was performed in a similar way as for the immunohistochemistry as desribed above. The extraction of histones was made from fresh tissue of carotid arteries, including again three study groups: healthy tissue, early, and advanced stage of AS. Each group consisted of 9 samples. For quantification, the ImageJ software was used and samples were normalized to the amount of histone H3. Furthermore, the state of methylation in a healthy tissue was set as 100%. The extent of H3K4 and H3K9 di-methylation (H3K4me2 and H3K9me2) is shown in *Figure 43*. Significant reduction of histone H3 methylation at K4 and K9 was observed in both early and advanced stages of AS. In carotid plaque from early stage of AS, a decrease to 28.5% ($p<0.01$) was found compared with healthy control tissue. In advanced AS, a significant reduction of H3K4 di-methylation to 39.3% ($p<0.05$) was seen. With regard to H3K9me2, a significant decrease to 12.0% ($p<0.05$) and to 25.2% ($p<0.01$) was observed for early stage and advanced stage of AS, respectively. In both cases, for

H3K4 and H3K9, no significant differences in histone di-methylation were observed between early and advanced of AS.

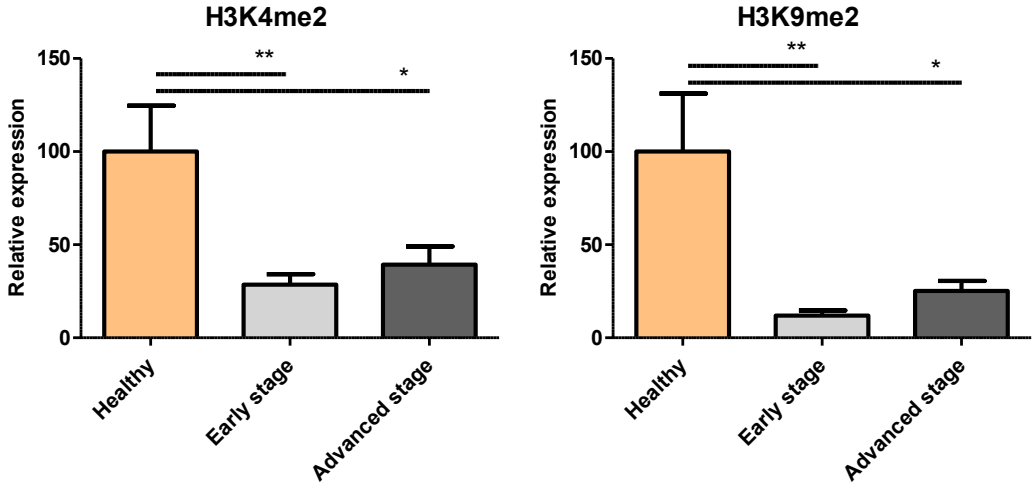

Figure 43. *Western blot analysis for di-methylation of histone H3 at lysine 4 (H3K4) and lysine 9 (H3K9). A statistically significant decrease for both H3K4me2 and H3K9me2 was observed with the progression of the AS. The expression of each modification in the control group was set as 100%.*

3.1.5 Analysis of histone methyltransferases (HMTs)

3.1.5.1 HMTs responsible for H3K4 methylation

Finally, to constitute the changes in histone methylation pattern in atherosclerotic lesions, the expression of methyltransferases, responsible for the transfer of methyl group to H3K4, was analyzed by quantitative SYBR-Green based RT-PCR (*Figure 44*). The analyzed methyltransferases were MLL1, SET1A, and SET1B. Their expression was evaluated at the mRNA level on tissue samples extracted from FFPE tissues. From all three HMTs, only the expression of *MLL1* could be detected. Interestingly, *MLL1* expression increased continuously with the progression of atherosclerosis, in early stage lesions by 2.63-fold (p=0.7658) and in advanced stage by 2.09-fold (p=0.5800), however without the postulated significance. For *SETD1A as well as for SETD1B* no expression was observed (*Figure 44*).

Figure 44. *Quantification of the expression of methyltransferase MLL1, SETD1a, and SETD1b responsible for H3K4 methylation. In contrast to the expression of MLL1, which continuously increased with the progression of atherosclerosis, no expression was observed for SETD1A and SETD1B. Expression of the control group was set as 100%.*

3.1.5.2 HMTs responsible for H3K9 methylation

Similar to results described before, the expression of methyltransferases responsible for the transfer of methyl group to H3K9 was evaluated (*Figure 45*). The expression of SUV39H1 and EHMT2 (G9a), responsible for the corresponding methylation, was analyzed at mRNA level from FFPE tissue samples as for H3K4. No expression was detected for both enzymes.

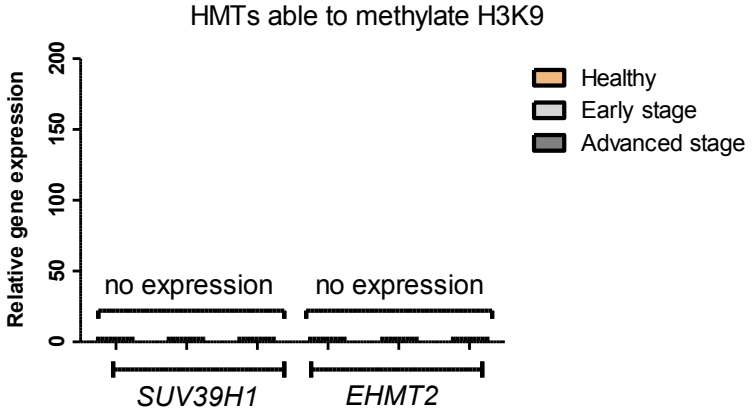

Figure 45. *Quantification of the expression of methyltransferase SUV39H1 and EHMT2 responsible for H3K9 methylation. No detectable expression was observed for both enzymes.*

3.2 RESULTS - Epigenetic changes in regenerative medicine

3.2.1 Isolation and characterization of the adipose derived mesenchymal stem cells (adMSCs)

Mesenchyme is a type of undifferentiated loose connective tissue derived mostly from mesoderm. Mesenchyme is characterized morphologically by a prominent ground substance matrix containing a loose aggregate of reticular fibrils and unspecialized cells. The cells are capable of developing into connective tissue, such as bone, cartilage, and adipose tissue. Adipose tissue contains a high amount of mesenchymal stem cells that can be easily isolated. These cells have been described to have high proliferative capacity and also a potential to differentiate into osteoblast, chondrocytes or adipocytes, if they are cultivated under appropriate conditions.

3.2.1.1 Analysis of cell morphology and phenotype

Mesenchymal stem cells (MSCs) have been classified as a heterogeneous population in terms of morphology, proliferation capacity, and differentiation potential. They display different phenotypes: large flattened cells, thin star-shaped cells, and fibroblast-like cells (spindle shape) as already described by Muraglia *et al.* [216] (Figure 46). By examining the cell isolated from adipose tissue, it was observed that MCSs are characterized morphologically by small cell body with few long and thin cell processes. The cell body contains round nucleus with large nucleolous, which is surrounded by finely scattered chromatin particles. Cells isolated from human adipose tissue in this study displayed the typical features of MSCs, as shown in Figure 46.

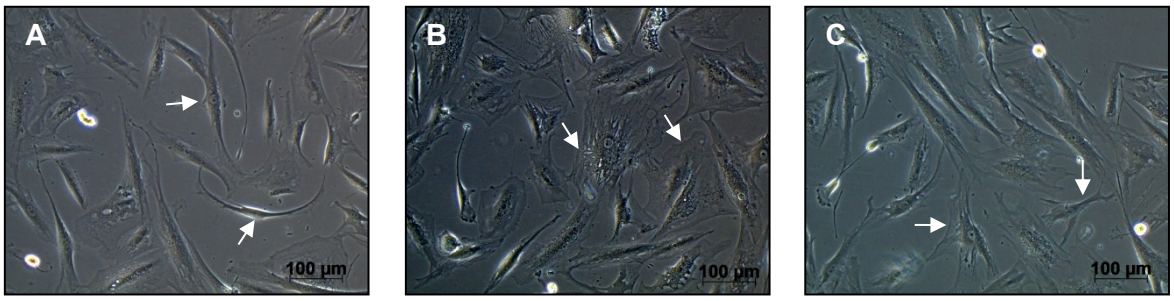

Figure 46. *Phenotype of cultured human adMSCs. Three phenotypes were observed in adMSC colonies: (A) spindle shape, (B)large flattened cells, and (C) star shaped cells as described by Muraglia et al [216].*

The population of freshly isolated adMSCs is in general heterogeneous. Therefore, to assure reproducibility of the following experiments, it was necessary to further characterize the cell population over the passages. Following cell isolation and their cultivation until

passage 3, flow cytometry analysis revealed mainly homogenous cell population with a characteristic expression pattern of the known MSCs markers CD90 and CD105, while being negative for hematopoietic marker CD14 and CD45 (*Figure 47*). This assay was performed in every passage up to the passage 3 for all CD markers mentioned. Based on the cell characterization, passage 3 was selected for all further experiments due to the best proliferation/homogeny ratio. The expression of MSC markers in passage three was as follows: CD90 and CD105 - 86% and 96%, respectively, CD14 and CD45 - 1.88% and 1.06%, respectively. The markers CD14 and CD45 showed a decrease to less than 2%, while CD90 and CD105 showed an increase for up to 96% in the third passage (for detailed results see *Table 19* and *Figure 48*)

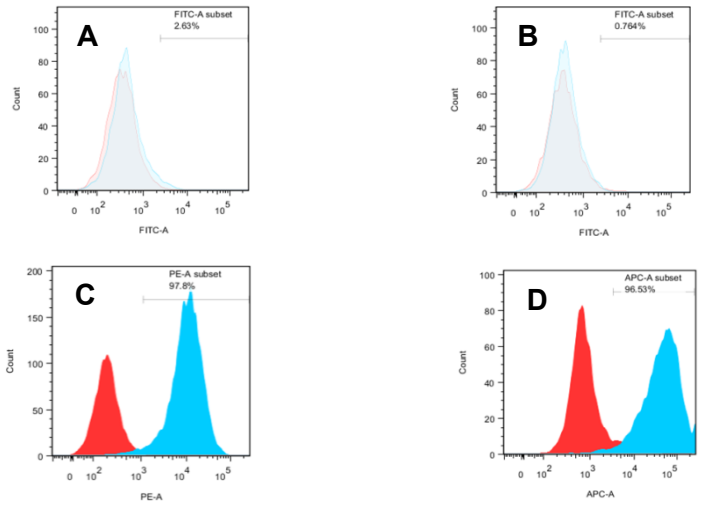

Figure 47. *FACS histograms for CD14, CD45, CD90, and CD105 used for characterization of adMSCs population. Cells were screened for (A) CD14, (B) CD45, (C) CD105, and (D) CD90 and their corresponding isotype controls. Each representative antibody is represented by the blue histograms, and the isotype control is red colored.*

Table 19. *Summary of adMSC characterization by FACS analysis.*

Passage number	CD14 positive cells	CD45 positive cells	CD 90 positive cells	CD 105 positive cells
Passage 0	8.4%	5.7%	73.72%	44.3%
Passage 1	3.4%	1.5%	77.7%	47%
Passage 2	3.12%	1.26%	81%	50%
Passage 3	1.88%	1.06%	86%	96.17%

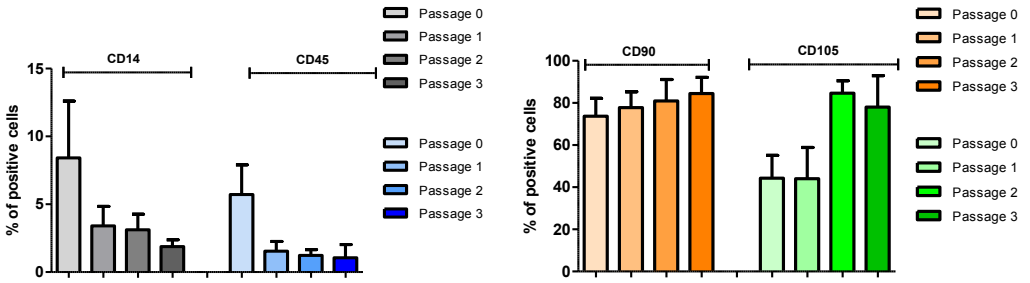

Figure 48. *FACS analysis of adMSCs for CD14, CD45, CD90, and CD105 during passages 0, 1, 2, and 3. The markers CD14 and CD45 showed a decrease while CD90 and CD105 showed an increase with the passage. The graphs represent the quantitative evaluation after setting the entire cell population as 100%.*

3.2.1.2 Immunocytological characterization

Cells isolated from adipose tissue were first cultivated under normal growth conditions. In the third passage they were screened for the known mesenchymal markers vimentin and endoglin *(Figure 49*). Vimentin is the cytoskeletal component responsible for maintaining cell integrity, and endoglin, also known as CD105, is a glycoprotein part of the transforming growth factor receptor complex that binds several members of the TGFbeta superfamily. The cells were proven to be homogenous with regard to these markers, with all cells positive for both antigens.

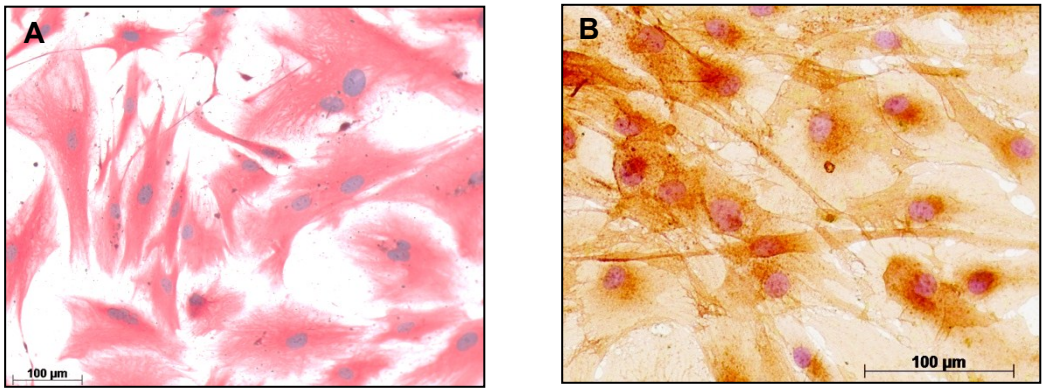

Figure 49. *AdMSC characterisation – vimentin and endoglin - ICC. (A) Red cells positive for the mesenchymal marker – vimentin (red); (B) CD105 - endoglin, is present on the membrane of all cells (brown); counter stain with Meyer's haematoxylin (nuclei are stained in blue).*

3.2.2 Analysis of cell proliferation

Ki-67, a marker of actively dividing cells, was used to determine the fraction of proliferating cells within the given population. Proliferating adMSCs in passage 3 were visualized by ICC staining. Cells were in average positive for Ki-67 at a rate of 52%, as shown in *Figure 50* (quantification was performed with ImageJ software).

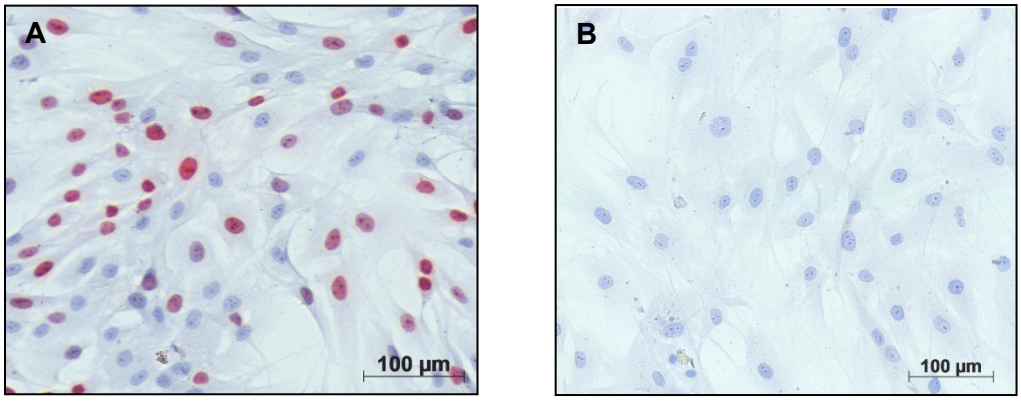

Figure 50. *Immunocytochemistry for the Ki-67 antigen on adipose-derived mesenchymal stem cells (A) adMSCs. in third passage, red stain represents the proliferating cells, positive for Ki-67; (B) Negative control IgG.*

3.2.3 Osteogenic and adipogenic differentiation

Since adMSCs are mesenchymal stem cells, they should have the capacity to undergo osteogenic, adipogenic, and chondrogenic differentiation. To prove their differentiation potential and their multipotent characteristics, the cells were seeded and cultivated in appropriate differentiation media.

3.2.3.1 Osteogenic differentiation

Osteogenic differentiation was assessed after 7, 14, and 21 days of cultivation in osteogenic differentiation medium by analyzing the presence of the alkaline phosphatase (ALP) enzyme, deposits of collagen III, and mineralized matrix.

ALP is a marker known to be necessary for mineralization of bone tissue, present in cells of the osteoblastic linage. The majority of isolated adMSCs cultivated under osteogenic conditions were positive for ALP and the results were similar to that of human osteoblast progenitor cells, compared with normal growth media (*Figure 51*).

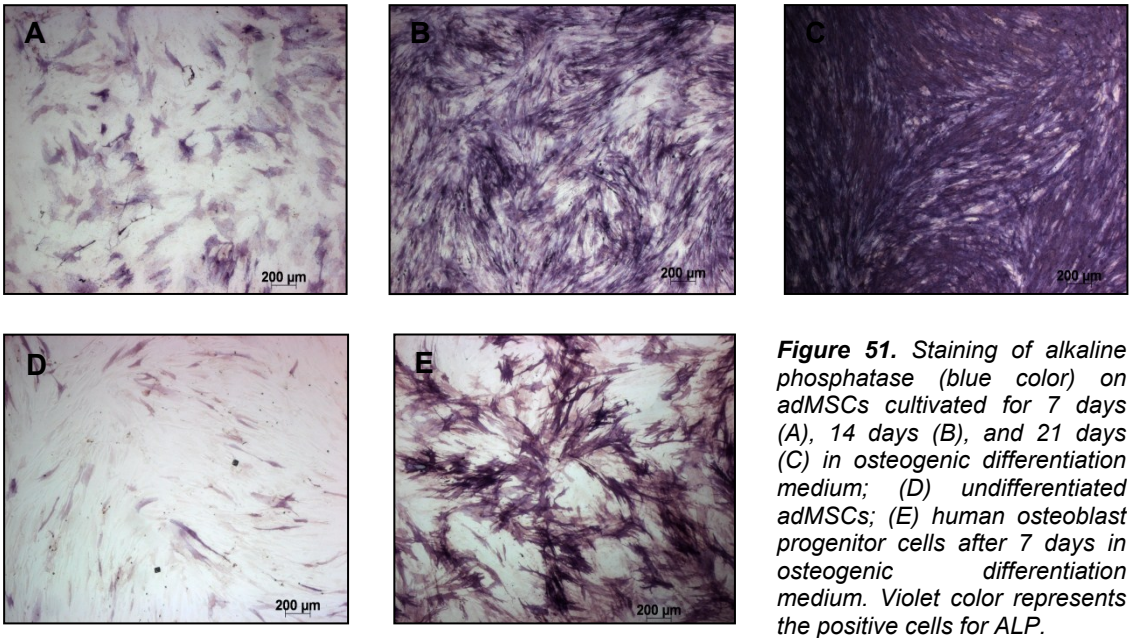

Figure 51. *Staining of alkaline phosphatase (blue color) on adMSCs cultivated for 7 days (A), 14 days (B), and 21 days (C) in osteogenic differentiation medium; (D) undifferentiated adMSCs; (E) human osteoblast progenitor cells after 7 days in osteogenic differentiation medium. Violet color represents the positive cells for ALP.*

Type-III collagen is a protein that is found in bone, cartilage, tendon and some other connective tissues. Therefore, adMSCs, cultivated in osteogenic medium, were tested also for their ability to synthesize collagen type III. Staining of differentiated adMSCs against collagen III revealed an increase in the production of the protein over the differentiation period, whereas under normal growth conditions the cells were not producing collagen type III (*Figure 52*).

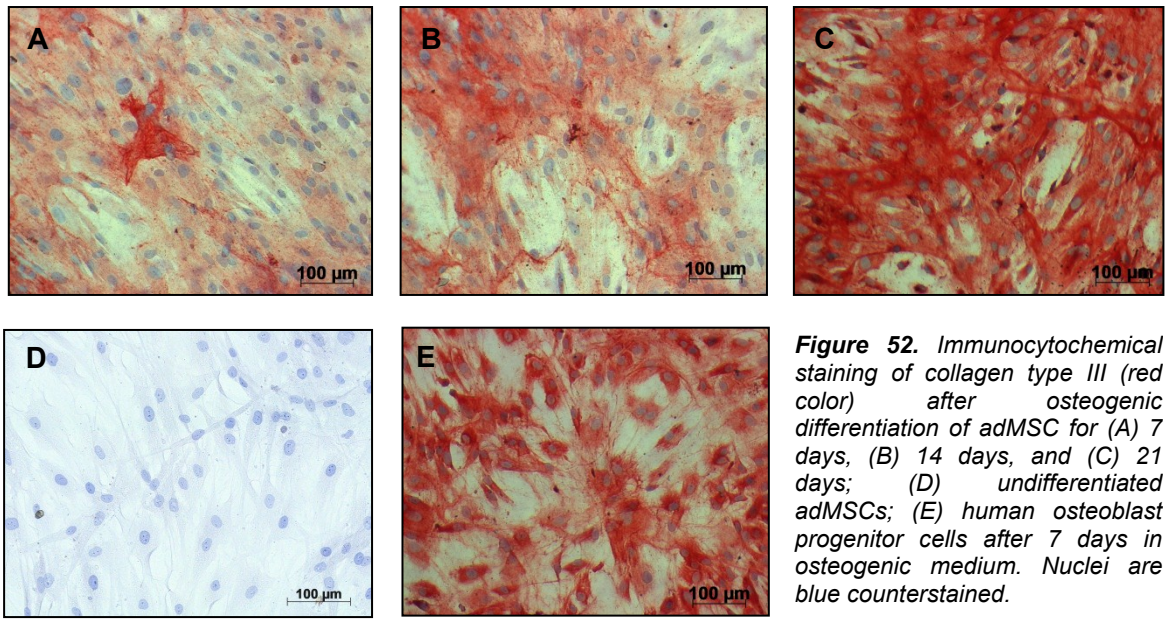

Figure 52. *Immunocytochemical staining of collagen type III (red color) after osteogenic differentiation of adMSC for (A) 7 days, (B) 14 days, and (C) 21 days; (D) undifferentiated adMSCs; (E) human osteoblast progenitor cells after 7 days in osteogenic medium. Nuclei are blue counterstained.*

Beside ALP activity and the production of extracellular matrix (ECM) during osteogenic differentiation, osteoblasts also produce mineralized matrix. For this reason, the matrix mineralization was tested using von Kossa staining after 7, 14, and 21 days, in order to prove the capacity of adMSCs to differentiate into osteogenic lineage (*Figure 53*). The

staining confirmed the ability of adMSCs to deposit calcium phosphate within the cell. The deposition was observed in direct progression with the differentiation time.

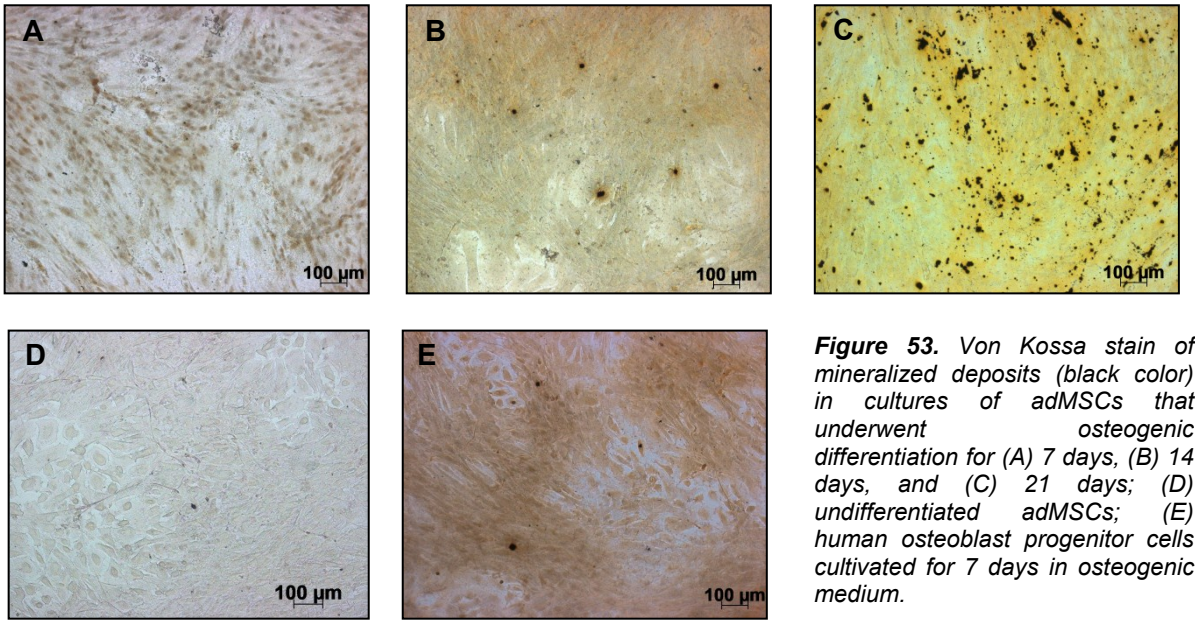

Figure 53. *Von Kossa stain of mineralized deposits (black color) in cultures of adMSCs that underwent osteogenic differentiation for (A) 7 days, (B) 14 days, and (C) 21 days; (D) undifferentiated adMSCs; (E) human osteoblast progenitor cells cultivated for 7 days in osteogenic medium.*

3.2.3.2 Adipogenic differentiation

As mentioned above, adMSCs also possess the ability to differentiate into the adipogenic lineage. The differentiation potential of the cells was tested by Oil Red O staining. The lipid droplets appeared after 2-3 days in adipogenic medium and their accumulation was equivalent to an adipocyte phenotype. Furthermore, the staining revealed large lipid vacuoles after 14 days of culture (*Figure 54*).

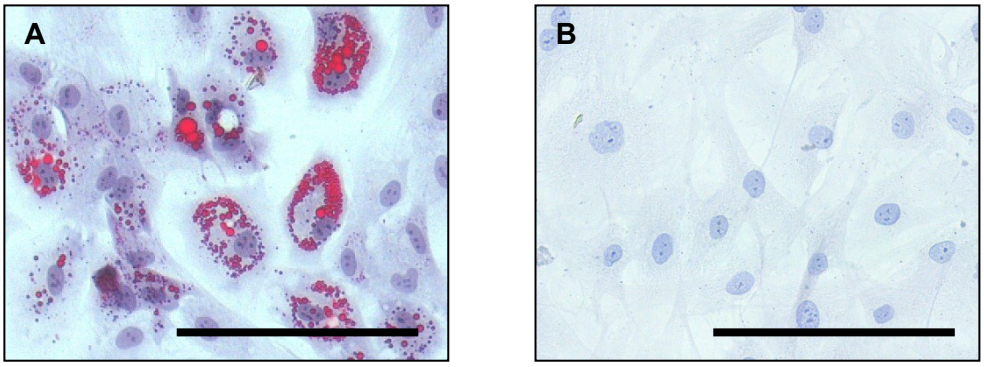

Figure 54. *Adipogenic differentiation of adMSCs. Morphological analysis of adMSCs cells under (A) adipogenic conditions for 14 days in comparison with (B) normal growth conditions; bar represents 100 µm.*

3.2.4 Effect of the epigenetic modifying drugs on adMSCs

3.2.4.1 Detection of the optimal concentration of epigenetic modifying drugs for adMSCs

To find the optimal non-toxic concentration of the epigenetic modifying drugs used in this study, different amount of 5-azacytidine (AZA), BIX-01294 (BIX), and valproic acid (VPA) were used and cell viability assay (MTT) was applied.

3.2.4.2 Effect of AZA on viability of adMSCs

The viability of cells treated with five different concentrations of AZA (2.5, 5, 10, 20, and 40 μM) and compared with non-treated cells. Cell viability was not significantly affected by the tested concentrations independent of the different time point used (24, 48, and 72 h (*Figure 55*). For this reason the two lowest AZA concentrations, 2.5 and 5 μM, were selected for further experiments.

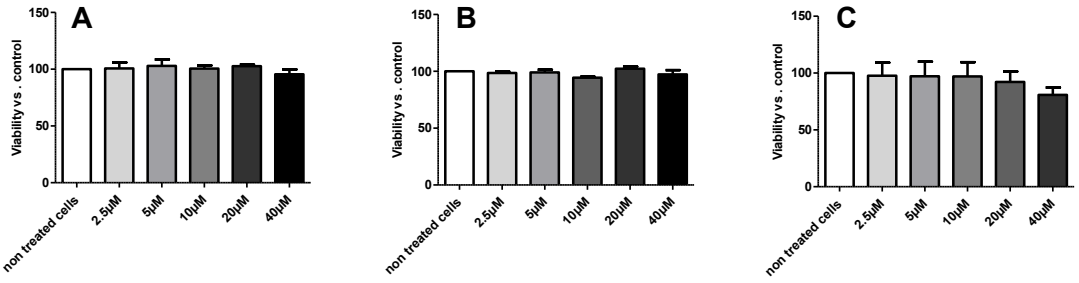

Figure 55. *Viability of adMSCs treated with five different concentrations of 5-azacytidine (AZA) for different time points: (A) 24 h, (B) 48 h, and (C) 72 h. Viability of the non-treated cells was set as 100%.*

3.2.4.3 Effect of BIX on viability of adMSCs

The tested concentrations of BIX were 0.625, 1.25, 2.5, 5, and 10 μM. As for AZA, the viability of the cells was measured 24, 48, and 72 h following treatment (*Figure 56*). In comparison with non-treated cells, a statistically significant decrease in cell viability was observed after exposing the cells to concentrations of 5μM and 10 μM BIX for all three time points. Following decrease in cell viability was observed using BIX: After 24 h and at the concentration of 5 μM to 44% ($p<0.001$), at 10 μM to 5% ($p<0.0001$); after 48 h at 5 μM to 8.5% ($p<0.0001$), and at 10 μM to 0.5% ($p<0.0001$); after 72 h at 2.5 μM to 52% ($p<0.05$), at 5 μM to 6% ($p<0.0001$), and at 10 μM to 3% ($p<0.0001$). Thus, for the next experiments BIX concentration of 0.625 and 1.25 μM were selected.

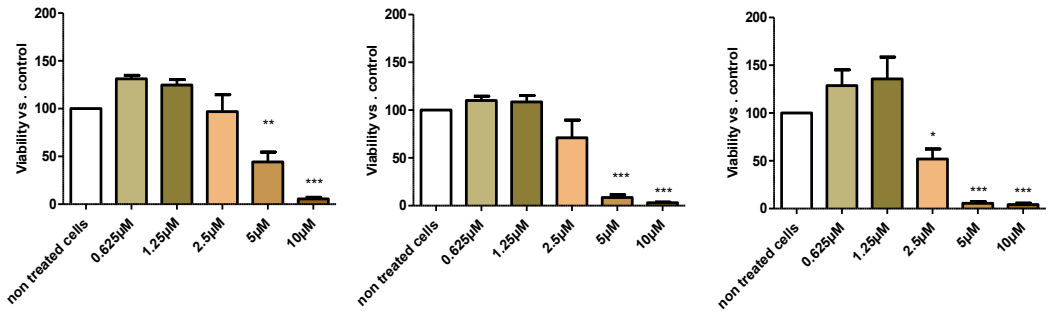

Figure 56. *MTT assay for BIX-01294 at different points of time: (A) 24 h, (B) 48 h, and (C) 72 h with five different concentrations. Viability of the non-treated cells is set as 100%.*

3.2.4.4 Effect of VPA on viability of adMSCs

Valproic acid was tested on adMSCs at concentrations of 100, 200, 400 and 800 µM, and 1.2 mM at three different time points, 24, 48, and 72 h (*Figure 57*). Compared with non-treated cells, significant decrease in cell viability was observed after 48 h at 100 µM to 53.8%, at 400µM to 56.5%, at 800µM to 50.66%, and at 1.2 mM to 54.1% (for all $p<0.05$); after 72 h significant decrease in viability was observed only for 1.2 mM to 43.21% ($p<0.05$). Consequently, for all future experiments the concentrations of 100 and 200 µM were chosen.

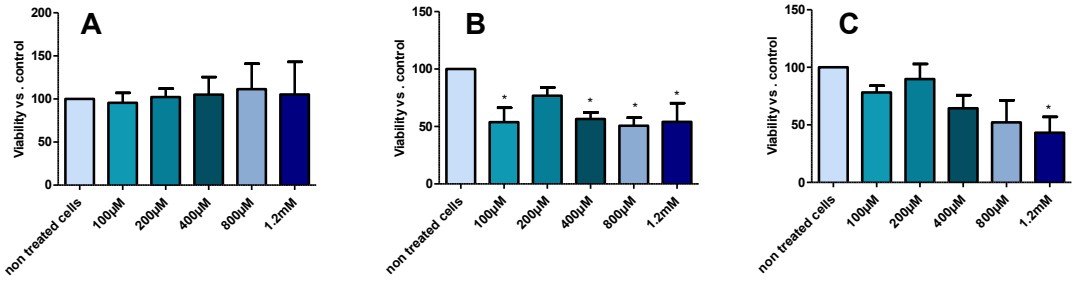

Figure 57. *MTT assay for VPA at different points of time: (A) 24 h, (B) 48 h, and (C) 72 h with five different concentrations. Viability of the non-treated cells is set as 100%.*

Finally, also combination of these chemical compounds was tested and compared with the non-treated cells for the above mentioned time points (24, 48, and 72 h). Based on the previous results for each of the compound, following concentrations were chosen: AZA 5 µM, BIX 1.25 µM, and VPA 200 µM). In addition several of these compounds and their selected concentration were tested. Various combinations were tested to verify the viability of the cells as follow: AZA and BIX; AZA and VPA, BIX and VPA, AZA, BIX, and VPA. No significant differences were observed after the treatment independent of the combination or time point used (*Figure 58*).

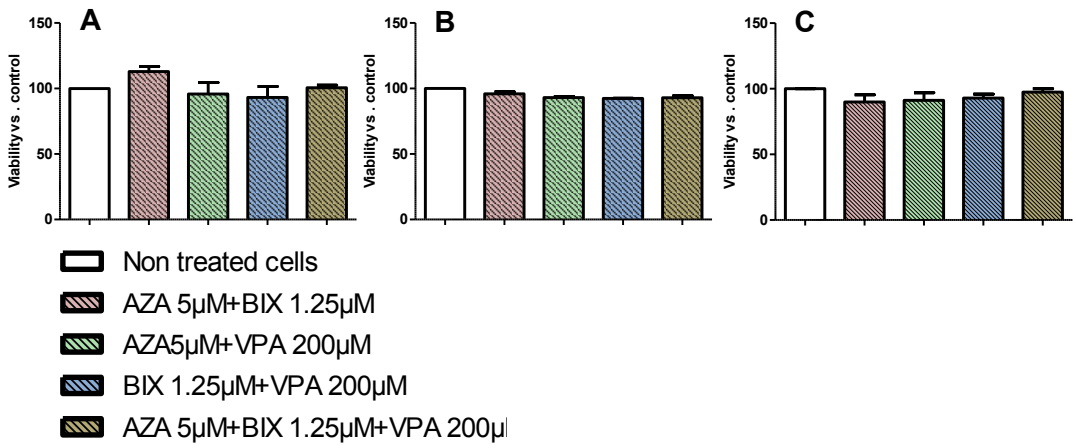

Figure 58. *MTT assay after treatment with a combination of AZA, BIX, and VPA for a time period of (A) 24 h, (B) 48 h, and (C) 72 h. Viability of the non-treated cells is set as 100%.*

3.2.5 *Effect of epigenetic modifying drugs on global DNA methylation*

Global DNA methylation was assessed as described in section Materials and methods. All three chemical compounds described above are known for their ability to modify epigenetic pattern; However, only AZA has been shown to have a direct effect on DNA methylation [136]. Changes in DNA methylation pattern have been already associated with the reprogramming capacity of the cells. Consequently, epigenetic drugs might also improve the reprogramming capacity of adMSCs used in this study. Optimized non-toxic concentrations of AZA (2.5μM and 5μM), BIX (0.625μM and 1.25μM), and VPA (100μM and 200μM) were used for cell treatment at three different time points (24, 48, and 72 h) as already tested before to determine the optimal concentration of these chemical compounds on global DNA methylation. The results are summarized in *Figure 59*.

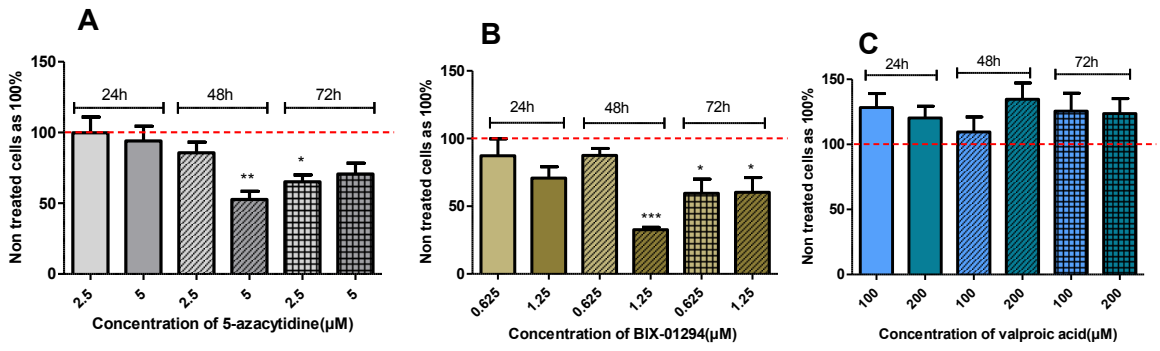

Figure 59. *Global DNA methylation after treatment with the epigenetic modifying drugs (A) 5-azacytididine; (B) BIX-01294; (C) valproic acid. The graphs represent the quantitative evaluation after setting the methylation in the non-treated cells as 100%.*

Following treatment of adMSCs with AZA for 24 hours no significant changes in DNA methylation pattern were observed. In contrast, global DNA methylation was decreased to 40.3% ($p<0.001$) using 5 μM AZA for 48 h, whereas 2.5 μM AZA for 72 h led to a decrease to

71.6% ($p<0.05$), compared with non-treated cells. In similar way, BIX treatment demonstrated significant changes in DNA methylation first after 48 hours of treatment. Using the higher non-toxic concentration of 1.25 μM, global DNA methylation was reduced to 49.80% ($p<0.0001$). Treatment of adMSCs with BIX for 72 hours led to a significant decrease in global DNA methylation for both concentrations applied. Using 0.625 μM the reduction went to 68.30% ($p<0.05$), by 1.25 μM to 68.35% ($p<0.05$), respectively. Treatment with valproic acid did not lead to any decrease in the global DNA methylation, but interestingly to a slight increase, even though not statistically significant (*Figure 59*).

3.2.6 Effect of epigenetic modifying drugs on the expression of pluripotency-related genes

OCT4A, *NANOG*, *SOX2*, *KLF4*, and *CMYC* were shown to induce pluripotency, if they are all expressed at the same time in human and mouse fibroblasts. A link between cell reprogramming and epigenetics connects these pluripotency markers with the chromatin remodeling. Thus, to analyse a possible effect of epigenetic modifying drugs on the differentiation potential of adMSCs, expression levels of the above mentioned genes were analyzed following treatment. The expression of the pluripotency-related markers was measured by real time PCR and quantified with the ΔCT method after normalization of each sample to housekeeping gene *GAPDH*. AdMSCs were treated again with 5μM AZA, 1.25 μM BIX, or 200 μM VPA for 48 h and non-treated cells were used as a control; their gene expression was set as 100%.

AZA and VPA had the tendency to increase the expression of *OCT4A* for up to 143.54% and 133.15%, respectively ($p=0.0705$ for both), statistical analysis showed however no significant differences. Only BIX treatment was able to significantly increase the expression of *OCT4A* up to 233.77% ($p=0.0112$) (*Figure 60A*). *SOX2* expression significantly increased to 263.36% ($p=0.0195$) after BIX treatment, while AZA or VPA did not have any significant effects (*Figure 60B*). For *NANOG* expression only BIX led to a significant increase to 152.93% ($p=0.0357$). Both AZA and VPA had a tendency to increase the expression of this marker to 147% and 142%, respectively ($p=0.09$ for both), but without significance (*Figure 60C*).

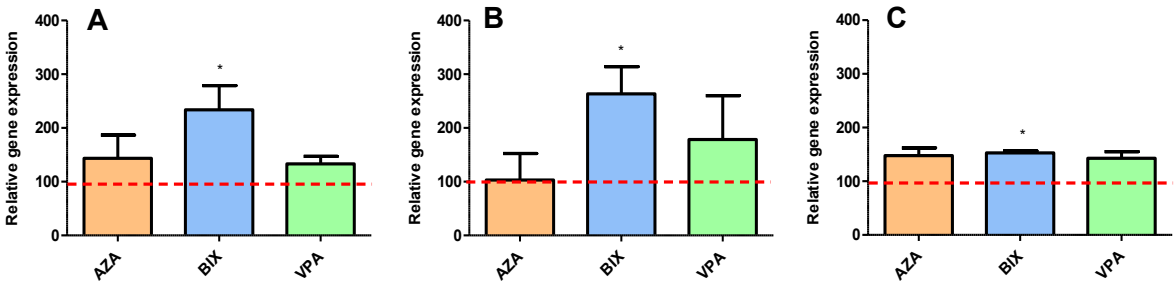

Figure 60. *Relative expression of pluripotency related genes: (A) OCT4A, (B) SOX2, (C) NANOG.*

Expression of the other pluripotency markers *KLF4* and *CMYC* did not significantly change after the treatment of adMSCs with none of these epigenetic modifying drugs (*Figure 61 A* and *B*).

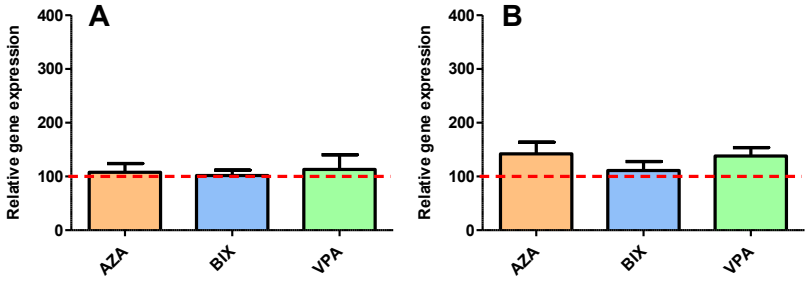

Figure 61. *Relative gene expression of (A) KLF4 and (B) CMYC after treatment with AZA, BIX, or VPA.*

In addition, a combination AZA, BIX, and VPA was tested to verify, whether the expression of pluripotency-related genes could be further increased. Combinations of each of the two substances and even all three did not lead to any significant increase in the expression of these genes compared to single treatment and was therefore not considered for further experiments.

3.2.7 Differentiation of adMSCs into endothelial cells

After proving the hypothesis that epigenetic modifying drugs, namely BIX and AZA, are able to modify the global DNA methylation, and also that BIX was able to significantly increase the expression of pluripotency related genes at mRNA level, the next step was to evaluate, whether the reprogramming capacity was increased as well. Therefore, adMSCs were pre-treated with AZA, BIX, and VPA for 48 h at the optimal non-toxic concentrations as described above and then the cells were cultured in endothelial medium for up to 14 days (*Figure 62*). Cells were microscopically analyzed after being stained for VCAM-1, von Willebrand Factor, VEGFR-2, and PECAM-1. In order to quantify the expression of the relevant endothelial cell markers (*VEGFR-2, VCAM-1*, *PECAM-1*, *F8*) and angiogenesis markers (*VEGF*, *PDGF*, *ANG-1*, and *ANG-2*), qPCR analysis was performed.

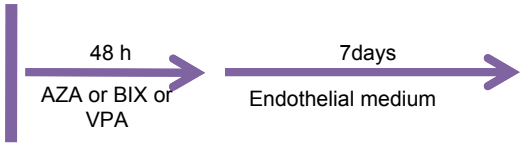

Figure 62. *Schematic view of the endothelial differentiation protocol using ICC.*

3.2.7.1 Evaluation of endothelial and angiogenenic markers by immunocytochemistry

During cultivation of adMSCs under endothelial conditions, the morphology of adMSCs changed with the time towards that of endothelial cells, showing the characteristical cobblestone-like shape. These changes were observed mostly in the group of epigenetic treated cells (*Figure 63*).

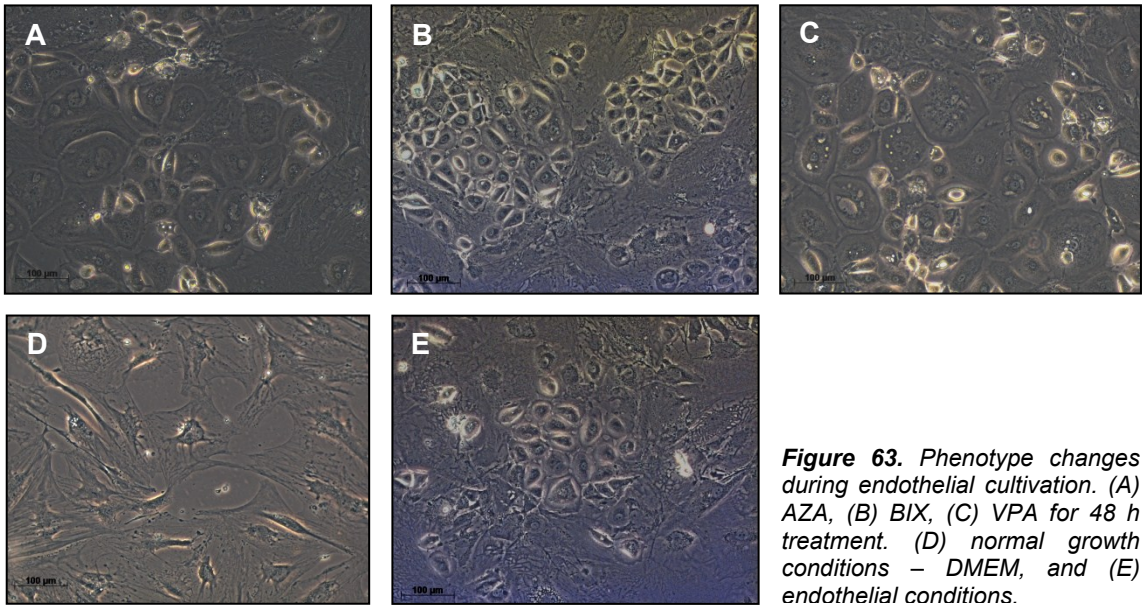

Figure 63. *Phenotype changes during endothelial cultivation. (A) AZA, (B) BIX, (C) VPA for 48 h treatment. (D) normal growth conditions – DMEM, and (E) endothelial conditions.*

To further characterize the differentiation process, ICC was performed after 7 days under endothelial cultivation conditions. The cells were stained against VCAM-1 (*Figure 64*), vWF (*Figure 65*), VEGFR-2 (*Figure 66*), and PECAM-1 (*Figure 67*). The increased number of positive cells in the group that received BIX treatment confirmed that BIX had the highest potential to increase the reprogramming capacity of adMSCs to differentiate into cells with endothelial characteristics for all endothelial markers used.

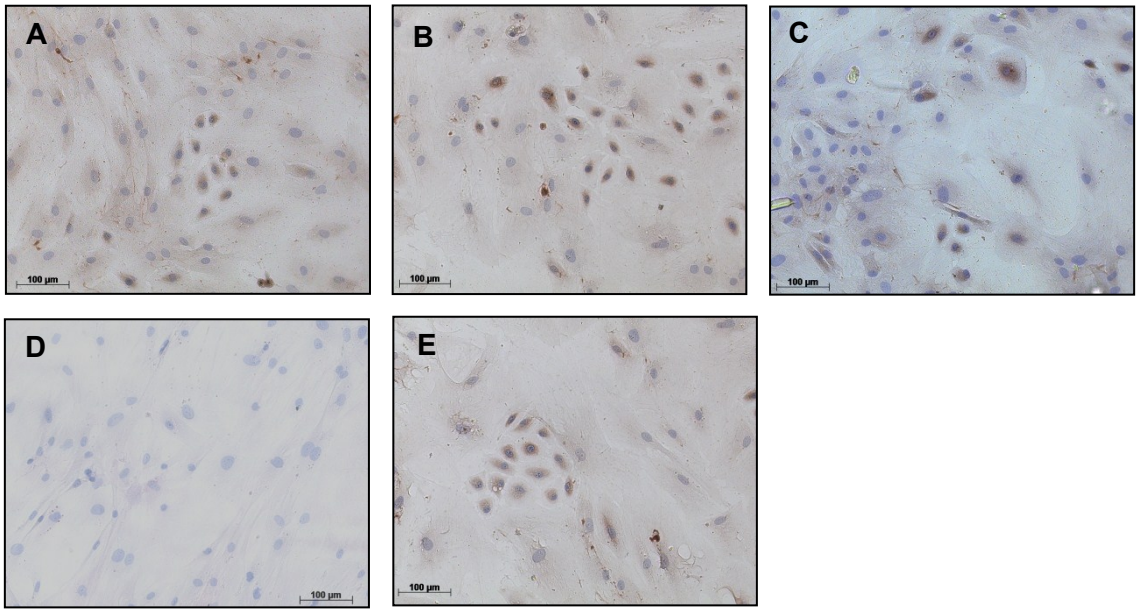

Figure 64. *VCAM-1 staining of adMSCs after 7 days under endothelial conditions. (A) AZA, (B) BIX, (C) VPA for 48 h treatment; (D) non-differentiating growth conditions (DMEM) and (E) adMSCs in endothelial medium without any epigenetic drug treatment.*

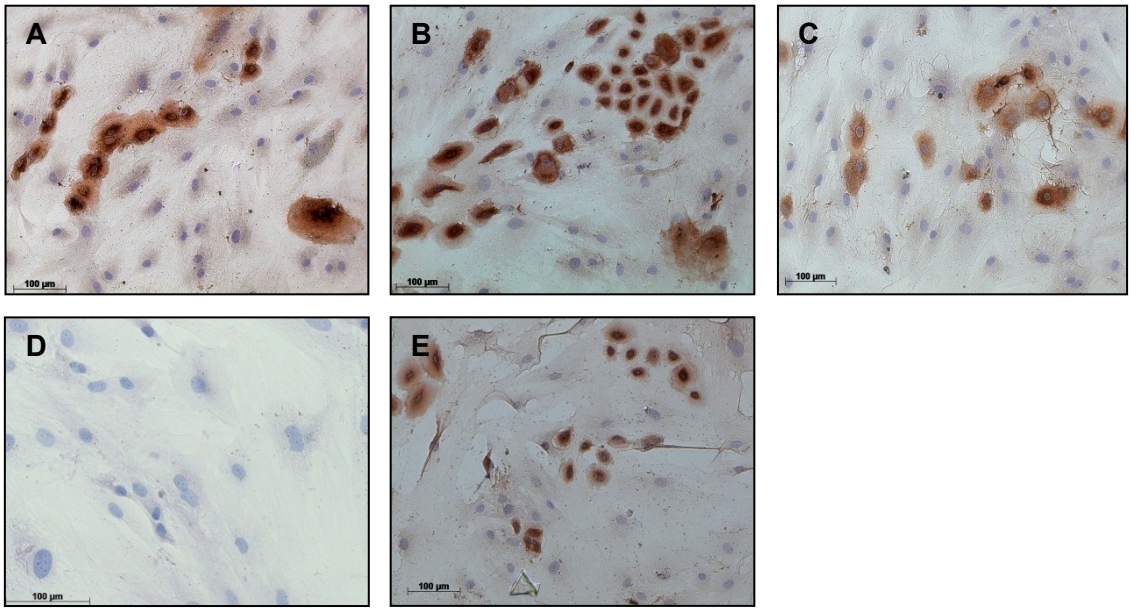

Figure 65. *Staining for von Willebrand Factor antigen after 7 days under endothelial conditions. (A) AZA, (B) BIX, (C) VPA for 48 h treatment; (D) non-differentiating growth conditions (DMEM) and (E) adMSCs in endothelial medium without any epigenetic drug treatment.*

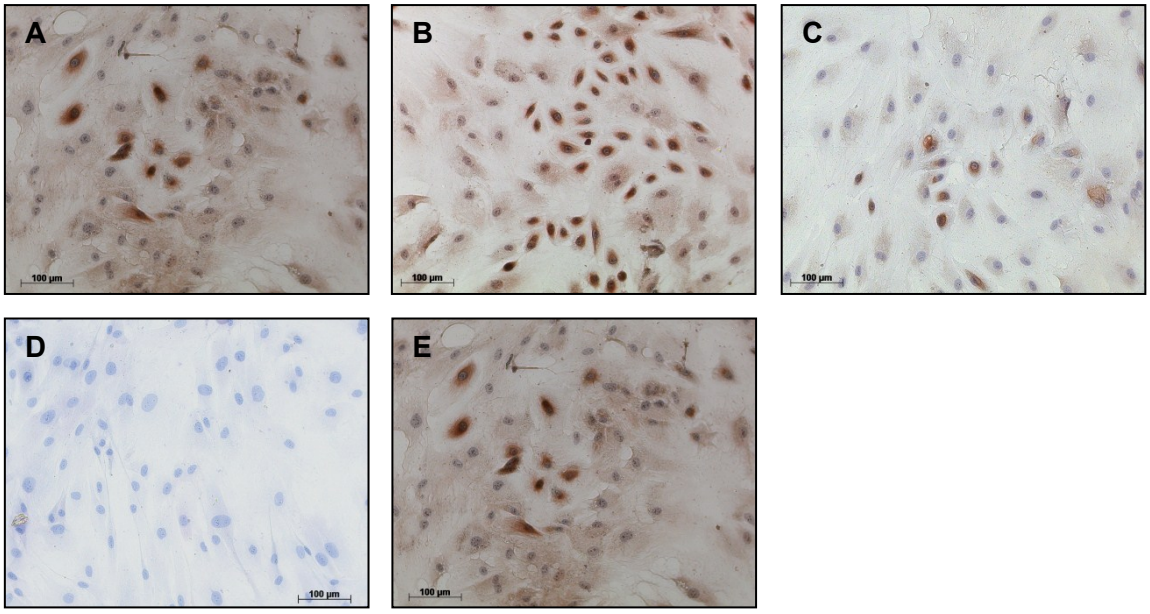

Figure 66. *Staining for the antigen VEGFR-2 after 7 days under endothelial conditions. (A) AZA, (B) BIX, (C) VPA for 48 h treatment; (D) non-differentiating growth conditions (DMEM) and (E) adMSCs in endothelial medium without any epigenetic drug treatment.*

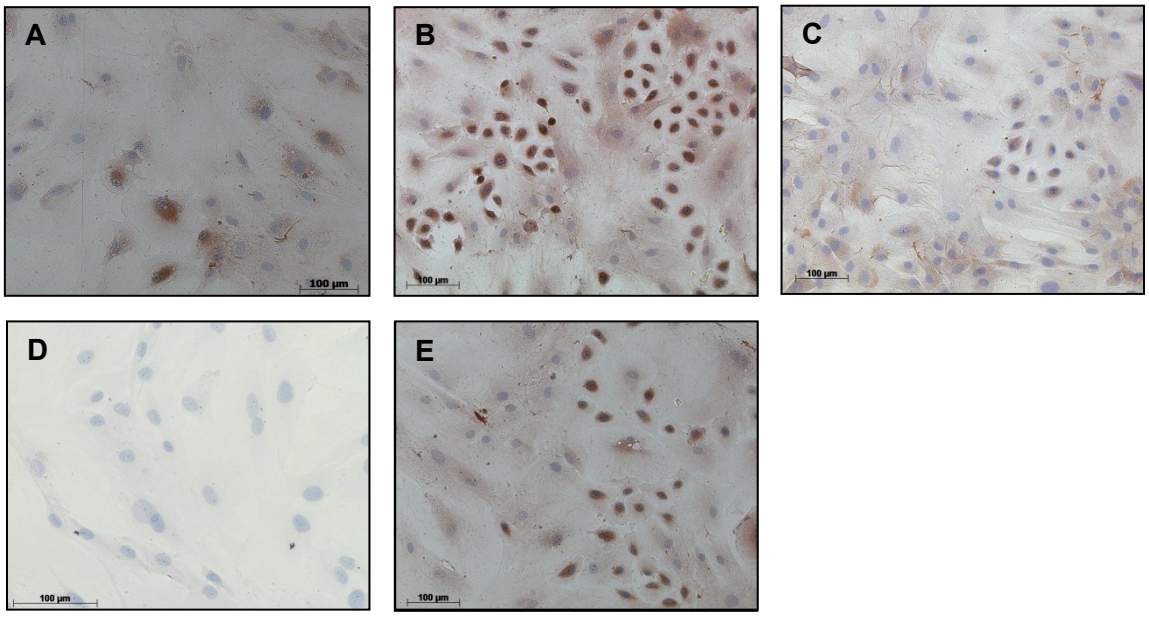

Figure 67. *Staining for the PECAM-1 antigen after 7 days under endothelial conditions. (A) AZA, (B) BIX, (C) VPA for 48 h treatment; (D) non-differentiating growth conditions (DMEM) and (E) adMSCs in endothelial medium without any epigenetic drug treatment.*

3.2.7.2 Evaluation of endothelial and angiogenesis markers at mRNA level

Since the most changes were observed in the group adMSCs that received a treatment with BIX before endothelial differentiation, the next experiments were performed only on these cells. *Figure 68* shows the protocol followed for the endothelial differentiation.

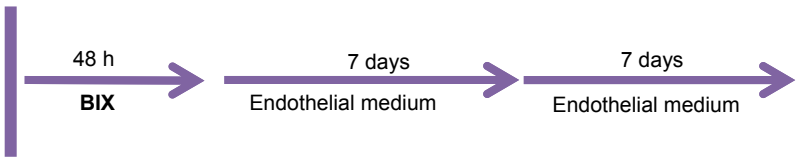

Figure 68. *Endothelial differentiation protocol for further characterization of the differentiation process at mRNA and protein level.*

The effect of BIX on the differentiation capacity of adMSCs into endothelial cells was determined analyzing the expression of genes activated in an endothelial lineage or involved in neovascularisation: *PECAM-1*, *VCAM-1*, *F8*, *VEGFR-2*, *VEGF*, *PDGF*, *ANG-1* and *ANG-2*. Two experimental groups of cells were compared: one group was cultured only in endothelial medium (EM), the other group was treated with BIX for 48 h before the endothelial medium was added (BIX plus EM). Gene expression was analyzed in adMSCs cultured for 7 and 14 days under endothelial conditions, and was normalized to *GAPDH*, with the EM group set as 100%. The results are presented in *Figure 69, 70, 71, and 72.*

PECAM-1 expression was increased by 2.91-fold (p=0.0500) after 7 days, and by 2.11-fold (p=0.0008) after 14 days of differentiation. As for *VCAM-1*, the increase was by 2.22-fold (p=0.0500) after 7 days and by 4.86-fold (p=0.0185) after 14 days of differentiation (*Figure 69*). Each of the increase was statistically significant.

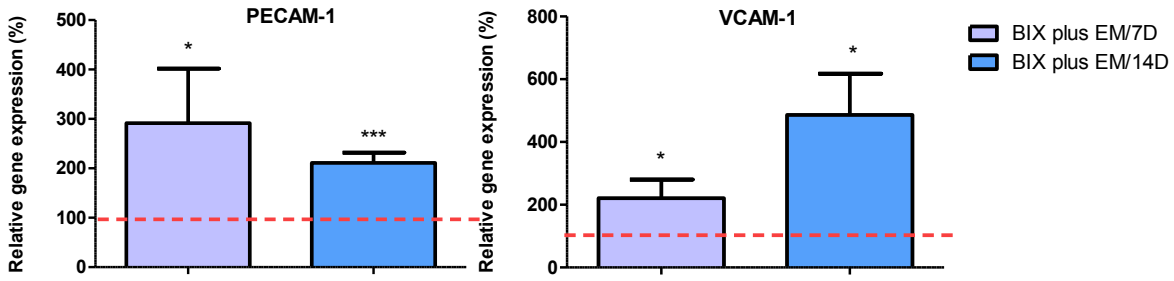

Figure 69. *Relative expression of PECAM-1 and VCAM-1 in the "BIX plus EM" group of cells after 7 and 14 days of endothelial medium; red line represents the expression of the same genes in the "EM" group of cells that was set as 100%.*

Von Willebrand factor gene expression was increased by 4.02-fold (p=0.0104) after 7 days and by 36-fold (p=0.0382) after 14 days in the "BIX plus EM" group. In the same group the expression of *VEGFR-2* was increased by 2.17-fold (p=0.0844) and by 4.53-fold (p=0.0235) after 7 and 14 days, respectively (*Figure 70*).

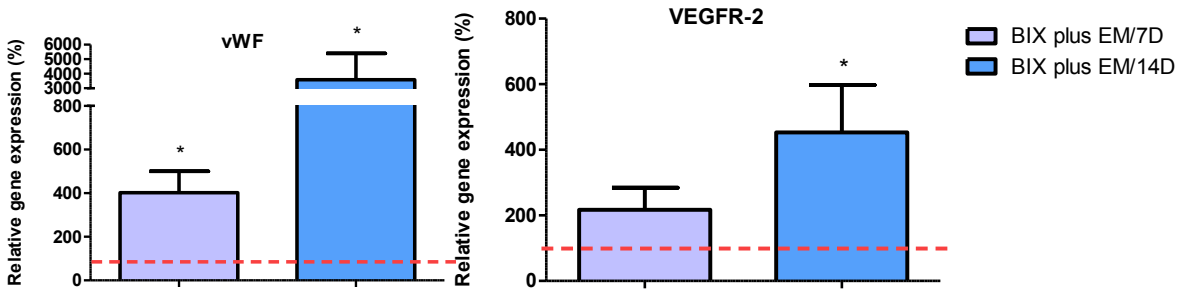

Figure 70. *Von Willebrand factor (vWF) and VEGFR-2 gene expression in the "BIX plus EM" group of cells after 7 and 14 days in endothelial medium; red line represents the expression of the same genes in the "EM" group of cells that was set as 100%.*

Expression of *VEGF* and *PDGF* was also analyzed. After 7 days under endothelial conditions, an increase of *VEGF* expression by 4.68-fold (p=0.0851) and by 2.34-fold (p=0.0131) after 14 days was observed. As for *PDGF*, similar increases were found by 2.78-fold (p=0.3655) after 7 days and by 5.21-fold (p=0.0017) after 14 days.

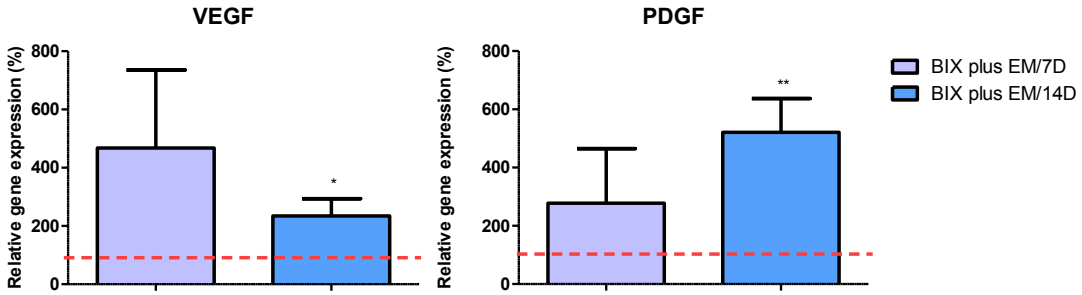

Figure 71. *VEGF and PDGF gene expression in the "BIX plus EM" group of cells after 7, and respectively 14 days in endothelial medium (EM). Red line represents the expression of the same genes in the "EM" group of cells that was set as 100%.*

In the “BIX plus EM” group significant changes in the expression of *ANG-1* and *-2* after 7 and 14 days were observed. Ang-1 expression was increased by 4.2-fold (p=0.0498) after 7 days and by 6.52-fold (p=0.0080) after 14 days, respectively. In contrast, expression of Ang-2 after 7 days under endothelial differentiation conditions presented a decrease by 0.40-fold (p=0.0498) and after 14 days by 0.64-fold (p=0.0498) in comparison with the EM group (*Figure 72*).

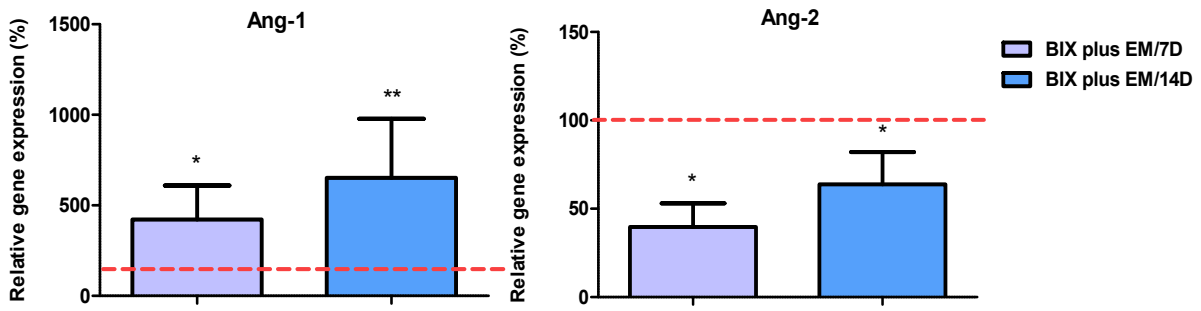

Figure 72. *Ang-1 and Ang-2 gene expression in the "BIX plus EM" group of cells after 7 and respectively 14 days in endothelial medium; red line represents the expression of the same genes in the "EM" group of cells that was set as 100%.*

3.2.7.3 Evaluation of endothelial and angiogenesis markers at protein level

In addition, to evaluate whether the increase in expression of endothelial and angiogenic factors take place also at protein level, selected markers specific for ECs showing significant differences in gene expression as shown above, VCAM-1 and VEGFR-2, were verified by western blot.

After quantification, results were normalized to the expression of GAPDH from the same samples. The amount of VCAM-1 protein was increased by 1.15-fold (p=0.0271) and by 2.04-fold (p=0.0286) after 7 and 14 days, respectively, compared with cells without BIX pre-treatment. The total amount of VEGFR-2 protein was increased after 7 days by 2.95-fold (p=0.0937) and after 14 days by 1.94-fold (p<0.0001) (*Figure 73*).

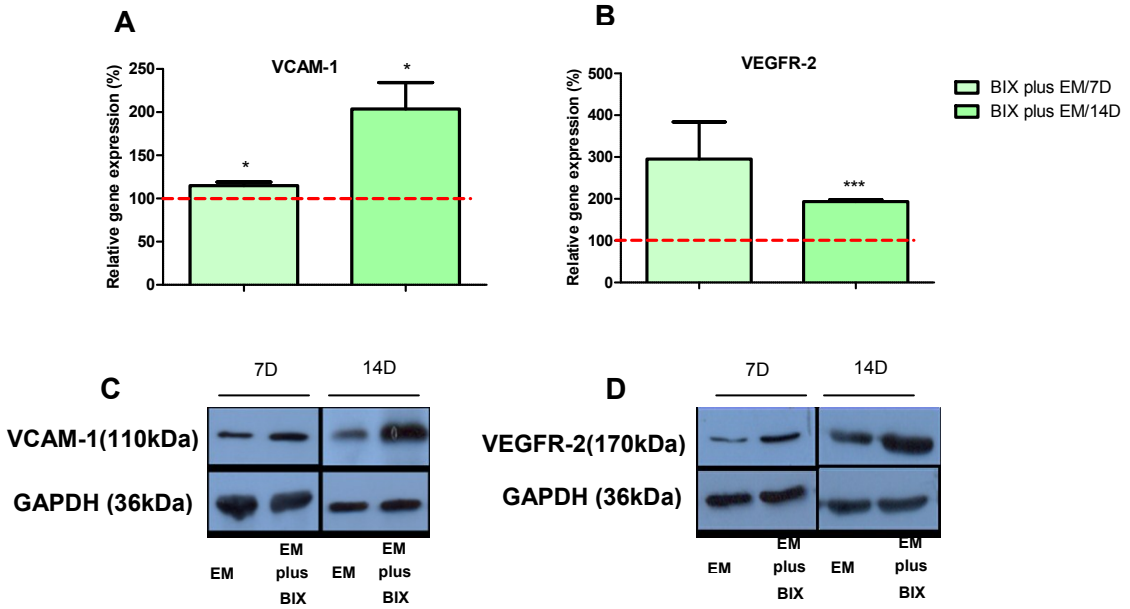

Figure 73. Western blot for VCAM-1 and VEGFR-2 in "BIX plus EM". *(A) VCAM-1 and (B) VEGFR-2 expression at protein level in the "BIX plus EM" group of cells after 7 and respectively 14 days of endothelial medium; red line represents the expression of the same genes in the "EM" group of cells that was set as 100% (C) representative blot for VCAM-1 and related GAPDH; (D) representative blot for VEGFR-2 and related GAPDH.*

3.2.7.4 Analysis of endothelial cell functionality

One of the typical tests for verifying the functionality of endothelial cells is the acLDL uptake assay. AcLDL is labeled with a carbocynine salt that emits fluorescent light at 488 nm (red). Since only endothelial cells and macrophages are able to metabolize acLDL, the red color will be observed only after metabolization of acLDL in this type of cells.

After adMSCs were cultivated in normal growth medium no cellular uptake was observed. In "EM"group of cells, low metabolization of labeled acLDL was observed (Figure 49). In contrast, cells it the group "BIX pus EM" presented the highest capacity to take up acLDL, *(Figure 74).*

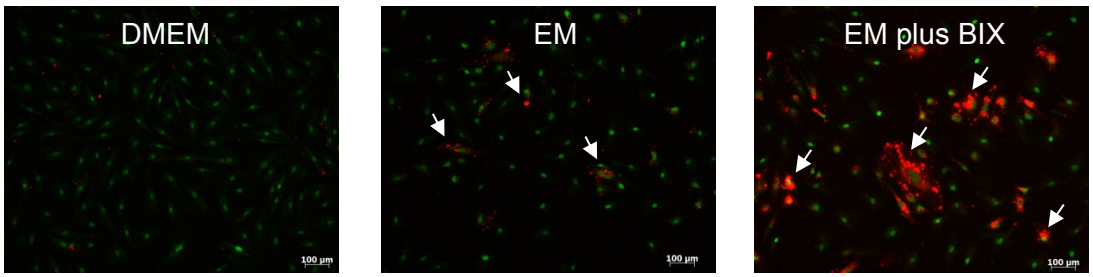

Figure 74. *AcLDL uptake into AdMSCs after 7 days under different cultivation conditions: DMEM (normal growth medium); EM (endothelial medium); EM plus BIX (AdMSCs have received BIX pre-treatment followed by cultivation in endothelial medium). Fluorescence staining for AcLDL labeled with DiI (red color), nuclear counterstaining with SybrGreen I Dye (green color).*

3.2.8 Autologous vessel for tissue engineering

3.2.8.1 Preparation of collagen based scaffold by decellularization of blood vessel

Decellularization of a collagen based scaffold can be done with several methods (physically, chemically, or enzymatic methods or these combined). In the present work, to obtain the acellular vessel scaffold, the chemical decellularization method was used. The acellular scaffold was obtained after optimization of the decellularization process with 0.66% SDS. Four time points were considered in order to establish the optimal protocol: 1, 24, 48, and 96 hours of treatment. Saphenous vein was washed with 0.66% SDS for the established time duration. The concentration of 0.66% SDS was previously established to be the lowest concentration that removed all the cellular components.

After treatment of the saphenous vein with 0.66% SDS at the different time points for up to 96 h, H&E staining was performed and the vessel was analyzed by light microscopy. Treatment of the vessel for 48 hours was considered to be sufficient to achieve complete cell removal (*Figure 75*).

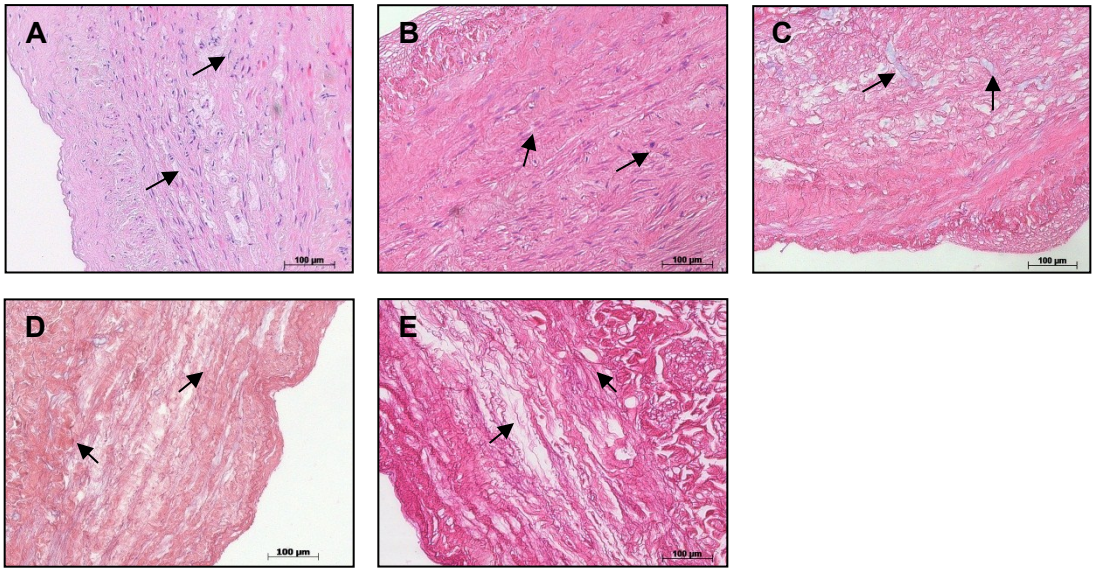

Figure 75. *H&E staining of the saphenous vein after treatment with SDS at different time points. (A) control vessel - not decellularized; (B) 1 h washing with 0.66% SDS; (C) 24 h washing with 0.66%SDS; (D) 48 h washing with 0.66% SDS; (E) 96 h washing with 0.66% SDS; blue color is representing the nuclear stain; original magnification 200x.*

Consequently, these conditions were used for the following experiments. As shown in *Figure 76*, the macroscopic structure and form the biological scaffold was unaffected and retained the shape and size of the original vessel.

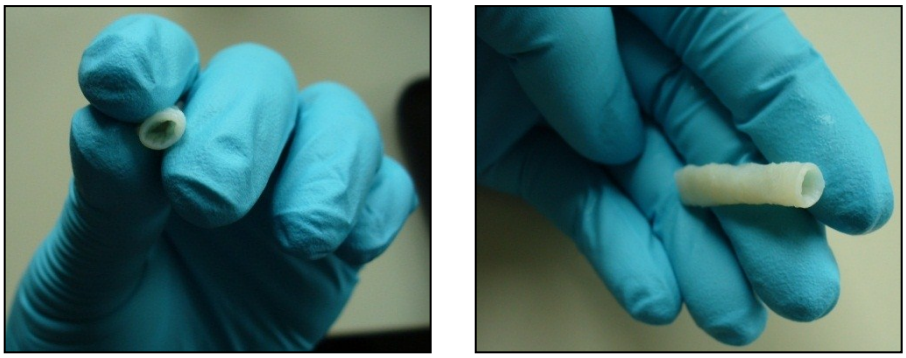

Figure 76. *Macroscopic view of the collagen-based scaffold after decellularization process. The biological scaffold maintained the shape and the size of the original vessel.*

3.2.8.2 Attachment of differentiated adMSCs on the decellularized blood vessel

Following the optimization of the decellularization protocol, the next step was to evaluate, whether endothelial cells, differentiated from adMSCs after BIX treatment, were able to attach to the previously established biological scaffold.

Various time points were tested for the optimal seeding time. The majority of cells attached already after 2.5 h in a Petri dish, therefore the same incubation time was assumed also for the attachment on the biological scaffold.

After the differentiated adMSCs were seeded onto the decellularized scaffold, the cell behavior was followed for up to 7 days. The scaffold and the cells were prepared as follows: cells have been suspended in small volume of growth medium and seeded into the lumen of the previously obtained matrix. The vessel segments were incubated in 5%CO_2 at 37°C for 2.5 h. Thereafter, the EM was added, and after 2 and 7 days of culture the constructs were histologically analyzed.

The staining applied verified the cell attachment. Two days following seeding, cells started to form a monolayer at the surface of the scaffold. In addition, some cells migrated into the deeper layers. After 7 days, a higher cell density was observed on the surface of the scaffold compared with the first time point. However, some cells seemed to detach from the scaffold (*Figure 77*).

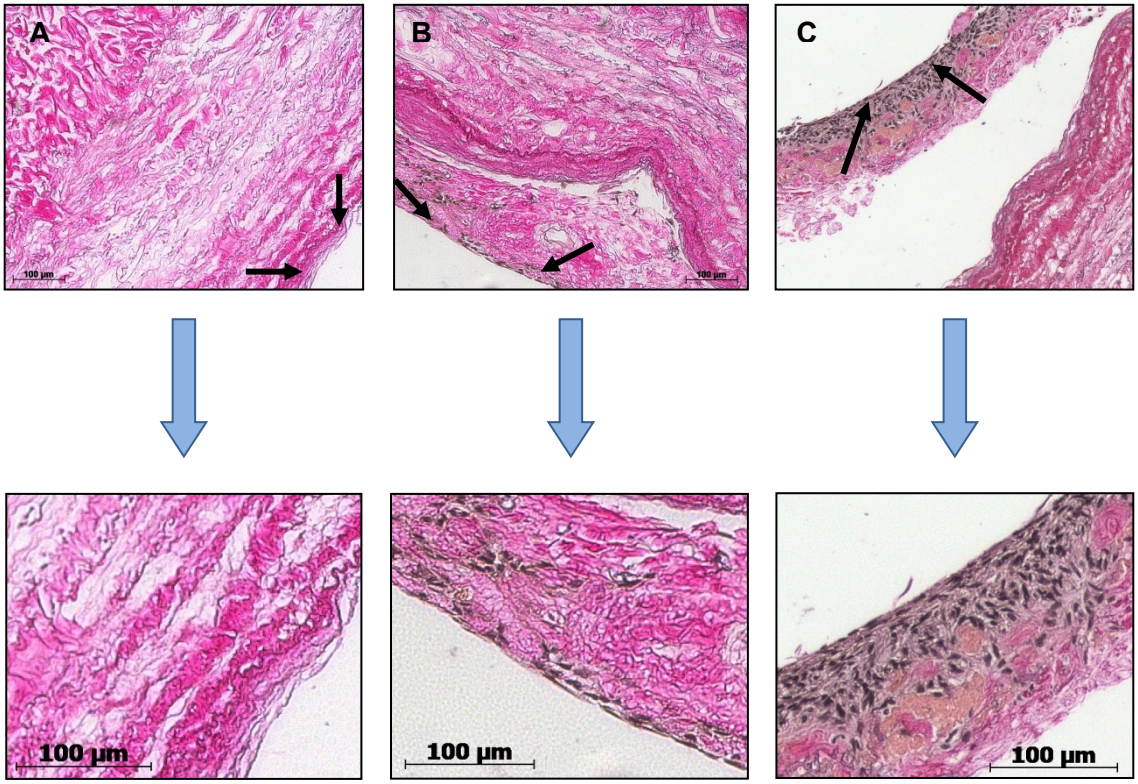

Figure 77. *Van Gieson's staining of biological scaffold. - (A) decellularized vessel; (B) 2 days after new cells were seeded; (C) 7 days after new cells were seeded. Lower part corresponding pictures are with a higher magnification. Black color represents the nuclear staining.*

3.2.9 The influence of donor age on the properties of adMSCs

By regular examination of the morphology of adMSCs in culture, differences were noticed between different cell populations. Since the isolation procedure and cultivation were standardized, the differences were assumed to be associated with origin of the adipose tissue from which the cells were isolated. The most plausible explanation was the different age of the donors, the adipose tissue was isolated. For this purpose, 13 donors were divided

into two groups, namely young (less than 50 years old) and elderly (more than 50 years old) as described in *Table 20*. The osteogenic and adipogenic differentiation potential of adMSCs were verified again in the third passage.

Table 20. *Study groups for the cells originating from elderly and young donors.*

Mean age (years)	Patient gender	Group
69±13.5 (60-88)	3 women 4 men	**elderly**
39±14 (21-49)	4 women 2 men	**young**

3.2.9.1 Osteogenic and adipogenic differentiation

3.2.9.1.1 Osteogenic differentiation

Following osteogenic differentiation for 7, 14, and 21 days, the two groups were examined for the presence of alkaline phosphatase (ALP). Quantitative assays revealed a 1.8-, 2.4-, and 2.1-fold ($p<0.05$) increase in ALP activity (*Figure 78 A*) in the groups of cells isolated from younger individuals at 7, 14, and 21 days of differentiation, respectively, compared to cells from elderly donors. Differences between the groups were observed also after staining for ALP (*Figure 78 B, C, and D)*.

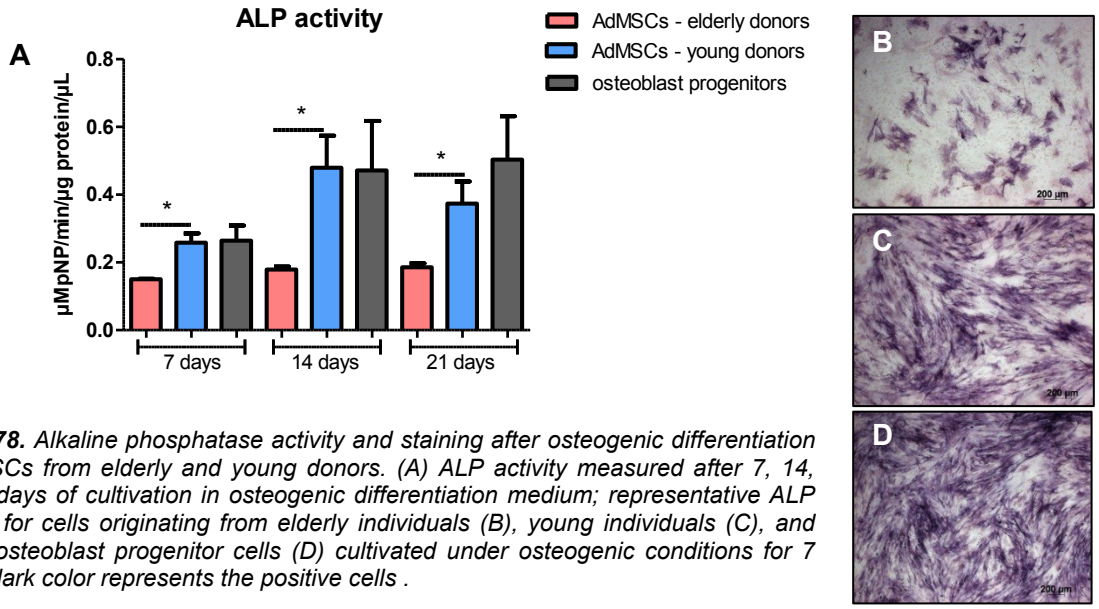

Figure 78. *Alkaline phosphatase activity and staining after osteogenic differentiation of adMSCs from elderly and young donors. (A) ALP activity measured after 7, 14, and 21 days of cultivation in osteogenic differentiation medium; representative ALP staining for cells originating from elderly individuals (B), young individuals (C), and human osteoblast progenitor cells (D) cultivated under osteogenic conditions for 7 days – dark color represents the positive cells .*

3.2.9.1.2 Adipogenic differentiation

Following adipogenic differentiation for 14 and 21 days, adMSCs from the two groups of donors were examined by Oil Red O staining (*Figure 79*) and quantified accordingly (*Figure 80*). Under adipogenic conditions, adMSCs changed their shape to round or squared and produced lipid droplets. After the staining of the droplets with Oil Red O and using typical light microscopy technique, it was observed that cells originating from younger individuals produced droplets larger in diameter than cells from elderly donors. On the other side, there were more droplets in the cells from the elderly group than in the young group. Moreover, all cells belonging to the elderly group contained lipid droplets. In contrast, in younger individuals also cells without droplets were found.

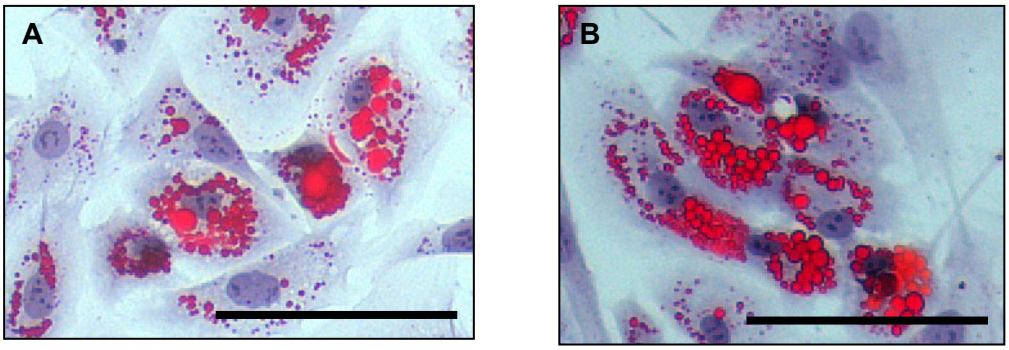

Figure 79. *Oil Red O staining in adMSCs under adipogenic differentiation conditions. AdMSCs from elderly (A) and young (B) donors, after 14 days under adipogenic conditions; scale bars represent 100 µm, magnification 200x.*

After solubilizing the lipid droplets in isopropanol, spectrophotometric quantification revealed no significant differences between populations from young and elderly donors after 14 and 21 days under adipogenic conditions. Nevertheless, production of oil droplets was increased up to 11-fold ($p<0.0001$) at day 21 compared to day 14 for both groups.

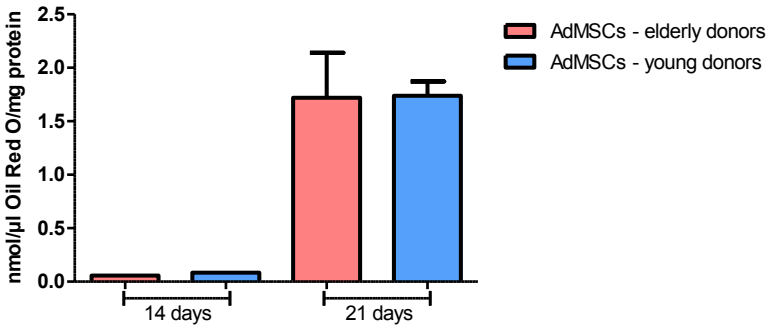

Figure 80. *Quantification of the adipogenic differentiation of adMSCs from young and elderly donors - Oil Red O quantification assay showed an 11-fold increase in lipid production after 21-days reference point compared to the 14-days point. No significant differences were observed between the young and elderly donors.*

3.2.9.2 Analysis of cell proliferation

Ki67 is a nuclear protein marker for cellular proliferation. It can be exclusively detected within the cell nucleus during all active phases of the cell cycle (G_1, S, G_2, and mitosis), but is absent in resting cells (G_0). Both study groups were stained for Ki67 to evaluate possible differences in cell proliferation.

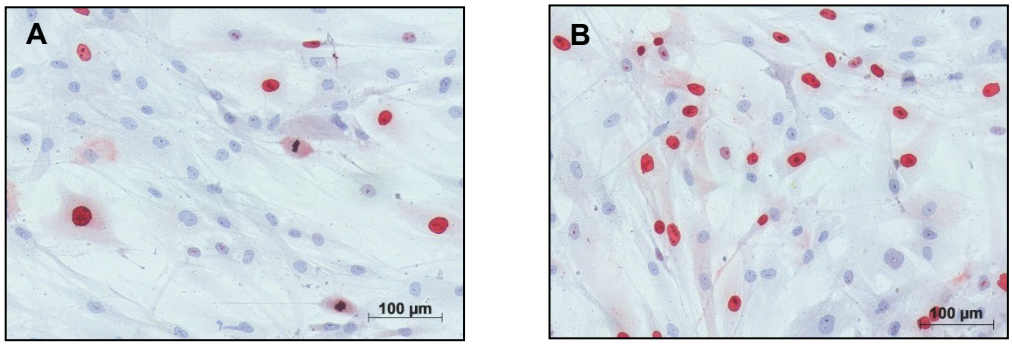

Figure 81. *Proliferating cells in the comparison groups – elderly and young. Staining for Ki67 antigen in adMSCs from elderly (A) and young (B) donors. Red color represents the positive cells.*

For cell populations originating from elderly donors, 29.04% were positive for Ki67 antigen (*Figure 81*). Regarding the cell population originating from younger donors, 66.26% were positive for this marker of proliferation Comparing these two study groups, younger donors demonstrated significant higher proliferation by 2.28-fold (p=0.0022) than elderly cell population (*Figure 82*).

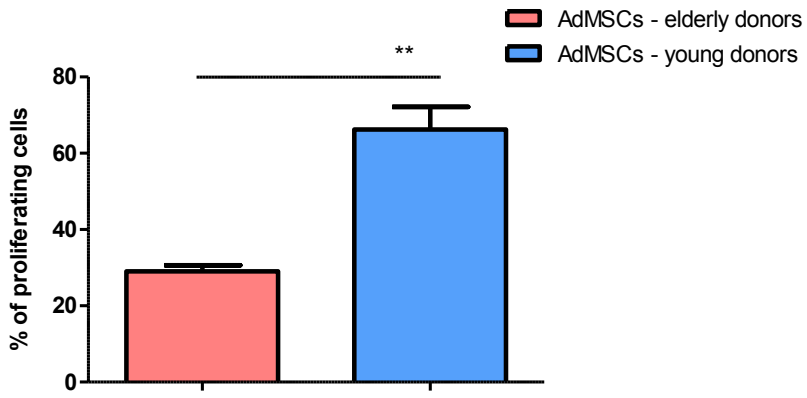

Figure 82. *Quantification of proliferation rate in young and elderly donors. Ki-67 staining was analyzed by the ImageJ software.*

3.2.9.3 Analysis of global DNA methylation

DNA was isolated from both study groups, elderly and young donors and the DNA methylation was evaluated by the MethyLight assay. After normalization to the control DNA (completely methylated DNA) that was set as 100%, it was observed that in cells from elderly donors the global DNA methylation was 32.36% ($p<0.05$) and that from young donors was 26.28% ($p<0.05$) compared to control (*Figure 83*). In elderly group it was observed an increase by 1.23-fold ($p=0.0186$) in global DNA methylation compared with the group of young donors.

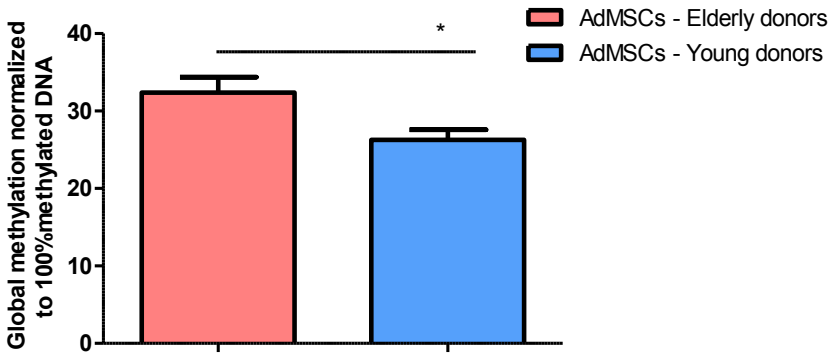

Figure 83. *Global DNA methylation in adMSCs from young and elderly donors. DNA-methylation was significantly lower in cells isolated from young patients.*

3.2.9.4 Expression of pluripotency-related genes

Since the global DNA methylation status was reduced in cells from young donors, the next step was to verify expression of pluripotency associated genes at mRNA level. The expression of *OCT4A*, *NANOG*, *SOX2*, *KLF4, and CMYC* was assessed using SybrGreen-based real time PCR and normalized to the expression for the housekeeping gene *GAPDH* (*Figure 84*).

In cells from young donors, expressions of genes *NANOG* and *SOX2* were significantly increased by 7.97-fold ($p=0.0415$) and 20-fold ($p=0.0415$), respectively, compared with the elderly group. *OCT4A*, *KLF4*, and *CMYC* showed a tendency to increase their expression in the cells from young donors by up to 11.74-fold ($p=0.3992$), 2.48-fold ($p=0.0603$), and 1.08-fold, respectively ($p=0.1524$), again compared to the elderly donors, however without statistical significance.

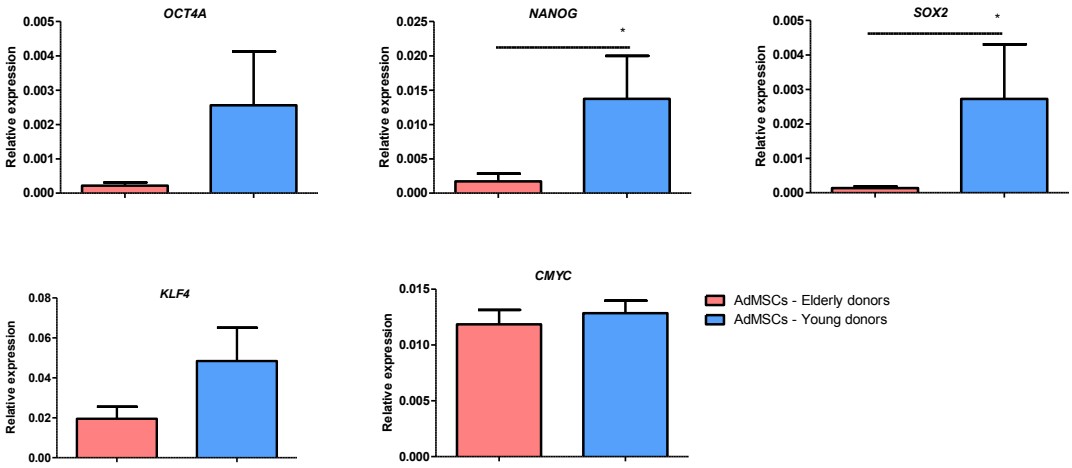

Figure 84. *Expression of pluripotency related genes in adMSCs originating from elderly and young donors. Statistically significant differences were observed for NANOG and SOX2 expression. Both markers had increased expression in the cells from young donors.*

4 DISCUSSION

4.1 Epigenetics and vascular disease – atherosclerosis

4.1.1 DNA methylation in early and advanced atherosclerotic plaque and serum

Chromatin is a flexible structure undergoing dynamic changes throughout the whole life. These heritable alternations of chromatin - leading to changes in gene expression or phenotype without influencing the underlying DNA sequence - are called epigenetics. The most interesting feature of epigenetics is that it can be affected by environmental interactions, giving the organism a feedback from surrounding conditions. Emerging evidences implicate a spectrum of epigenetic changes in the pathophysiology of atherosclerosis.

The results of the present study showed significant changes in the epigenetic pattern in advanced atherosclerosis, especially DNA- and histone-methylation, which was the aim of the current thesis. Furthermore, epigenetic changes correlated with the severity of atherosclerosis in carotid lesions. Thus, results confirmed the important role of epigenetics in atherosclerosis.

Characterization of carotid AS plaques had shown the classical morphology of atherosclerosis lesions, as described by Herbert Stary in accordance with AHA [75, 76]. Following plaque classification two study groups were built: early and advanced stage of atherosclerosis. The early stage comprised lesions type I, II, and III. For these stages, histopathology showed typical morphology of the AS plaque with macrophages infiltration and intimal thickening [76]. For the advanced stage lesions of type V, VI, and VII were chosen. The typical morphology for each lesion type observed was lipid core (type V) accompanied by thrombotic deposits (type VI), and necrotic core with calcified lesions (VII) [75]. Type IV, the first potential clinical lesion, characterized by a massive aggregate of extracellular lipid (a lipid core) without any fibrotic cap, thrombosis or hemorrhage, was excluded from the current study because very few patients, who underwent CEA in the Department of Vascular Surgery, had this type of lesion. In addition, type VIII, consisting entirely or almost entirely of scar collagen with minimal or absent lipid deposition and small vessel lumen, was also excluded from the study. As mentioned for type IV, type VIII was also

seldom in the biobank of the Department for Vascular end Endovascular Surgery, from which the plaques were selected.

DNA methylation can affect gene expression by preventing the access of transcription factors to the CpG nucleotides. A decreased level of methylation especially in the promoter region of a gene is usually acknowledged as transcriptional active site, while the hypermethylation status is associated with transcriptionally silent state of gene activity. So far, very little is known about the changes in DNA methylation in atherosclerotic lesions and almost nothing in carotid plaques. Therefore, at first, the global DNA methylation status was analyzed. For this purpose three repetitive elements (LINE1, Satα, and Alu1) were selected. They are acknowledged as a surrogate marker for estimating global methylation levels [214]. Repetitive elements represent a large percentage of the human genome; approximately 45% of the genome is represented by interspersed repeats from transposable elements and tandem of simple sequences (DNA satellites) or complex sequences [214].

In the current work, DNA methylation was investigated by the method of Weisenberger *et al.* [214], who validated MethyLight, a Taqman-based real time PCR assay based on methylation of DNA repetitive elements. The results showed that the hypomethylation of DNA was significantly associated with the severity of atherosclerosis in the analyzed carotid plaques. Compared with healthy vessels, global DNA methylation diminished to 60% in early stages of atherosclerosis and was further reduced to 30% in advanced atherosclerotic lesions. Consequently, the level of DNA methylation in the repetitive DNA sequences LINE1 and SATα might also serve as an epigenetic marker of progression of atherosclerotic lesions. These results were confirmed by blood analysis, with significantly reduced methylation of DNA from serum of patients with advanced carotid artery stenosis, compared to healthy individuals. These results confirm the work of Castillo-Diaz and colleagues [92], who observed extensive DNA demethylation in human coronary samples of atherosclerosis. Interestingly, these data were in discordance with the work of Stenvinkel and colleagues [217], who found global DNA hypermethylation in blood samples of patients with cardiovascular disease. However, Stenvinkel included patients with chronic kidney disease (CKD) and analysed, in contrast to the present study, peripheral blood leucocytes. CKD is frequently associated with chronic inflammation, which has been already suggested to be associated with with general genome hypomethylation but selective gene hypermethylation and silencing [218]. These discrepancies confirm the importance of epigenetic changes in various diseases. Mechanistically, loss of DNA methylation may have several causes. For example, it could be a consequence of abnormal cellular proliferation, a local deficiency of methyl donors, or both. Early studies have suggested that e.g. certain

premalignant conditions may lead to decreased tissue folate content and, thus, a local deficiency in methyl donors [219].

4.1.2 DNA methyltransferases in atherosclerotic lesions

Methylation of DNA is provided by adding a methyl group at the nucleotide, mainly at the promoter site. The methylation of DNA is directed by a family of DNA methyltransferases (DNMTs) with DNMT1, DNMT3A, and DNMT3B as only functional known members. The role of DNA methylation and DNMTs in cancer and developmental studies has been extensively examined. In contrast, the expression pattern of DNMTs in atherosclerosis is so far unknown. The results from the DNA methylation experiments in this study demonstrated significant hypomethylation in advanced atherosclerotic lesions. The next logical explanation for these changes would be alternations in the expression of DNMTs.

The results reported in this work showed that the expression of *DMNT1* decreases with the progression of AS, which was in accordance with the study of Hiltunen *et al.* [13]. DNMT1 is a methyltransferase responsible to maintain methylation of DNA within the cell. Thus, a decrease in the expression of *DNMT1* might be one of the principal causes in the reduction of the level of global DNA methylation found in the carotid tissue and in serum from patients with high graded carotid artery stenosis. DNMT1 is constitutively expressed and methylates newly replicated DNA only when the template nucleotides are methylated. Consequently, the function of DNMT1 is to maintain global methylation after replication of DNA. Our results suggest however the function of DNMT1 also in the maintenance of DNA methylation, which would explain the significant demethylation in atherosclerosis.

In agreement with results obtained for global DNA methylation and decreased expression of *DNMT1*, it was found that the expression of methylcytosine dioxigenase *TET1* (Ten-eleven translocation 1) increases with the progression of atherosclerosis. This protein is an enzyme involved in the demethylation process, responsible for the intermediate form 5-hidroxymethylation. It catalyzes the conversion of the modified genomic base 5-methylcytosine (5mC) into 5-hydroxymethylcytosine (5hmC). It initiates a process leading to cytosine demethylation through deamination into 5-hydroxymethyluracil (5hmU) and subsequent replacement by unmethylated cytosine by the base excision repair system playing an important role in transcriptional regulation [220]. By controlling the levels of 5mC and 5hmC, it may regulate gene expression [21, 22, 221]. In conclusion, if DNMT1 does not function properly, it does not add methyl groups to maintain methylation. In addition, if the

demethylase TET1 has an increased function, the results are that the genome wide demethylation will be induced.

De novo methylation process is provided with the help of DNMT3A and DNMT3B. Notably, *DNMT3A* expression was not found in the analyzed samples. *DNM3B* expression level was found to be decreased in the atherosclerotic tissue, again corresponding with AS progression. The expression of *DNMT3B* was however up to 1000-fold lower than the expression of *DNMT1*. These results are in agreement with the study of Spin et al. [222] and indicated a significant downregulation of *DNMT3A* and *3B* in e.g. SMCs during de-differentiation. In contrast, the work of Yiden et al [85] correlated genome wide hypomethylation induced *in vitro* in vascular smooth muscle cells (VSMCs) by homocysteine (Hcy) with increased levels of *DNMT3A* and *DNMT3B*. Since in the current work the level of *DNMT3B* is decreased, it might be possible that Hcy is not the primary trigger of AS, but an intermediary step in the progression of atherosclerosis. Nevertheless, the increased levels of Hcy may contribute, together with oxidative stress, apoptosis and inflammation to the progression of AS.

4.1.3 Correlation of methylated K4 and K9 of histone H3 with smooth muscle cells, inflammatory cells, and the progress of atherosclerosis

Based on the obtained results it was concluded that global DNA methylation might be used as a potential marker for the progression of AS. However, DNA methylation is just a part of the vast epigenetic apparatus. Transcription factors can bind more easily the hypomethylated promoter region of a gene, but only if this area of genome is accessible. Histone modifications play an important role in chromatin remodeling and changes to the histone tails control the state of the chromatin. Especially histone methylation is a highly interesting modification that, depending on the site of methylation, can lead either to gene activation or silencing. Furthermore, there is clear evidence that DNA and histone methylations are tightly controlled [223]. The histone H3 with an unmethylated K4 is required for DNA methylation [224]. In addition, methylation of histone H3 on K9 participates in DNA methylation as well, mediated by DNMT1 [120]. Because de-methylation seems to be the most important modification of H3K4 and H3K9 [225], this modification was analyzed in the present study in order to find out whether it corresponds with the progression of atherosclerosis and whether these changes can be associated with a certain type of cells, e.g. smooth muscle cells or inflammatory cells.

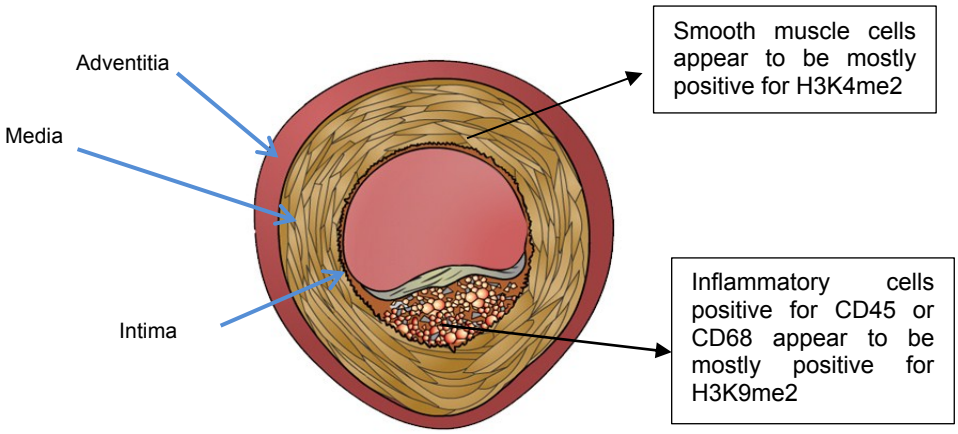

By staining of consecutive slices it was possible to connect the presence of smooth muscle cells in all stages of atherosclerosis and control tissue with the H3K4me2 positive cells. Interesting was to observe that with the progression of AS the smooth muscle cells were weaker stained in comparison with the control tissue. The reason for this is currently unknown and must be further investigated.

In contrast to skeletal and cardiac myocytes, mature vascular smooth muscle cells (VSMC) have the capability to modulate their phenotype towards an earlier state (de-differentiate) in response to multiple environmental signals, particularly under stimuli associated with vascular injury and diseases. These “de-differentiated” VSMCs present down-regulated markers and contractile proteins. Under this phenotype the cell may migrate, proliferate, produce extracellular matrix (ECM), and remodeling factors [222]. In the current study, VSMCs positive for H3K4me2 and their decreasing expression with the progression of atherosclerosis correlates with the phenotype changes in a vascular injury that leads to AS. Since H3K4 methylation is a reversible modification [226], the de-differentiated VSMCs could be, under favorable conditions, induced to re-differentiate into normal contractile state, and methylation of H3K4 may be regarded as a potential target for drug therapy in AS.

Regarding histone H3K9 methylation, VSMCs in control tissue were almost all negative. In AS samples these cells were increasingly positive with the progression of the disease. H3K9me2 is a marker known to be acting as a suppressor of transcriptional activity, by involvement in the suppression of contractile proteins of the normal VSMCs. This hypothesis is reinforced by the study of Lockman et al. [227], where the overexpression of histone demethylase was associated with decreased expression of H3K9me2 and with increased expression of transgelin. The other way around, the increased expression of H3K9me2 is associated with down-regulation of transgelin in normal VSMCs. By contrast, another study [228] showed that *in vitro* demethylation of the K9 lysine may trigger conversion to the transcriptionally viable euchromatin during SMC differentiation. The exact

mechanism is far from being understood due to high complexity of the H3K9me2 modification involvement in many different pathways.

The epigenetic modifications of the inflammatory cells within AS plaque must not be ignored. Consecutive tissue sections from the investigated samples were stained for CD45, CD68, and H3K4me2, and matching areas were compared. It was observed that almost all CD45-positive cells and all CD68-positive cells, both in early and advanced stage, were slightly positive for H3K4me2. Additionally, by western bot analysis of the AS samples, a significant decrease in the expression of H3K4me2 was observed with the progression of AS. Di-methylation of H3K4 has been reported as a boundary marker, preventing the spread of "repressive modifications" into the active regions, or directing modifying activities to the locus in a developmentally appropriate manner [229]. Histone H3K4 di-methylation has been shown to enhance the NF-κB-dependent expression of inflammatory genes in macrophages [230]. Correlations between increased H3K4 methylation and induction of transcription are also observed at most, but not all, loci where transcription is induced. Thus, H3K4 methylation may be used to control chromatin activity [231].

Nearly all CD45 positive cells were also positive for H3K9me2 in the immunohistological analysis of corresponding areas. Additionally, the western blot analysis of the tissue samples confirmed these results, amount of H3K9me2 positive cells increased with the progression of AS and with accumulation of inflammatory cells. The study of Tachibana concludes that H3K9me2 is dispensable in the B-cell lineage and/or other differentiated cells and that B cells require minimal levels of H3K9me2 [53]. Therefore, not surprisingly, the CD68 positive cells presented same characteristics for these two histone markers, as shown in the present work. Tissue- and/or stage-specificity of leucocyte development are controlled at many genetic and epigenetic levels beyond the simple presence of H3K9me2. More important might be that hypoxia is influencing the H3K9me2 with a concomitant loss of a specific histone demethylase activity that is followed by increased H3K9 methylation [232]. In the context of AS, it is already well recognized that hypoxia plays an important role in the progression of this disease [233].

In conclusion, methylation of H3K4me2 might be associated with changes in the phenotype of VSMCs and the methylation of H3K9me2 seems to be associated with inflammatory cells in atherosclerotic lesions. The western blot analysis of fresh samples, in controls, early and advanced stage AS, revealed interestingly a decrease in the di-methylation of both H3K4 and H3K9. A possible explanation for the discrepancy between IHC and western blot might be the involvement of other epigenetic mechanisms, such as histone acetylation/deacetylation. DNA methylation and histone deacethylation play also an

important role in the regulation of the H3K4me2. A recent study on T cells showed that AZA or trichostatin A (histone deacetylase inhibitor) were able to also affect di-methylation of K4 beside their known effects on DNA methylation and histone deacetylation [225]. Such results demonstrate that the processes of DNA methylation, histone methylation, and histone acetylation are connected and more complex than currently thought.

4.1.4 Gene expression of histone methyltransferases

Methylation of histones is accomplished by histone methyltransferases (HMTs). HMTs are enzymes, which catalyze the transfer of one to three methyl groups from S-adenosyl methionine to lysine or arginine residues of histone proteins. Responsible for adding a methyl group to the H3K4 site are HMTs containing the human SET1 (hSET1) domain. Among them are MLL1, SETD1A and SETD1B. The expression analysis showed that only *MLL1* increased continuously with the progression of AS.

The MLL1 gene product is required for control of vertebrate HOX gene expression and thus involved in many developmental processes [234]. It is a candidate for establishing the patterns of H3K4 methylation. MLL1 has H3K4 methyltransferase activity [58, 235], but is unable to generate tri-methylation of H3K4 *in vitro* [235]. Furthermore, MLL1 has links to B-cell development, as translocations in the *MLL1* gene can cause malignancy in pre-B cells suggesting the involvement of H3K4 methylation pattern in malignancy [236, 237]. In addition, it has been shown that MLL1 is involved in tumor angiogenesis by recruiting and sustaining of the blood vessels, but without a direct connection to H3K4me2 [224]. There is so far no data linking *MLL1* expression, methylation of H3K4, and atherosclerosis. The mutual connection might be the inflammation process. MLL1 was suggested to be recruited to its target genes by activated NF-κB and regulates their transcription [238]. In the present work, immunohistological analysis of the inflammatory cells and western blot analysis showed a decrease in the expression of the H3K4me2 with the progression of AS, but the *MLL1* expression was increased. This suggests that other processes are involved in AS, and that the mechanisms are more complex involving also other methyltransferases.

The histone methyltransferase hSET1 has been shown to be differentially over-expressed in the malignant cells [239]. SETD1A and SETD1B are both components of the HMT complexes able to mono-, di-, or tri-methylate H3K4, and have non-redundant roles [239]. In carotid tissue affected by AS, as well as in control tissue, the expressions of *SETD1A* and *SETD1B* were undetectable. This would suggest that these two methyltransferases are not playing an important role in the vascular wall. SETD1B was reported to methylate H3K4 only if H3K9 was not already methylated [240] and so affect the

methylation of H3K9. Moreover, *SETD1B* was shown to be down-regulated at the beginning of VSMC de-differentiation [53, 56]. In agreement with the presented results, methylation at K9 might occur ahead of the methylation of K4, thus being hindered by the first process.

HMTs responsible for di-methylation of K9 are SUV39H1 and EHMT2 (also known as G9a). Their expression was not detected in this study, independent of the tissue analyzed. During the de-differentiation process of the VSMCs, *EHMT2* (*G9a*) was shown to be down-regulated in the first stages of the differentiation and up-regulated in the late phase. In B lymphocytes, G9a serves as the major H3K9 di-methylattransferase, but is not the only HMT involved in this process since the global H3K9me2 was reduced in the absence of G9a but not absent [53, 241].

4.1.5 Conclusion

In summary, genomic hypomethylation occurs with the progression of atherosclerotic lesions. This is in a direct correlation with the failure to function of the methyltransferase DNMT1. In agreement with the increased expression of *TET1*, associated with a demethylation at the nucleotide level, the DNA is globally hypomethylated. Thus, the synergetic effect of DNMT1 and TET1 might be the main mechanism leading to DNA hypomethylation. As for histone modifications, the other component of the epigenetic code, di-methylation of H3K4 and H3K9 decreases with the progression of the atherosclerosis. Furthermore, H3K4me2 was mainly observed to exist in vascular smooth muscle cells and H3K9me2 was associated with inflammatory cells. Since the expression of *SETD1A* and *-B* was not found in atherosclerotic lesions, it can be concluded that they do not play a major role in the methylation of H3K4. MLL1 seems to have a compensatory mechanism to methylate H3K4. However, other mechanisms might also have implications in maintaining this modification. Methyltransferases SUV39H1 and G9a were not found to be involved in the methylation of the H3K9 in atherosclerosis. In conclusion, the presented results have brought new insights to understanding the epigenetic changes that occur within vascular disorders, especially atherosclerosis.

4.1.6 Future directions

The necessity to understand human epigenome has already been well recognized. Much effort has been addressed to associate changes in epigenetics with cancer progression and malignancy. In contrast, the cardiovascular field has not yet experienced such attention. The first results achieved in this field, as also confirmed by data of the current study, are promising and can contribute to better understand the mechanisms leading to

progression of atherosclerosis and other CVDs [242-245]. A particularly challenging task specific to atherosclerosis will be to define the epigenome of every cell type participating in the vascular lesion – VSMCs, macrophages, immune cells, and endothelial cells at different stages of the disease. A next task would be to incorporate these data into clinical studies, addressing the level of CVDs risk associated with specific epigenome. It is likely that epigenetic changes imposed by environmental and nutritional factors may contribute to the disease progression and could also serve as target to improve future therapeutic strategies.

4.2 Epigenetics and regenerative medicine

Vascular grafts are currently under a continuous development and so far they cannot reproduce the biologically sophisticated functions of native vessels. Currently available synthetic vascular grafts require a pre-treatment with anticoagulants due to the need to control thromboembolism, and the bio-prosthetics undergo structure deterioration and calcification [190]. Also for soft and hard tissue there remains the challenge of reconstruction, implantation, and plastic surgery. Nowadays, there is a high need for a suitable reconstruction of vessels (e.g. carotid artery), soft tissue (e.g. skin, liver, lung), and hard tissue (e.g. bone) defects resulting after atherosclerosis plaque removal, deep burns, trauma, or tumor resection. The biggest challenge of tissue engineering is to find a suitable cell or tissue application that is provided with a vascular network, which has the purpose to sustain and support the functions of the tissue.

4.2.1 AdMSC population characterization

Mesenchymal stem cells, compared to somatic cells, show attributes like plasticity, adherence and have a high proliferation rate, thus being suitable for induction of pluripotency. Until now it was considered that the main source of MSCs is the bone marrow, from which the cells can be isolated for experimental and clinical use. However, it was recently discovered that MSCs can also be obtained successfully from other sources such as adipose tissue [246]. In contrast to the bone marrow, the adMSCs are easily available. They can be isolated from larger quantities of adipose tissue, thus yielding higher amounts of cells.

Proper isolation of adMSCs is necessary to gain a homogenous cell population for reliable experimental data. At present there is still a lack of standardized methods for isolation of these cells [246]. Furthermore, there are still no definitive cell surface markers for a clear identification of adMSCs. Therefore, prior to treating the adMSCs with epigenetic drugs, the cells isolated from adipose tissue in this study were characterized appropriately. With regard to the intended experiments, different passages were tested concerning cell proliferation, viability, and commonly used negative and positive markers of this cell population. AdMSCs possess a non-hematopoietic phenotype and should be therefore negative for the hematopoietic markers *CD14* and *CD45*. This cell characteristic was confirmed by FACS analysis revealing less than 2% hematopoietic cells in the isolated adMSC population. Positive markers for adMSCs include cell-surface molecules CD90 and CD105. CD90 (THY-1) is a GPI-anchored cell-surface protein and is used as a marker of stem cells [247]. CD105 (ENDOGLIN) is a part of the TGF-beta receptor complex and has been found on endothelial cells, activated monocytes/macrophages, fibroblasts, smooth

muscle cells, and also on mesenchymal stem cells [248]. The isolated adMSCs were highly homogenous for these markers, with more than 85% positive cells.

Antigen Ki-67 is a nuclear protein that is associated with cellular proliferation and ribosomal RNA transcription [249]. The cell population isolated from adipose tissue presented more than 50% proliferating cells. However, it is to note that adMSCs from different donors varied markedly in their proliferative state.

Moreover, the studied adMSCs were positive for the intermediate filament vimentin, which is known to be expressed in mesenchymal cells. Vimentin, together with tubuline-based microtubules and actin microfilaments are forming the cellular cytoskeleton. This marker is generally used as developmental marker for cells and tissues [250].

The best characteristics concerning proliferation, viability, homogeneity, and structural composition of adMSCs were found for passage three. Therefore, this passage was used for the whole experimental design.

4.2.2 Differentiation potential as part of cell characterization

Another feature of MSCs is their differentiation potential. They should be capable to achieve adipogenic, osteogenic, and chondrogenic characteristics using proper cultivation conditions. In perfect agreement with other studies [251], adMSCs used in the present work showed the ability to differentiate towards the adipogenic and osteogenic lineages.

4.2.3 Epigenetic changes produced by epigenetic modifying drugs led to increase in expression of pluripotency related genes

So far, several approaches have been used to generate stem-like cells from adult human somatic cells. In this study a novel strategy was followed to induce pluripotency by altering epigenetics pattern using epigenetic-modifying drugs 5-azacytidine (AZA), BIX-01294 (BIX), and valproic acid (VPA). These chemical compounds have been already used on cancer cells in order to modify their epigenetic pattern, with benefits for the clinical outcome [252].

Human adMSCs were treated with increasing concentrations of all three epigenetic drugs to find the optimal sub-toxic dosage. With the exception of AZA, the other epigenetic-modifying drugs BIX and VPA achieve their best effect on epigenetics using their maximal sub-toxic concentrations. Using AZA no significant toxicity was observed up to a concentration of 40 μM, independent of the tested treatment time. However, maximal

reduction in the global DNA methylation was achieved at 2.5 and 5 µM after 48 hours. Therefore, these conditions were also used for the experiments in this study. In contrast to BIX and VPA, AZA is unstable in aqueous solution [141], which could explain the low toxic effect of AZA on adMSCs in present experiments.

AZA is a chemical analogue of cytidine and is incorporated into DNA during cell replication. The incorporation inhibits methyltransferase activity, thereby causing DNA demethylation. AZA concentrations of 5, 10 and 50 µM showed already a significant reduction of DNA methylation on mouse embryonic fibroblasts without any changes in the relation between cell growth and cell viability [253]. These data confirm the present experimental results with no toxic effect of AZA on adMSCs for up to 40 µM [151]. Using AZA, the results demonstrated significant reduction in DNA methylation by 50%, compared with non-treated controls. However, regarding expression of the pluripotency markers analyzed in this study, such as *POU5F1*, *NANOG*, *KLF4*, *SOX2* and *CMYC*, no significant changes at mRNA levels were observed for *KLF4* and *CMYC* following treatment of adMSCs with AZA. In case of *POU5F1,* an increase in expression for up to 1.84-fold was found. Following BIX treatment significant reduction in global DNA-methylation for up to 70% was observed. These were interesting results because BIX-01294 influences especially histone methylation at the position H3K9 by inhibiting G9a-histone methyltransferase [5, 31]. BIX was already tested on different cells such as mouse embryonic stem cells and HeLa cells with a concentration of 4.1 µM, leading to the most efficient demethylation at the histone level [124]. One could suppose that G9a-histone methyltransferases also influence the expression of DNMTs (dinucleotide methyltransferases) as described [148, 254], and may therefore change DNA methylation [255]. Also, the G9a-histonmethyltransferase was reported to indirectly mediate the expression of *POU5F1* during cell differentiation influencing both global DNA methylation and expression of pluripotency genes. The presented results confirmed this presumption, observing not only significant reduction in DNA methylation but also a significant increase in the expression of pluripotency genes *POU5F1*, *NANOG*, and *CMYC* by 5.41-, 3.04-, and 2.39-fold respectively. These data presume that the specific inhibition of histone methyl tranferases (HMTs) by BIX is more involved in the activation of the specific pluripotency genes than in inhibition of DNMTs (by AZA). However, similar to the effect of AZA, the expression profile of the pluripotency genes strongly depended on the individual donors.

In contrast to AZA and BIX, no significant changes in DNA methylation were observed following treatment of adMSCs with VPA. The possible explanation is that VPA, although inhibiting histone deacetylases (HDAC), does not influence DNMTs or HMTs, which are known to positively regulate gene expression. The choice for using VPA was based on the

supposition that there is a common regulation mechanism between HDACs and HMTs [252]. Histone acetylation plays an important role in the regulation of gene expression. A study in mouse models demonstrated that only a subset of genes (7%) is deregulated by HDACs [256]. In addition, some studies have shown that VPA can also be used as a differentiating agent [157]. The results in the present study led to the assumption that the expression of long interspersed nuclear elements *LINE1* is not regulated by HDACs and that in adMSCs VPA may induce a more undifferentiated state by up-regulation of stemness modulating genes.

Pluripotent embryonal carcinomas are good potential models to study the mechanisms that control differentiation during embryogenesis, or even as positive control for specific pluripotency related factors [257]. The pluripotent human embryonal carcinoma cell line NTERA-2 clone D1, also known as NT2/D1, is a sub clone derived from the parent line NTERA-2. These cells have been cited to be positive for all pluripotency related markers verified also in the present study: POU5F1, NANOG, SOX2, KLF4, and CMYC [258]. Therefore mRNA from these cells was used as positive control for the quantitative expression analysis.

Interestingly, *KLF4* and *CMYC* native expressions in adMSCs were 1000- to 2000-fold higher than native expressions of *POU4F1* and *NANOG,* and were comparable with the expression levels in NTERA-2 cell line used as positive control. This is probably due to the feature of adMSCs, which are not yet fully differentiated, to have high proliferative potential and therefore possess some properties of stem cells [259]. The CMYC protein is a transcription factor that activates expression of a great number of genes involved in the control of DNA replication [260]. Thus, CMYC activation may result in cell proliferation and growth. KLF4 plays an important role in regulation of cell growth, differentiation and embryogenesis [261]. Generally, KLF4 has an inhibitory effect on cell proliferation in adult tissue [262]. However, KLF4 has also been shown to cooperate with CMYC to influence stem cell self-renewal [262]. In pluripotent cells, however, KLF4 may suppress apoptosis induced by CMYC. The CMYC in turn may neutralize the cytostatic effect of KLF4 by suppressing P21 [258]. Thus, the balance between KLF4 and CMYC might be essential in the establishment of an immortalized state of induced pluripotent stem cells.

Interesting is the fact that both *CMYC* and *KLF4* expressions were not affected by BIX, which led to the hypothesis that G9a does not affect the expression of these two oncogenes, or they are regulated by an independent mechanism.

Again, as already mentioned above, these results strongly depended on the individual donor. Moreover, no correlation was observed between the expression of the pluripotency genes and patient characteristics, such as demographic data and known accompanying diseases. The only link seemed to be the amount of proliferating cells, which corresponds with the age of each donor.

4.2.4 Epigenetic changes induced by BIX improve the endothelial differentiation

So far, several approaches have been used to generate endothelial cells from mesenchymal stem cells. In the present study a novel strategy was followed, by which the potential of adMSCs to differentiate into cells with endothelial features was significantly improved.

The hypothesis was based on the assumption that modifying the epigenetic pattern with the epigenetic modifying drug BIX, the most effective epigenetic compound found in the present study, allows the cells to enter a pre-differentiation state and from this point they could be directed to different cell types under appropriate cell culture conditions. To verify this theory, cells were divided into two groups: “EM” – cells cultivated in endothelial medium, and “EM plus BIX” – cells that received a pre-treatment with BIX, and then were cultivated in endothelial medium.

To evaluate the capacity of adMSCs to differentiate into ECs were analyzed known vascular-specific markers. VEGF is a critical regulator of vascular formation that binds to VEGFR-2. It initiates the formation of immature vessels by vasculogenesis or angiogenic sprouting by cell mitogenesis and migration. In the current study, increased levels of VEGF were found both after 7 and 14 days in the BIX plus EM group.

Other factors necessary for vascular formation are angiopoetins [263]. ANG-1 is required for further remodeling and maturation of the initially immature vessels. In the present findings this marker was significantly increased after 14 days in “BIX plus EM” group. ANG-2 is the antagonist of ANG-1, binding to the same receptor – TIE-2. The results showed a significant decrease of ANG-2 in BIX-treated cells, decrease that is naturally occurring during endothelial differentiation and new blood vessel formation.

Active endothelial cells express also VCAM-1 during angiogenesis [264]. This is why the cells were further characterized for VCAM-1 expression and localization. As expected, following pretreatment of adMSCs with BIX, expression of this endothelial marker was significantly increased as well.

PDGF is involved in the maturation of nascent vessels and in the recruitment of pericytes and smooth-muscle cells that coat the new vessels. It is produced by smooth-muscle cells, activated macrophages, and endothelial cells [265]. In comparison to the non-treated cells, the expression of PDGF was increased in the “EM plus BIX” group.

Von Willebrand factor (vWF) is a glycoprotein present in blood plasma and produced constitutively in endothelial cells by the Weibel-Palade bodies [266]. The primary function of vWF is to bind other proteins, especially FACTOR VIII (F8), and is important in platelet adhesion to injured sites. Factor VIII is bound to vWF while inactive in circulation, and is released from vWF by the action of thrombin. F8 and vWF are often used as specific markers for endothelial cells. The differentiated adMSCs were positive for vWF, which is usual for all endothelial cells, and by quantification of the expression of the *F8* gene it has been observed that BIX treatment induced a significant increase in expression of this marker. In a previous study by Collazo et al. [111] was shown that 7 days of differentiation was enough to increase the expression of *vWF*, but not of *VCAM-1*. In the present work it is shown an improvement of *VCAM-1, F8,* and also *VEGFR-2* expression after 7 and even more after 14 days of differentiation, if the cells received BIX as a pre-treatment. Furthermore, the cells treated with epigenetic drug BIX were positive also for the CD31 (PECAM-1) marker. In contrast, undifferentiated cells showed no specific staining for these markers.

The functionality of the endothelial cells was investigated with the ac-LDL uptake assay. DiI-Ac-LDL is taken up via the “scavenger” cell pathway of LDL metabolism and is characteristic for endothelial cells [267, 268]. Results showed that the cells of “BIX plus EM” group are able to metabolize the ac-LDL. The assay performed on cells of the “EM” group was also positive, but with clearly fewer positive cells. These results are in agreement with the above described data regarding the expression of endothelial related genes in both groups.

In summary, BIX treatment led to an overall increase in expression of endothelial and angiogenic markers, facilitating the differentiation process of adMSCs into endothelial cells.

4.2.5 Endothelial cells differentiated from BIX pre-treated adMSCs for vascular grafts

Nowadays there are several vascular grafts used for bypasses. Unfortunately the grafts manufactured from synthetic material possess low patency rates, with high risks of trombogenicity, occlusion, infection, and lack of self-healing in comparison with the autologous grafts. First, decellularization of vessels has been investigated as a promising

solution in replacing the synthetic scaffolds [269]. Furthermore, the epigenetically modified adMSCs were tested after differentiation towards endothelial cells for their capacity to attach to decellularized saphenous vein. Two days after being seeded onto the grafts, cells displayed good attachment and adaptation to the new environment at the surface of the scaffolds. After 7 days in culture, there were an increased number of cells on the construct that were organized in multiple layers. These results were in agreement with previous, where autologous cells were seeded onto a similar scaffold [270, 271]. These first results confirmed the usefulness of natural decellularized scaffolds and the possibility to seed autologous differentiated endothelial cells. Further studies must be performed, to see whether the endothelial characteristics are kept under these conditions.

4.2.6 Cell proliferation, DNA methylation, and pluripotency markers related to donor age

Finally, a special concern was dedicated to the source of the mesenchymal stem cells. A high variation in the gene expression and global DNA methylation was observed in adMSCs. However, no correlation was found between the demographic data, gender or medical history of the donors. Until now, several studies have reported variances in the differentiation potential of adult stem cells originating from donors with different ages [272, 273]. In accordance with these studies an increase in the osteogenic differentiation potential was observed also in the adMSCs of the “young donors” group. No differences were found for the adipogenic differentiation. Thus, the adult stem cells originating from younger donors show an increase in the reprogramming capacity towards osteogenic lineage. Additionally in the present study was found an increased number of Ki67 positive adMSCs in the group of “young donors”. Currently there are only few studies that have investigated the amount of proliferating adMSCs originating from young and elderly donors [171, 274]. The difference in the number of the proliferating cells may be partly responsible for the variability in the differentiation potential of adMSCs.

Furthermore, analyzed cells from younger donors had a decreased global DNA methylation level compared with cells from elderly donors. DNA methylation is one of the main components of epigenetics. An alteration in its pattern is associated with a change in the reprogramming capacity of the cells, a decreased level being associated with an increased transcription activity. This hypothesis is supported by the study of Hupkes *et al.* [275], where a decreased global DNA methylation, and subsequently a change in the epigenetic pattern, directs the differentiation of mouse myoblasts from muscle to bone cells. Similarly, in the present work, the decreased level of DNA methylation in adMSCs from younger donors presented an increased differentiation potential into osteoblasts.

Nevertheless, no studies have found so far any connection between global DNA methylation status or expression of pluripotency related genes and the age of the donors in adMSCs. Somatic cells have already been reprogrammed into pluripotent stem cells by introducing a combination of several transcription factors (TFs), such as *Oct3/4*, *Sox2*, *Klf4* and *c-Myc* [276]. Thus, an increased expression in these TFs is associated with an increased reprogramming capacity. In the present study the decreased level of genomic methylation is in agreement with the statistically significant increased expression of pluripotency related genes *NANOG* and *SOX2*, in the cells from the "young donors" group. The promoters of pluripotency genes such as *nanog* and *Oct4* have been showed that are stably silenced by DNA methylation in somatic cells in mice [277], which likely interferes with transcription factor binding and gene activation during reprogramming. Similarly, this process might occur in adMSCs from elderly donors, where the reprogramming genes might be silenced through DNA methylation, therefore they possess a decreased differentiation potential in comparison with the cells from younger donors.

In summary, proper epigenetic changes might reverse the effect of aging on cells from elderly patients. These cells could then be used with a greater success rate in cell therapies based on autologous transplantation.

4.2.7 Conclusion

For future therapeutic developments of autologous and allogenic pluripotent stem cells, adMSCs are a promising cell source that can be easily harvested. Furthermore, a chemical approach for targeted epigenetics might be a feasible and safe method to improve pluripotency of somatic cells. In the present study, the epigenetic-modifying drugs AZA and BIX were able not only to significantly reduce global DNA methylation in adMSCs but also to increase the expression of genes for pluripotency such as *POU5F1* and *NANOG*. Thus, reactivation of the native pluripotency genes by epigenetic changes using chemical compounds might represent a promising approach in future regenerative medicine. Furthermore, due to epigenetic changes, BIX was able to enhance the differentiation of adMSCs into cells with endothelial features. The treatment with the epigenetic modifying drug BIX is also able to decrease global DNA methylation. These epigenetic changes were responsible for the increase of the expression of the pluripotency related genes. Subsequently, expression of endothelial and angiogenic markers was increased. Further studies are necessary to investigate the feasibility of applying these cells *in vivo*, by e.g. producing autologous vascular grafts.

4.2.8 Future directions

In order to better understand and manipulate the epigenetic pattern, the present study has to be continued by analysis of other histone modifications, improvements of the differentiation capacity of adMSC, examination of other epigenetic processes such as ATP-dependent chromatin remodeling and DNA methylation at specific promoter regions in adMSCs, nuclear packaging and localization of gene loci of specific cell types (e.g. endothelial cells) in adMSCs. The inherent plasticity of the adMSC lineage has presented remarkable insights and unique challenges regarding the understanding of the control of cellular differentiation. This might bring research closer to optimization of differentiation towards particular tissues that are required in regenerative medicine. Cells that are epigenetically modified to change from one linage to another, without insertion of foreign nucleic material, could be a safe and ethically approved way to an almost unlimited choice of tissue engineering applications.

5 SUMMARY

The present work evaluated two aspects of epigenetics: involvement in vascular disease and applicability in regenerative medicine.

5.1 Epigenetics and vascular disease

Epigenetic regulation of gene activity is a fundamental mechanism that occurs in all eukaryotic cells and is indispensable for development, tissue regeneration or maintaining of cell phenotype. Defects in epigenetics have already been connected to various diseases. DNA and histone methylation significantly contribute to the regulation of gene expression. So far, no sufficient data are available about epigenetic modifications in atherosclerotic lesions.

In the current study, carotid plaques of patients with high grade carotid artery stenosis in early (type II-III, n=20) and advanced (type V-VII, n=20) stage of atherosclerosis (AS), as well as 10 control vessels, and 10 healthy individuals were included. Carotid lesions were characterized by histology and immunohistochemistry (IHC). Global DNA methylation was analyzed by Methylight assay. Expressions of DNA methyltransferases (*DNMT1*, *DNMT3A*, and *DNMT3B*), demethylase *TET1*, and histone methyltransferases (HMT) *MLL1*, *SED1A*, and *SETD1B* for H3K4 and SUV39H1, and *G9a* for H3K9 were analyzed by quantitative real time PCR. Methylation of histone H3 at lysine K4 and K9 in atherosclerotic plaques was evaluated by western blot and by IHC in correlation with smooth muscle cells and inflammatory cells.

Global DNA methylation in carotid plaque decreased continuously with the progression of AS and correlated significantly with the genome-wide hypomethylation of free DNA from blood serum in patients with carotid artery stenosis. Expression of *DNMT1* was decreased, *DNMT3A* and *DNMT3A* exhibited very low expression within AS. In contrast, *TET1* expression was found to increase with the progression of the disease. Tissue slices stained for smooth muscle cells were found also to be positive for H3K4 and the intensity of staining decreased with the progression of AS. Smooth muscle cells were found mostly negative for H3K9 in all study groups. Inflammatory cells, positive for CD45 and CD68, were only slightly stained for H3K4, both in early and advanced stage of AS. The amount of inflammatory cells positive for H3K9 increased with the severity of AS. Western blot analysis revealed decreased level of methylation for H3K4 and H3K9, negatively corresponding with the progression of AS. Regarding HMTs responsible for methylation of lysine K4 analyzed in

this study, expression of *MLL1* increased in correlation with the severity of AS. *SETD1A* and *SETD1B* were not expressed in the analyzed samples. HMTs responsible for methylation of lysine K9, *SUV39H1* and *G9a*, showed no expression in AS specimens or in controls.

In conclusion, the level of DNA methylation and histone methylation was found to be significantly associated with the severity of atherosclerosis in patients with carotid artery stenosis. Thus, epigenetic changes seem to play a substantial role during atherosclerotic plaque progression.

5.2 Epigenetics and regenerative medicine

Chromatin remodeling plays an essential role in regulation of gene transcription. Thus, appropriate changes in the chromatin of somatic cells may lead to the induction of pluripotency. The aim of the present study was to evaluate the effect of epigenetic drugs 5-azacytidine (AZA), BIX-01294 (BIX), and valproic acid (VPA) on DNA methylation and expression of pluripotency genes *OCT4A*, *NANOG*, *KLF4*, *SOX2*, and *CMYC* in human adipose-derived mesenchymal stem cells (adMSCs) and to evaluate their potential to differentiate into cells with endothelial characteristics.

AdMSCs were isolated from human abdominal adipose tissue and characterized morphologically, by FACS analysis, and regarding their osteogenic and adipogenic differentiation potential. Viability assay (MTT) was used to determine the optimal dosage of epigenetic modifying drugs on adMSCs. Global DNA methylation was determined by MethyLight assay, and expression of pluripotency and endothelial genes by SYBRgreen-based real-time PCR. Immunocytochemistry and western blot were used in order to characterize the differentiated cells into endothelial lineage analyzing various endothelial and angiogenic factors such as vWF, VCAM-1, PECAM, VEGFR-2, Ang-1, and -2.

The optimal population of adMSCs with the best homogenous properties was found in passage three of culture, with 86% of cells positive for CD90, CD105 and 98% negative for CD14, CD45. The optimal sub-toxic concentrations of AZA, BIX, and VPA were observed after 48 hours of treatment using 2.5, 1.25, and 100 µM, respectively. Global DNA methylation status of adMSCs treated with the epigenetic modifying drugs was significantly reduced by BIX and AZA but was not affected by VPA. Pluripotency related genes *OCT4A*, *SOX2*, and *NANOG* showed significant increased expressions after treatment with BIX. AdMSCs cultured under endothelial conditions and pre-treated with BIX were observed to undergo changes in the phenotype towards endothelial cells. Up to 20% of cells were positive for endothelial and angiogenic markers tested in this study. The functionality of the

adMSC-derived endothelial cells was verified by their capacity to take up ac-LDL. Experiments concerning autologous grafts showed that decellularized native saphenous veins remained stable and adMSCs-derived endothelial cells were able to attach to this scaffold.

In conclusion, epigenetic modifying drugs AZA and BIX were able to significantly reduce global DNA methylation. Furthermore, BIX led also to a significant increase in the expression of genes for pluripotency and following differentiation the expression of endothelial and angiogenic genes. These adMSC-derived endothelial cells showed all characteristics of an endothelial lineage. Thus, targeted epigenetic modification using appropriate chemical compounds might represent a promising and feasible approach in regenerative medicine.

6 REFERENCES

1. Berger, S.L., et al., *An operational definition of epigenetics.* Genes Dev, 2009. **23**(7): p. 781-3.

2. McGarvey, K.M., et al., *DNA methylation and complete transcriptional silencing of cancer genes persist after depletion of EZH2.* Cancer Res, 2007. **67**(11): p. 5097-102.

3. Brinkman, A.B., et al., *Histone modification patterns associated with the human X chromosome.* EMBO Rep, 2006. **7**(6): p. 628-34.

4. Lachner, M., R.J. O'Sullivan, and T. Jenuwein, *An epigenetic road map for histone lysine methylation.* J Cell Sci, 2003. **116**(Pt 11): p. 2117-24.

5. Lachner, M. and T. Jenuwein, *The many faces of histone lysine methylation.* Curr Opin Cell Biol, 2002. **14**(3): p. 286-98.

6. Rodenhiser, D. and M. Mann, *Epigenetics and human disease: translating basic biology into clinical applications.* CMAJ, 2006. **174**(3): p. 341-8.

7. Bird, A., *DNA methylation patterns and epigenetic memory.* Genes Dev, 2002. **16**(1): p. 6-21.

8. Choi, S.H., et al., *Identification of preferential target sites for human DNA methyltransferases.* Nucleic Acids Res, 2011. **39**(1): p. 104-18.

9. Cooper, M.P. and J.F. Keaney, Jr., *Epigenetic control of angiogenesis via DNA methylation.* Circulation, 2011. **123**(25): p. 2916-8.

10. Osborne F.X. Almeida, D.S., Carsten Wotjak, Günther Schütz. *Epigenetic programming*. 2012; Available from: http://www.mpipsykl.mpg.de/en/research/themes/aging/spengler_02/index.html.

11. Miranda, T.B. and P.A. Jones, *DNA methylation: the nuts and bolts of repression.* J Cell Physiol, 2007. **213**(2): p. 384-90.

12. Matouk, C.C. and P.A. Marsden, *Epigenetic regulation of vascular endothelial gene expression.* Circ Res, 2008. **102**(8): p. 873-87.

13. Hiltunen, M.O., et al., *DNA hypomethylation and methyltransferase expression in atherosclerotic lesions.* Vasc Med, 2002. **7**(1): p. 5-11.

14. Ling, C. and L. Groop, *Epigenetics: a molecular link between environmental factors and type 2 diabetes.* Diabetes, 2009. **58**(12): p. 2718-25.

15. Perini, G., et al., *In vivo transcriptional regulation of N-Myc target genes is controlled by E-box methylation.* Proc Natl Acad Sci U S A, 2005. **102**(34): p. 12117-22.

16. Comb, M. and H.M. Goodman, *CpG methylation inhibits proenkephalin gene expression and binding of the transcription factor AP-2.* Nucleic Acids Res, 1990. **18**(13): p. 3975-82.

17. Wenger, R.H., et al., *Oxygen-regulated erythropoietin gene expression is dependent on a CpG methylation-free hypoxia-inducible factor-1 DNA-binding site.* Eur J Biochem, 1998. **253**(3): p. 771-7.

18. Prokhortchouk, A., et al., *The p120 catenin partner Kaiso is a DNA methylation-dependent transcriptional repressor.* Genes Dev, 2001. **15**(13): p. 1613-8.

19. Chan, G.C., et al., *Epigenetic basis for the transcriptional hyporesponsiveness of the human inducible nitric oxide synthase gene in vascular endothelial cells.* J Immunol, 2005. **175**(6): p. 3846-61.

20. Fuks, F., et al., *The methyl-CpG-binding protein MeCP2 links DNA methylation to histone methylation.* J Biol Chem, 2003. **278**(6): p. 4035-40.

21. Tahiliani, M., et al., *Conversion of 5-methylcytosine to 5-hydroxymethylcytosine in mammalian DNA by MLL partner TET1.* Science, 2009. **324**(5929): p. 930-5.

22. Kriaucionis, S. and N. Heintz, *The nuclear DNA base 5-hydroxymethylcytosine is present in Purkinje neurons and the brain.* Science, 2009. **324**(5929): p. 929-30.

23. Branco, M.R., G. Ficz, and W. Reik, *Uncovering the role of 5-hydroxymethylcytosine in the epigenome.* Nat Rev Genet, 2012. **13**(1): p. 7-13.

24. Hajkova, P., et al., *Genome-wide reprogramming in the mouse germ line entails the base excision repair pathway.* Science, 2010. **329**(5987): p. 78-82.

25. Ko, M., et al., *Impaired hydroxylation of 5-methylcytosine in myeloid cancers with mutant TET2.* Nature, 2010. **468**(7325): p. 839-43.

26. Ito, S., et al., *Role of Tet proteins in 5mC to 5hmC conversion, ES-cell self-renewal and inner cell mass specification.* Nature, 2010. **466**(7310): p. 1129-33.

27. Szwagierczak, A., et al., *Sensitive enzymatic quantification of 5-hydroxymethylcytosine in genomic DNA.* Nucleic Acids Res, 2010. **38**(19): p. e181.

28. Ficz, G., et al., *Dynamic regulation of 5-hydroxymethylcytosine in mouse ES cells and during differentiation.* Nature, 2011. **473**(7347): p. 398-402.

29. Xu, Y., et al., *Genome-wide regulation of 5hmC, 5mC, and gene expression by Tet1 hydroxylase in mouse embryonic stem cells.* Mol Cell, 2011. **42**(4): p. 451-64.

30. Frauer, C., et al., *Different binding properties and function of CXXC zinc finger domains in Dnmt1 and Tet1.* PLoS One, 2011. **6**(2): p. e16627.

31. Zhang, H., et al., *TET1 is a DNA-binding protein that modulates DNA methylation and gene transcription via hydroxylation of 5-methylcytosine.* Cell Res, 2010. **20**(12): p. 1390-3.

32. Kouzarides, T., *Chromatin modifications and their function.* Cell, 2007. **128**(4): p. 693-705.

33. Kimura, A.P., S.A. Liebhaber, and N.E. Cooke, *Epigenetic modifications at the human growth hormone locus predict distinct roles for histone acetylation and methylation in placental gene activation.* Mol Endocrinol, 2004. **18**(4): p. 1018-32.

34. Rice, J.C. and C.D. Allis, *Histone methylation versus histone acetylation: new insights into epigenetic regulation.* Curr Opin Cell Biol, 2001. **13**(3): p. 263-73.

35. Briggs, S.D., et al., *Histone H3 lysine 4 methylation is mediated by Set1 and required for cell growth and rDNA silencing in Saccharomyces cerevisiae.* Genes Dev, 2001. **15**(24): p. 3286-95.

36. Wang, H., et al., *Purification and functional characterization of a histone H3-lysine 4-specific methyltransferase.* Mol Cell, 2001. **8**(6): p. 1207-17.

37. Sedkov, Y., et al., *Methylation at lysine 4 of histone H3 in ecdysone-dependent development of Drosophila.* Nature, 2003. **426**(6962): p. 78-83.

38. Rea, S., et al., *Regulation of chromatin structure by site-specific histone H3 methyltransferases.* Nature, 2000. **406**(6796): p. 593-9.

39. Nakayama, J., et al., *Role of histone H3 lysine 9 methylation in epigenetic control of heterochromatin assembly.* Science, 2001. **292**(5514): p. 110-3.

40. Tachibana, M., et al., *Set domain-containing protein, G9a, is a novel lysine-preferring mammalian histone methyltransferase with hyperactivity and specific selectivity to lysines 9 and 27 of histone H3.* J Biol Chem, 2001. **276**(27): p. 25309-17.

41. Schultz, D.C., et al., *SETDB1: a novel KAP-1-associated histone H3, lysine 9-specific methyltransferase that contributes to HP1-mediated silencing of euchromatic genes by KRAB zinc-finger proteins.* Genes Dev, 2002. **16**(8): p. 919-32.

42. Cao, R., et al., *Role of histone H3 lysine 27 methylation in Polycomb-group silencing.* Science, 2002. **298**(5595): p. 1039-43.

43. Vojnic, E., et al., *Structure and carboxyl-terminal domain (CTD) binding of the Set2 SRI domain that couples histone H3 Lys36 methylation to transcription.* J Biol Chem, 2006. **281**(1): p. 13-5.

44. Feng, Q., et al., *Methylation of H3-lysine 79 is mediated by a new family of HMTases without a SET domain.* Curr Biol, 2002. **12**(12): p. 1052-8.

45. Krogan, N.J., et al., *The Paf1 complex is required for histone H3 methylation by COMPASS and Dot1p: linking transcriptional elongation to histone methylation.* Mol Cell, 2003. **11**(3): p. 721-9.

46. Huyen, Y., et al., *Methylated lysine 79 of histone H3 targets 53BP1 to DNA double-strand breaks.* Nature, 2004. **432**(7015): p. 406-11.

47. Szyf, M. and N. Detich, *Regulation of the DNA methylation machinery and its role in cellular transformation.* Prog Nucleic Acid Res Mol Biol, 2001. **69**: p. 47-79.

48. Weidle, U.H. and A. Grossmann, *Inhibition of histone deacetylases: a new strategy to target epigenetic modifications for anticancer treatment.* Anticancer Res, 2000. **20**(3A): p. 1471-85.

49. Kramer, O.H., M. Gottlicher, and T. Heinzel, *Histone deacetylase as a therapeutic target.* Trends Endocrinol Metab, 2001. **12**(7): p. 294-300.

50. Simonini, M.V., et al., *The benzamide MS-275 is a potent, long-lasting brain region-selective inhibitor of histone deacetylases.* Proc Natl Acad Sci U S A, 2006. **103**(5): p. 1587-92.

51. Terry L. Sheppard, A.D., *The human protein methyltransferases*, in *Nature Chemical Biology*2011, Nature: Nature Publishing Group.

52. Dillon, S.C., et al., *The SET-domain protein superfamily: protein lysine methyltransferases.* Genome Biol, 2005. **6**(8): p. 227.

53. Tachibana, M., et al., *G9a histone methyltransferase plays a dominant role in euchromatic histone H3 lysine 9 methylation and is essential for early embryogenesis.* Genes Dev, 2002. **16**(14): p. 1779-91.

54. Albert, M. and K. Helin, *Histone methyltransferases in cancer.* Semin Cell Dev Biol, 2010. **21**(2): p. 209-20.

55. Lee, J.S. and A. Shilatifard, *A site to remember: H3K36 methylation a mark for histone deacetylation.* Mutat Res, 2007. **618**(1-2): p. 130-4.

56. Dodge, J.E., et al., *Histone H3-K9 methyltransferase ESET is essential for early development.* Mol Cell Biol, 2004. **24**(6): p. 2478-86.

57. Rayasam, G.V., et al., *NSD1 is essential for early post-implantation development and has a catalytically active SET domain.* EMBO J, 2003. **22**(12): p. 3153-63.

58. Milne, T.A., et al., *MLL targets SET domain methyltransferase activity to Hox gene promoters.* Mol Cell, 2002. **10**(5): p. 1107-17.

59. Varambally, S., et al., *The polycomb group protein EZH2 is involved in progression of prostate cancer.* Nature, 2002. **419**(6907): p. 624-9.

60. Croonquist, P.A. and B. Van Ness, *The polycomb group protein enhancer of zeste homolog 2 (EZH 2) is an oncogene that influences myeloma cell growth and the mutant ras phenotype.* Oncogene, 2005. **24**(41): p. 6269-80.

61. Bracken, A.P., et al., *EZH2 is downstream of the pRB-E2F pathway, essential for proliferation and amplified in cancer.* EMBO J, 2003. **22**(20): p. 5323-35.

62. Kleer, C.G., et al., *EZH2 is a marker of aggressive breast cancer and promotes neoplastic transformation of breast epithelial cells.* Proc Natl Acad Sci U S A, 2003. **100**(20): p. 11606-11.

63. van der Vlag, J. and A.P. Otte, *Transcriptional repression mediated by the human polycomb-group protein EED involves histone deacetylation.* Nat Genet, 1999. **23**(4): p. 474-8.

64. O'Carroll, D., et al., *The polycomb-group gene Ezh2 is required for early mouse development.* Mol Cell Biol, 2001. **21**(13): p. 4330-6.

65. Allfrey, V.G., R. Faulkner, and A.E. Mirsky, *Acetylation and Methylation of Histones and Their Possible Role in the Regulation of Rna Synthesis.* Proc Natl Acad Sci U S A, 1964. **51**: p. 786-94.

66. Bannister, A.J. and T. Kouzarides, *Regulation of chromatin by histone modifications.* Cell Res, 2011. **21**(3): p. 381-95.

67. Yang, X.J. and E. Seto, *HATs and HDACs: from structure, function and regulation to novel strategies for therapy and prevention.* Oncogene, 2007. **26**(37): p. 5310-8.

68. Yang, X.J. and E. Seto, *The Rpd3/Hda1 family of lysine deacetylases: from bacteria and yeast to mice and men.* Nat Rev Mol Cell Biol, 2008. **9**(3): p. 206-18.

69. Dovey, O.M., C.T. Foster, and S.M. Cowley, *Histone deacetylase 1 (HDAC1), but not HDAC2, controls embryonic stem cell differentiation.* Proc Natl Acad Sci U S A, 2010. **107**(18): p. 8242-7.

70. *Cardiovascular diseases (CVDs)* 2011, World Health Organization.

71. Shekaran, A. and A.J. Garcia, *Extracellular matrix-mimetic adhesive biomaterials for bone repair.* J Biomed Mater Res A, 2011. **96**(1): p. 261-72.

72. Pelisek, J., et al., *Multiple biological predictors for vulnerable carotid lesions.* Cerebrovasc Dis, 2009. **28**(6): p. 601-10.

73. Stary, H.C., et al., *A definition of initial, fatty streak, and intermediate lesions of atherosclerosis. A report from the Committee on Vascular Lesions of the Council on Arteriosclerosis, American Heart Association.* Arterioscler Thromb, 1994. **14**(5): p. 840-56.

74. Virmani, R., et al., *Lessons from sudden coronary death: a comprehensive morphological classification scheme for atherosclerotic lesions.* Arterioscler Thromb Vasc Biol, 2000. **20**(5): p. 1262-75.

75. Stary, H.C., et al., *A definition of advanced types of atherosclerotic lesions and a histological classification of atherosclerosis. A report from the Committee on Vascular Lesions of the Council on Arteriosclerosis, American Heart Association.* Arterioscler Thromb Vasc Biol, 1995. **15**(9): p. 1512-31.

76. Stary, H.C., et al., *A definition of initial, fatty streak, and intermediate lesions of atherosclerosis. A report from the Committee on Vascular Lesions of the Council on Arteriosclerosis, American Heart Association.* Circulation, 1994. **89**(5): p. 2462-78.

77. Gluckman, P.D., et al., *Effect of in utero and early-life conditions on adult health and disease.* N Engl J Med, 2008. **359**(1): p. 61-73.

78. Waterland, R.A. and K.B. Michels, *Epigenetic epidemiology of the developmental origins hypothesis.* Annu Rev Nutr, 2007. **27**: p. 363-88.

79. Roseboom, T., S. de Rooij, and R. Painter, *The Dutch famine and its long-term consequences for adult health.* Early Hum Dev, 2006. **82**(8): p. 485-91.

80. Xue, F. and K.B. Michels, *Intrauterine factors and risk of breast cancer: a systematic review and meta-analysis of current evidence.* Lancet Oncol, 2007. **8**(12): p. 1088-100.

81. Breton, C.V., et al., *Prenatal tobacco smoke exposure affects global and gene-specific DNA methylation.* Am J Respir Crit Care Med, 2009. **180**(5): p. 462-7.

82. Fraga, M.F. and M. Esteller, *Epigenetics and aging: the targets and the marks.* Trends Genet, 2007. **23**(8): p. 413-8.

83. Baccarelli, A., et al., *Rapid DNA methylation changes after exposure to traffic particles.* Am J Respir Crit Care Med, 2009. **179**(7): p. 572-8.

84. Hoffmann, B., et al., *Residential traffic exposure and coronary heart disease: results from the Heinz Nixdorf Recall Study.* Biomarkers, 2009. **14 Suppl 1**: p. 74-8.

85. Yideng, J., et al., *Homocysteine-mediated expression of SAHH, DNMTs, MBD2, and DNA hypomethylation potential pathogenic mechanism in VSMCs.* DNA Cell Biol, 2007. **26**(8): p. 603-11.

86. Ingrosso, D. and A.F. Perna, *Epigenetics in hyperhomocysteinemic states. A special focus on uremia.* Biochim Biophys Acta, 2009. **1790**(9): p. 892-9.

87. Ordovas, J.M. and C.E. Smith, *Epigenetics and cardiovascular disease.* Nat Rev Cardiol, 2010. **7**(9): p. 510-9.

88. Yideng, J., et al., *Homocysteine-mediated PPARalpha,gamma DNA methylation and its potential pathogenic mechanism in monocytes.* DNA Cell Biol, 2008. **27**(3): p. 143-50.

89. Castro, R., et al., *Increased homocysteine and S-adenosylhomocysteine concentrations and DNA hypomethylation in vascular disease.* Clin Chem, 2003. **49**(8): p. 1292-6.

90. Sharma, P., et al., *Detection of altered global DNA methylation in coronary artery disease patients.* DNA Cell Biol, 2008. **27**(7): p. 357-65.

91. Lund, G., et al., *DNA methylation polymorphisms precede any histological sign of atherosclerosis in mice lacking apolipoprotein E.* J Biol Chem, 2004. **279**(28): p. 29147-54.

92. Castillo-Diaz, S.A., et al., *Extensive demethylation of normally hypermethylated CpG islands occurs in human atherosclerotic arteries.* Int J Mol Med, 2010. **26**(5): p. 691-700.

93. Shima, K., et al., *MGMT promoter methylation, loss of expression and prognosis in 855 colorectal cancers.* Cancer Causes Control, 2011. **22**(2): p. 301-9.

94. Turunen, M.P. and S. Yla-Herttuala, *Epigenetic regulation of key vascular genes and growth factors.* Cardiovasc Res, 2011. **90**(3): p. 441-6.

95. Laukkanen, M.O., et al., *Local hypomethylation in atherosclerosis found in rabbit ec-sod gene.* Arterioscler Thromb Vasc Biol, 1999. **19**(9): p. 2171-8.

96. Jackson-Grusby, L., et al., *Loss of genomic methylation causes p53-dependent apoptosis and epigenetic deregulation.* Nat Genet, 2001. **27**(1): p. 31-9.

97. Xu, S.S., S. Alam, and A. Margariti, *Epigenetics in Vascular Disease - Therapeutic Potential of New Agents.* Curr Vasc Pharmacol, 2012.

98. Mitro, N., et al., *Insights in the regulation of cholesterol 7alpha-hydroxylase gene reveal a target for modulating bile acid synthesis.* Hepatology, 2007. **46**(3): p. 885-97.

99. Dje N'Guessan, P., et al., *Statins control oxidized LDL-mediated histone modifications and gene expression in cultured human endothelial cells.* Arterioscler Thromb Vasc Biol, 2009. **29**(3): p. 380-6.

100. Cyr, A.R. and F.E. Domann, *The redox basis of epigenetic modifications: from mechanisms to functional consequences.* Antioxid Redox Signal, 2011. **15**(2): p. 551-89.

101. Boquest, A.C., A. Noer, and P. Collas, *Epigenetic programming of mesenchymal stem cells from human adipose tissue.* Stem Cell Rev, 2006. **2**(4): p. 319-29.

102. Takahashi, K. and S. Yamanaka, *Induction of pluripotent stem cells from mouse embryonic and adult fibroblast cultures by defined factors.* Cell, 2006. **126**(4): p. 663-76.

103. Yu, J., et al., *Induced pluripotent stem cell lines derived from human somatic cells.* Science, 2007. **318**(5858): p. 1917-20.

104. Gearhart, J., E.E. Pashos, and M.K. Prasad, *Pluripotency redux--advances in stem-cell research.* N Engl J Med, 2007. **357**(15): p. 1469-72.

105. Cotterman, R., et al., *N-Myc regulates a widespread euchromatic program in the human genome partially independent of its role as a classical transcription factor.* Cancer Res, 2008. **68**(23): p. 9654-62.

106. Yamanaka, S. and K. Takahashi, *[Induction of pluripotent stem cells from mouse fibroblast cultures].* Tanpakushitsu Kakusan Koso, 2006. **51**(15): p. 2346-51.

107. Thomson, M., et al., *Pluripotency factors in embryonic stem cells regulate differentiation into germ layers.* Cell, 2011. **145**(6): p. 875-89.

108. Gontan, C., et al., *Sox2 is important for two crucial processes in lung development: branching morphogenesis and epithelial cell differentiation.* Dev Biol, 2008. **317**(1): p. 296-309.

109. Snykers, S., et al., *Hepatic differentiation of mesenchymal stem cells: in vitro strategies.* Methods Mol Biol, 2011. **698**: p. 305-14.

110. Fawzy El-Sayed, K.M., et al., *Adult Mesenchymal Stem Cells Explored in the Dental Field.* Adv Biochem Eng Biotechnol, 2012.

111. Colazzo, F., et al., *Induction of mesenchymal to endothelial transformation of adipose-derived stem cells.* J Heart Valve Dis, 2010. **19**(6): p. 736-44.

112. Konno, M., et al., *Efficiently differentiating vascular endothelial cells from adipose tissue-derived mesenchymal stem cells in serum-free culture.* Biochem Biophys Res Commun, 2010. **400**(4): p. 461-5.

113. Caplan, A.I., *Review: mesenchymal stem cells: cell-based reconstructive therapy in orthopedics.* Tissue Eng, 2005. **11**(7-8): p. 1198-211.

114. Pittenger, M.F., et al., *Multilineage potential of adult human mesenchymal stem cells.* Science, 1999. **284**(5411): p. 143-7.

115. Oswald, J., et al., *Mesenchymal stem cells can be differentiated into endothelial cells in vitro.* Stem Cells, 2004. **22**(3): p. 377-84.

116. Zuk, P.A., et al., *Human adipose tissue is a source of multipotent stem cells.* Mol Biol Cell, 2002. **13**(12): p. 4279-95.

117. Fischer, L.J., et al., *Endothelial differentiation of adipose-derived stem cells: effects of endothelial cell growth supplement and shear force.* J Surg Res, 2009. **152**(1): p. 157-66.

118. Rossant, J., *Stem cells and early lineage development.* Cell, 2008. **132**(4): p. 527-31.

119. Luckey, C.J., Y. Lu, and J.A. Marto, *Understanding the first steps in embryonic stem cell exit from the pluripotent state.* Transfusion, 2011. **51 Suppl 4**: p. 118S-24S.

120. Rottach, A., H. Leonhardt, and F. Spada, *DNA methylation-mediated epigenetic control.* J Cell Biochem, 2009. **108**(1): p. 43-51.

121. Hong, C.P., J. Park, and T.Y. Roh, *Epigenetic regulation in cell reprogramming revealed by genome-wide analysis.* Epigenomics, 2011. **3**(1): p. 73-81.

122. Feng, B., et al., *Molecules that promote or enhance reprogramming of somatic cells to induced pluripotent stem cells.* Cell Stem Cell, 2009. **4**(4): p. 301-12.

123. Venolia, L., et al., *Transformation with DNA from 5-azacytidine-reactivated X chromosomes.* Proc Natl Acad Sci U S A, 1982. **79**(7): p. 2352-4.

124. Kubicek, S., et al., *Reversal of H3K9me2 by a small-molecule inhibitor for the G9a histone methyltransferase.* Mol Cell, 2007. **25**(3): p. 473-81.

125. Shi, Y., et al., *Induction of pluripotent stem cells from mouse embryonic fibroblasts by Oct4 and Klf4 with small-molecule compounds.* Cell Stem Cell, 2008. **3**(5): p. 568-74.

126. Patel, M. and S. Yang, *Advances in Reprogramming Somatic Cells to Induced Pluripotent Stem Cells.* Stem Cell Rev, 2010.

127. Wernig, M., et al., *In vitro reprogramming of fibroblasts into a pluripotent ES-cell-like state.* Nature, 2007. **448**(7151): p. 318-24.

128. Rideout, W.M., 3rd, K. Eggan, and R. Jaenisch, *Nuclear cloning and epigenetic reprogramming of the genome.* Science, 2001. **293**(5532): p. 1093-8.

129. Lin, X., et al., *Reversal of GSTP1 CpG island hypermethylation and reactivation of pi-class glutathione S-transferase (GSTP1) expression in human prostate cancer cells by treatment with procainamide.* Cancer Res, 2001. **61**(24): p. 8611-6.

130. Brueckner, B., et al., *Epigenetic reactivation of tumor suppressor genes by a novel small-molecule inhibitor of human DNA methyltransferases.* Cancer Res, 2005. **65**(14): p. 6305-11.

131. Fang, M.Z., et al., *Tea polyphenol (-)-epigallocatechin-3-gallate inhibits DNA methyltransferase and reactivates methylation-silenced genes in cancer cell lines.* Cancer Res, 2003. **63**(22): p. 7563-70.

132. Chavez-Blanco, A., et al., *Antineoplastic effects of the DNA methylation inhibitor hydralazine and the histone deacetylase inhibitor valproic acid in cancer cell lines.* Cancer Cell Int, 2006. **6**: p. 2.

133. Cihak, A., *Biological effects of 5-azacytidine in eukaryotes.* Oncology, 1974. **30**(5): p. 405-22.

134. Hardman, J.G. and N.M. Gajraj, *Epidural blood patch.* Br J Hosp Med, 1996. **56**(6): p. 268-9.

135. Locklin, R.M., R.O. Oreffo, and J.T. Triffitt, *Modulation of osteogenic differentiation in human skeletal cells in Vitro by 5-azacytidine.* Cell Biol Int, 1998. **22**(3): p. 207-15.

136. Seeliger, C., et al., *Decrease of global Methylation improves significantly hepatic Differentiation of Ad-MSCs: Possible future Application for Urea Detoxification.* Cell Transplant, 2012.

137. Snykers, S., et al., *Role of epigenetics in liver-specific gene transcription, hepatocyte differentiation and stem cell reprogrammation.* J Hepatol, 2009. **51**(1): p. 187-211.

138. Snykers, S., et al., *In vitro differentiation of embryonic and adult stem cells into hepatocytes: state of the art.* Stem Cells, 2009. **27**(3): p. 577-605.

139. Burlacu, A., et al., *Promoting effect of 5-azacytidine on the myogenic differentiation of bone marrow stromal cells.* Eur J Cell Biol, 2008. **87**(3): p. 173-84.

140. Pharmacopoeia, M.T.E., London, England, 1989, Reynolds, J. E. F.: The Pharmaceutical Press. p. p. 599.

141. Haaf, T., *The effects of 5-azacytidine and 5-azadeoxycytidine on chromosome structure and function: implications for methylation-associated cellular processes.* Pharmacol Ther, 1995. **65**(1): p. 19-46.

142. Jenuwein, T. and C.D. Allis, *Translating the histone code.* Science, 2001. **293**(5532): p. 1074-80.

143. Jackson, J.P., et al., *Dimethylation of histone H3 lysine 9 is a critical mark for DNA methylation and gene silencing in Arabidopsis thaliana.* Chromosoma, 2004. **112**(6): p. 308-15.

144. Stancheva, I., *Caught in conspiracy: cooperation between DNA methylation and histone H3K9 methylation in the establishment and maintenance of heterochromatin.* Biochem Cell Biol, 2005. **83**(3): p. 385-95.

145. Meissner, A., et al., *Genome-scale DNA methylation maps of pluripotent and differentiated cells.* Nature, 2008. **454**(7205): p. 766-70.

146. Ooi, S.K., et al., *DNMT3L connects unmethylated lysine 4 of histone H3 to de novo methylation of DNA.* Nature, 2007. **448**(7154): p. 714-7.

147. Otani, J., et al., *Structural basis for recognition of H3K4 methylation status by the DNA methyltransferase 3A ATRX-DNMT3-DNMT3L domain.* EMBO Rep, 2009. **10**(11): p. 1235-41.

148. Epsztejn-Litman, S., et al., *De novo DNA methylation promoted by G9a prevents reprogramming of embryonically silenced genes.* Nat Struct Mol Biol, 2008. **15**(11): p. 1176-83.

149. PubChem, C. *BIX 01294 - Compound Summary, BIX-01294*. 2012; Available from: http://pubchem.ncbi.nlm.nih.gov/summary/summary.cgi?cid=25150857#x395.

150. Chang, Y., et al., *Structural basis for G9a-like protein lysine methyltransferase inhibition by BIX-01294.* Nat Struct Mol Biol, 2009. **16**(3): p. 312-7.

151. Feldman, N., et al., *G9a-mediated irreversible epigenetic inactivation of Oct-3/4 during early embryogenesis.* Nat Cell Biol, 2006. **8**(2): p. 188-94.

152. Grunstein, M., *Histone acetylation in chromatin structure and transcription.* Nature, 1997. **389**(6649): p. 349-52.

153. Rosenberg, G., *The mechanisms of action of valproate in neuropsychiatric disorders: can we see the forest for the trees?* Cell Mol Life Sci, 2007. **64**(16): p. 2090-103.

154. Porubek, D.J., M.P. Grillo, and T.A. Baillie, *The covalent binding to protein of valproic acid and its hepatotoxic metabolite, 2-n-propyl-4-pentenoic acid, in rats and in isolated rat hepatocytes.* Drug Metab Dispos, 1989. **17**(2): p. 123-30.

155. Phiel, C.J., et al., *Histone deacetylase is a direct target of valproic acid, a potent anticonvulsant, mood stabilizer, and teratogen.* J Biol Chem, 2001. **276**(39): p. 36734-41.

156. Eyal, S., et al., *The activity of antiepileptic drugs as histone deacetylase inhibitors.* Epilepsia, 2004. **45**(7): p. 737-44.

157. Gottlicher, M., et al., *Valproic acid defines a novel class of HDAC inhibitors inducing differentiation of transformed cells.* EMBO J, 2001. **20**(24): p. 6969-78.

158. Kramer, O.H., et al., *The histone deacetylase inhibitor valproic acid selectively induces proteasomal degradation of HDAC2.* EMBO J, 2003. **22**(13): p. 3411-20.

159. Hahn, P. and M. Novak, *Development of brown and white adipose tissue.* J Lipid Res, 1975. **16**(2): p. 79-91.

160. Hull, D. and M.M. Segall, *Distinction of brown from white adipose tissue.* Nature, 1966. **212**(5061): p. 469-72.

161. Rosen, E.D. and B.M. Spiegelman, *Adipocytes as regulators of energy balance and glucose homeostasis.* Nature, 2006. **444**(7121): p. 847-853.

162. Gallagher, D., et al., *Healthy percentage body fat ranges: an approach for developing guidelines based on body mass index.* American Journal of Clinical Nutrition, 2000. **72**(3): p. 694-701.

163. Trayhurn, P., *Endocrine and signalling role of adipose tissue: new perspectives on fat.* Acta Physiol Scand, 2005. **184**(4): p. 285-293.

164. Cinti, S. and M. Morroni, *Brown adipocyte precursor cells: a morphological study.* Ital J Anat Embryol, 1995. **100 Suppl 1**: p. 75-81.

165. Tang, W., et al., *White fat progenitor cells reside in the adipose vasculature.* Science, 2008. **322**(5901): p. 583-6.

166. Seale, P., S. Kajimura, and B.M. Spiegelman, *Transcriptional control of brown adipocyte development and physiological function--of mice and men.* Genes Dev, 2009. **23**(7): p. 788-97.

167. Kirkland, J.L., C.H. Hollenberg, and W.S. Gillon, *Age, anatomic site, and the replication and differentiation of adipocyte precursors.* Am J Physiol, 1990. **258**(2 Pt 1): p. C206-10.

168. Mantovani, C., et al., *Morphological, molecular and functional differences of adult bone marrow- and adipose-derived stem cells isolated from rats of different ages.* Exp Cell Res, 2012.

169. Onate, B., et al., *The subcutaneous adipose tissue reservoir of functionally active stem cells is reduced in obese patients.* FASEB J, 2012.

170. Alt, E.U., et al., *Aging alters tissue resident mesenchymal stem cell properties.* Stem Cell Res, 2012. **8**(2): p. 215-25.

171. Chen, H.T., et al., *Proliferation and differentiation potential of human adipose-derived mesenchymal stem cells isolated from elderly patients with osteoporotic fractures.* J Cell Mol Med, 2012. **16**(3): p. 582-93.

172. Hauner, H., M. Wabitsch, and E.F. Pfeiffer, *Differentiation of adipocyte precursor cells from obese and nonobese adult women and from different adipose tissue sites.* Horm Metab Res Suppl, 1988. **19**: p. 35-9.

173. Gronthos, S., et al., *Surface protein characterization of human adipose tissue-derived stromal cells.* J Cell Physiol, 2001. **189**(1): p. 54-63.

174. Caplan, A.I., *All MSCs are pericytes?* Cell Stem Cell, 2008. **3**(3): p. 229-30.

175. Crisan, M., et al., *A perivascular origin for mesenchymal stem cells in multiple human organs.* Cell Stem Cell, 2008. **3**(3): p. 301-13.

176. Chang, W., et al., *Phorbol myristate acetate differentiates human adipose-derived mesenchymal stem cells into functional cardiogenic cells.* Biochem Biophys Res Commun, 2012.

177. Fang, C.H., et al., *In Vivo Differentiation of Human Amniotic Epithelial Cells into Cardiomyocyte-Like Cells and Cell Transplantation Effect on Myocardial Infarction in Rats: Comparison with Cord Blood and Adipose Tissue-Derived Mesenchymal Stem Cells.* Cell Transplant, 2012.

178. De Ugarte, D.A., et al., *Differential expression of stem cell mobilization-associated molecules on multi-lineage cells from adipose tissue and bone marrow.* Immunol Lett, 2003. **89**(2-3): p. 267-70.

179. Jaager, K., et al., *RNA-Seq Analysis Reveals Different Dynamics of Differentiation of Human Dermis- and Adipose-Derived Stromal Stem Cells.* PLoS One, 2012. **7**(6): p. e38833.

180. Huss, F.R. and G. Kratz, *Adipose tissue processed for lipoinjection shows increased cellular survival in vitro when tissue engineering principles are applied.* Scand J Plast Reconstr Surg Hand Surg, 2002. **36**(3): p. 166-71.

181. von Heimburg, D., et al., *Comparison of viable cell yield from excised versus aspirated adipose tissue.* Cells Tissues Organs, 2004. **178**(2): p. 87-92.

182. Requicha, J.F., et al., *Effect of Anatomical Origin and Cell Passage Number on the Stemness and Osteogenic Differentiation Potential of Canine Adipose-Derived Stem Cells.* Stem Cell Rev, 2012.

183. Huang, G.T., S. Gronthos, and S. Shi, *Mesenchymal stem cells derived from dental tissues vs. those from other sources: their biology and role in regenerative medicine.* J Dent Res, 2009. **88**(9): p. 792-806.

184. Boxall, S.A. and E. Jones, *Markers for characterization of bone marrow multipotential stromal cells.* Stem Cells Int, 2012. **2012**: p. 975871.

185. Sabapathy, V., et al., *Long-term cultured human term placenta-derived mesenchymal stem cells of maternal origin displays plasticity.* Stem Cells Int, 2012. **2012**: p. 174328.

186. Zuk, P.A., *The Adipose-derived Stem Cell: Looking Back and Looking Ahead.* Mol Biol Cell, 2010.

187. Rathore, A., et al., *Development of tissue engineered vascular grafts and application of nanomedicine.* Wiley Interdiscip Rev Nanomed Nanobiotechnol, 2012. **4**(3): p. 257-72.

188. Madden, R.L., et al., *A comparison of cryopreserved vein allografts and prosthetic grafts for hemodialysis access.* Ann Vasc Surg, 2005. **19**(5): p. 686-91.

189. Cho, S.W., et al., *Evidence for in vivo growth potential and vascular remodeling of tissue-engineered artery.* Tissue Eng Part A, 2009. **15**(4): p. 901-12.

190. Watanabe, M., et al., *Tissue-engineered vascular autograft: inferior vena cava replacement in a dog model.* Tissue Eng, 2001. **7**(4): p. 429-39.

191. Yacoub, M.H., *The Ross operation--an evolutionary tale.* Asian Cardiovasc Thorac Ann, 2006. **14**(1): p. 1-2.

192. Chard, R.B., et al., *Aorta-coronary bypass grafting with polytetrafluoroethylene conduits. Early and late outcome in eight patients.* J Thorac Cardiovasc Surg, 1987. **94**(1): p. 132-4.

193. Goyal, A., et al., *Development of a model system for preliminary evaluation of tissue-engineered vascular conduits.* J Pediatr Surg, 2006. **41**(4): p. 787-91.

194. O'Brien, B. and W. Carroll, *The evolution of cardiovascular stent materials and surfaces in response to clinical drivers: a review.* Acta Biomater, 2009. **5**(4): p. 945-58.

195. Alberts, B., J.H. Wilson, and T. Hunt, *Molecular biology of the cell*. 5th ed. 2008, New York: Garland Science. xxxiii, 1601, 90 p.

196. Weinberg, C.B. and E. Bell, *A blood vessel model constructed from collagen and cultured vascular cells.* Science, 1986. **231**(4736): p. 397-400.

197. Yao, L., J. Liu, and S.T. Andreadis, *Composite fibrin scaffolds increase mechanical strength and preserve contractility of tissue engineered blood vessels.* Pharm Res, 2008. **25**(5): p. 1212-21.

198. L'Heureux, N., et al., *A completely biological tissue-engineered human blood vessel.* FASEB J, 1998. **12**(1): p. 47-56.

199. Bassiouny, H.S., et al., *Anastomotic intimal hyperplasia: mechanical injury or flow induced.* J Vasc Surg, 1992. **15**(4): p. 708-16; discussion 716-7.

200. Schmidt, C.E. and J.M. Baier, *Acellular vascular tissues: natural biomaterials for tissue repair and tissue engineering.* Biomaterials, 2000. **21**(22): p. 2215-31.

201. Dahl, S.L., et al., *Decellularized native and engineered arterial scaffolds for transplantation.* Cell Transplant, 2003. **12**(6): p. 659-66.

202. Rodriguez, M., et al., *Development of a mechanically tuneable 3D scaffold for vascular reconstruction.* J Biomed Mater Res A, 2012.

203. Aurich, H., et al., *Hepatocyte differentiation of mesenchymal stem cells from human adipose tissue in vitro promotes hepatic integration in vivo.* Gut, 2009. **58**(4): p. 570-81.

204. Kern, S., et al., *Comparative analysis of mesenchymal stem cells from bone marrow, umbilical cord blood, or adipose tissue.* Stem Cells, 2006. **24**(5): p. 1294-301.

205. Drexler, H., et al., *DSMZ Catalogue of Human And Animal Cell Lines*: www.dsmz.de.

206. Gundle, R. and J.N. Beresford, *The isolation and culture of cells from explants of human trabecular bone.* Calcif Tissue Int, 1995. **56 Suppl 1**: p. S8-10.

207. Sigma-Aldrich. Available from: http://www.sigmaaldrich.com/sigma-aldrich/technical-documents/articles/biofiles/colorimetric-alkaline.html.

208. Dragunow, M., et al., *Image-based high-throughput quantification of cellular fat accumulation.* J Biomol Screen, 2007. **12**(7): p. 999-1005.

209. Skehan, P., et al., *New colorimetric cytotoxicity assay for anticancer-drug screening.* J Natl Cancer Inst, 1990. **82**(13): p. 1107-12.

210. Knepper, M.A., et al., *Concentration of solutes in the renal inner medulla: interstitial hyaluronan as a mechano-osmotic transducer.* Am J Physiol Renal Physiol, 2003. **284**(3): p. F433-46.

211. Stary, H.C., et al., *A definition of advanced types of atherosclerotic lesions and a histological classification of atherosclerosis. A report from the Committee on Vascular Lesions of the Council on Arteriosclerosis, American Heart Association.* Circulation, 1995. **92**(5): p. 1355-74.

212. *World Medical Association Declaration of Helsinki. Recommendations guiding physicians in biomedical research involving human subjects.* Cardiovasc Res, 1997. **35**(1): p. 2-3.

213. Rieder, E., et al., *Decellularization protocols of porcine heart valves differ importantly in efficiency of cell removal and susceptibility of the matrix to recellularization with human vascular cells.* J Thorac Cardiovasc Surg, 2004. **127**(2): p. 399-405.

214. Weisenberger, D.J., et al., *Analysis of repetitive element DNA methylation by MethyLight.* Nucleic Acids Res, 2005. **33**(21): p. 6823-36.

215. Redgrave, J.N., et al., *Critical cap thickness and rupture in symptomatic carotid plaques: the oxford plaque study.* Stroke, 2008. **39**(6): p. 1722-9.

216. Muraglia, A., R. Cancedda, and R. Quarto, *Clonal mesenchymal progenitors from human bone marrow differentiate in vitro according to a hierarchical model.* J Cell Sci, 2000. **113 (Pt 7)**: p. 1161-6.

217. Stenvinkel, P., et al., *Impact of inflammation on epigenetic DNA methylation - a novel risk factor for cardiovascular disease?* J Intern Med, 2007. **261**(5): p. 488-99.

218. Teitell, M. and B. Richardson, *DNA methylation in the immune system.* Clin Immunol, 2003. **109**(1): p. 2-5.

219. Kim, Y.I., et al., *Colonic mucosal concentrations of folate correlate well with blood measurements of folate status in persons with colorectal polyps.* Am J Clin Nutr, 1998. **68**(4): p. 866-72.

220. Ono, R., et al., *LCX, leukemia-associated protein with a CXXC domain, is fused to MLL in acute myeloid leukemia with trilineage dysplasia having t(10;11)(q22;q23).* Cancer Res, 2002. **62**(14): p. 4075-80.

221. Guo, J.U., et al., *Hydroxylation of 5-methylcytosine by TET1 promotes active DNA demethylation in the adult brain.* Cell, 2011. **145**(3): p. 423-34.

222. Spin, J.M., T. Quertermous, and P.S. Tsao, *Chromatin remodeling pathways in smooth muscle cell differentiation, and evidence for an integral role for p300.* PLoS One, 2010. **5**(12): p. e14301.

223. Cheng, X. and R.M. Blumenthal, *Coordinated chromatin control: structural and functional linkage of DNA and histone methylation.* Biochemistry, 2010. **49**(14): p. 2999-3008.

224. Hu, Z., et al., *MLL/AF-4 leukemic cells recruit new blood vessels but do not incorporate into capillaries in culture or in a NOD/SCID xenograft model.* Leukemia, 2009. **23**(5): p. 990-3.

225. Zhou, Y., et al., *Histone modifications and methyl-CpG-binding domain protein levels at the TNFSF7 (CD70) promoter in SLE CD4+ T cells.* Lupus, 2011. **20**(13): p. 1365-71.

226. Paul, T.A., et al., *Signatures of polycomb repression and reduced H3K4 trimethylation are associated with p15INK4b DNA methylation in AML.* Blood, 2010. **115**(15): p. 3098-108.

227. Lockman, K., J.M. Taylor, and C.P. Mack, *The histone demethylase, Jmjd1a, interacts with the myocardin factors to regulate SMC differentiation marker gene expression.* Circ Res, 2007. **101**(12): p. e115-23.

228. Lachner, M., et al., *Methylation of histone H3 lysine 9 creates a binding site for HP1 proteins.* Nature, 2001. **410**(6824): p. 116-20.

229. Morshead, K.B., et al., *Antigen receptor loci poised for V(D)J rearrangement are broadly associated with BRG1 and flanked by peaks of histone H3 dimethylated at lysine 4.* Proc Natl Acad Sci U S A, 2003. **100**(20): p. 11577-82.

230. Miao, F., et al., *In vivo chromatin remodeling events leading to inflammatory gene transcription under diabetic conditions.* J Biol Chem, 2004. **279**(17): p. 18091-7.

231. Perkins, E.J., B.L. Kee, and D.A. Ramsden, *Histone 3 lysine 4 methylation during the pre-B to immature B-cell transition.* Nucleic Acids Res, 2004. **32**(6): p. 1942-7.

232. Tausendschon, M., N. Dehne, and B. Brune, *Hypoxia causes epigenetic gene regulation in macrophages by attenuating Jumonji histone demethylase activity.* Cytokine, 2011. **53**(2): p. 256-62.

233. Fang, G., et al., *Chronic Intermittent Hypoxia Exposure Induces Atherosclerosis in ApoE Knockout Mice: Role of NF-kappaB p50.* Am J Pathol, 2012.

234. Yu, B.D., et al., *Altered Hox expression and segmental identity in Mll-mutant mice.* Nature, 1995. **378**(6556): p. 505-8.

235. Nakamura, T., et al., *ALL-1 is a histone methyltransferase that assembles a supercomplex of proteins involved in transcriptional regulation.* Mol Cell, 2002. **10**(5): p. 1119-28.

236. Ernst, P., J. Wang, and S.J. Korsmeyer, *The role of MLL in hematopoiesis and leukemia.* Curr Opin Hematol, 2002. **9**(4): p. 282-7.

237. Collins, E.C. and T.H. Rabbitts, *The promiscuous MLL gene links chromosomal translocations to cellular differentiation and tumour tropism.* Trends Mol Med, 2002. **8**(9): p. 436-42.

238. Wang, X., et al., *MLL1, a Histone H3K4 Methyltransferase, Regulates the Expression of TNFalpha-mediated NF-kappaB Downstream Genes.* J Cell Sci, 2012.

239. Yadav, S., et al., *hSET1: a novel approach for colon cancer therapy.* Biochem Pharmacol, 2009. **77**(10): p. 1635-41.

240. Lee, J.H., et al., *Identification and characterization of the human Set1B histone H3-Lys4 methyltransferase complex.* J Biol Chem, 2007. **282**(18): p. 13419-28.

241. Stewart, M.D., J. Li, and J. Wong, *Relationship between histone H3 lysine 9 methylation, transcription repression, and heterochromatin protein 1 recruitment.* Mol Cell Biol, 2005. **25**(7): p. 2525-38.

242. Guil, S. and M. Esteller, *DNA methylomes, histone codes and miRNAs: tying it all together.* Int J Biochem Cell Biol, 2009. **41**(1): p. 87-95.

243. Baron, U., et al., *DNA methylation analysis as a tool for cell typing.* Epigenetics, 2006. **1**(1): p. 55-60.

244. Eckhardt, F., et al., *DNA methylation profiling of human chromosomes 6, 20 and 22.* Nat Genet, 2006. **38**(12): p. 1378-85.

245. Weber, M., et al., *Chromosome-wide and promoter-specific analyses identify sites of differential DNA methylation in normal and transformed human cells.* Nat Genet, 2005. **37**(8): p. 853-62.

246. Locke, M., J. Windsor, and P.R. Dunbar, *Human adipose-derived stem cells: isolation, characterization and applications in surgery.* ANZ J Surg, 2009. **79**(4): p. 235-44.

247. Bradley, J.E., G. Ramirez, and J.S. Hagood, *Roles and regulation of Thy-1, a context-dependent modulator of cell phenotype.* Biofactors, 2009. **35**(3): p. 258-65.

248. Pierelli, L., et al., *CD105 (endoglin) expression on hematopoietic stem/progenitor cells.* Leuk Lymphoma, 2001. **42**(6): p. 1195-206.

249. Bullwinkel, J., et al., *Ki-67 protein is associated with ribosomal RNA transcription in quiescent and proliferating cells.* J Cell Physiol, 2006. **206**(3): p. 624-35.

250. Eriksson, J.E., et al., *Introducing intermediate filaments: from discovery to disease.* J Clin Invest, 2009. **119**(7): p. 1763-71.

251. Witkowska-Zimny, M. and K. Walenko, *Stem cells from adipose tissue.* Cell Mol Biol Lett, 2011. **16**(2): p. 236-57.

252. Szyf, M., *Epigenetics, DNA methylation, and chromatin modifying drugs.* Annu Rev Pharmacol Toxicol, 2009. **49**: p. 243-63.

253. Balana, B., Nicoletti, C., Zahanich, I., Graf, E. M., Christ, T., Boxberger, S., Ravens, U., *5-Azacytidine induces changes in electrophysiological properties of human mesenchymal stem cells.* Cell Res, 2006. **16**(12): p. 949-60.

254. Esteve, P.O., et al., *Direct interaction between DNMT1 and G9a coordinates DNA and histone methylation during replication.* Genes Dev, 2006. **20**(22): p. 3089-103.

255. Schlesinger, Y., et al., *Polycomb-mediated methylation on Lys27 of histone H3 pre-marks genes for de novo methylation in cancer.* Nat Genet, 2007. **39**(2): p. 232-6.

256. Zupkovitz, G., et al., *Negative and positive regulation of gene expression by mouse histone deacetylase 1.* Mol Cell Biol, 2006. **26**(21): p. 7913-28.

257. Simoes, P.D. and T. Ramos, *Human pluripotent embryonal carcinoma NTERA2 cl.D1 cells maintain their typical morphology in an angiomyogenic medium.* J Negat Results Biomed, 2007. **6**: p. 5.

258. Takahashi, K., et al., *Induction of pluripotent stem cells from adult human fibroblasts by defined factors.* Cell, 2007. **131**(5): p. 861-72.

259. Peroni, D., et al., *Stem molecular signature of adipose-derived stromal cells.* Exp Cell Res, 2008. **314**(3): p. 603-15.

260. Dominguez-Sola, D., et al., *Non-transcriptional control of DNA replication by c-Myc.* Nature, 2007. **448**(7152): p. 445-U3.

261. Shields, J.M., R.J. Christy, and V.W. Yang, *Identification and characterization of a gene encoding a gut-enriched Kruppel-like factor expressed during growth arrest.* J Biol Chem, 1996. **271**(33): p. 20009-17.

262. Nandan, M.O. and V.W. Yang, *The role of Kruppel-like factors in the reprogramming of somatic cells to induced pluripotent stem cells.* Histol Histopathol, 2009. **24**(10): p. 1343-55.

263. Holash, J., et al., *Vessel cooption, regression, and growth in tumors mediated by angiopoietins and VEGF.* Science, 1999. **284**(5422): p. 1994-8.

264. Michiels, C., *Endothelial cell functions.* J Cell Physiol, 2003. **196**(3): p. 430-43.

265. Kourembanas, S. and D.V. Faller, *Platelet-derived growth factor production by human umbilical vein endothelial cells is regulated by basic fibroblast growth factor.* J Biol Chem, 1989. **264**(8): p. 4456-9.

266. Metcalf, D.J., et al., *Formation and function of Weibel-Palade bodies.* J Cell Sci, 2008. **121**(Pt 1): p. 19-27.

267. Unger, R.E., et al., *In vitro expression of the endothelial phenotype: comparative study of primary isolated cells and cell lines, including the novel cell line HPMEC-ST1.6R.* Microvasc Res, 2002. **64**(3): p. 384-97.

268. Voyta, J.C., et al., *Identification and isolation of endothelial cells based on their increased uptake of acetylated-low density lipoprotein.* J Cell Biol, 1984. **99**(6): p. 2034-40.

269. Margariti, A., et al., *Direct reprogramming of fibroblasts into endothelial cells capable of angiogenesis and reendothelialization in tissue-engineered vessels.* Proc Natl Acad Sci U S A, 2012. **109**(34): p. 13793-8.

270. Dong, J.D., et al., *Mesenchymal stem cell-based tissue engineering of small-diameter blood vessels.* Vascular, 2011. **19**(4): p. 206-13.

271. Quint, C., et al., *Decellularized tissue-engineered blood vessel as an arterial conduit.* Proc Natl Acad Sci U S A, 2011. **108**(22): p. 9214-9.

272. Kretlow, J.D., et al., *Donor age and cell passage affects differentiation potential of murine bone marrow-derived stem cells.* BMC Cell Biol, 2008. **9**: p. 60.

273. de Girolamo, L., et al., *Human adipose-derived stem cells isolated from young and elderly women: their differentiation potential and scaffold interaction during in vitro osteoblastic differentiation.* Cytotherapy, 2009. **11**(6): p. 793-803.

274. Fossett, E. and W.S. Khan, *Optimising human mesenchymal stem cell numbers for clinical application: a literature review.* Stem Cells Int, 2012. **2012**: p. 465259.

275. Hupkes, M., et al., *DNA methylation restricts spontaneous multi-lineage differentiation of mesenchymal progenitor cells, but is stable during growth factor-induced terminal differentiation.* Biochim Biophys Acta, 2011. **1813**(5): p. 839-49.

276. Okita, K. and S. Yamanaka, *Induced pluripotent stem cells: opportunities and challenges.* Philos Trans R Soc Lond B Biol Sci, 2011. **366**(1575): p. 2198-207.

277. Gidekel, S. and Y. Bergman, *A unique developmental pattern of Oct-3/4 DNA methylation is controlled by a cis-demodification element.* J Biol Chem, 2002. **277**(37): p. 34521-30.

7 APPENDIX

7.1 Abbreviations

Official gene symbols in this work were mentioned according to the Guidelines for Human Gene Nomenclature found at http://www.GeneNames.org/Guidelines.html.

5hmC	5-hydroxymethylcytosine
5mC	5-methylcytosine
acetylCoA	acetyl Coenzyme A
adMSCs	adipose derived mesenchymal stem cells
AHA	American Heart Association
ALP	alkaline phosphatase
Alu1	DNA repetitive sequence
ANG-1	Angiopoetin 1
ANG-2	Angiopoetin 2
APAAP	Alkaline Phosphatase-Anti Alkaline Phosphatase
APC	allophycocyanin
AS	atherosclerosis
ASVD	arteriosclerotic vascular disease
AZA	5-azacytidine
BAT	brown adipose tissue
BCIP	5,5'-dibromo-4,4'-dichloro-indigo phosphate
BIX	BIX-01294
BM-MSCs	bone marrow mesenchymal stem cells
CEA	carotid endarterectomy
CMYC	transcription factor essential for achieving pluripotency
CVDs	cardiovascular diseases
DiI	1,1\'-dioctadecyl – 3,3,3\',3\'-tetramethyl-indocarbocyanine perchlorate
DiL-Ac-LDL	acetylated low density protein labeled with DiL
DMEM	Dulbecco's modified Eagle medium
DMSO	dimethyl sulfoxide
DNMT1	DNA Methyl Transferase 1, maintenance of the DNA methylation
DNMT3A	DNA Methyl Transferase 3A, de novo methylation
DNMT3B	DNA Methyl Transferase 3B, maintenance of the DNA methylation and *de novo* methylation
DNMTs	DNA methyltransferases

dsDNS	double stranded DNA
ECM	extracellular matrix
ECs	endothelial cells
EHMT2	methyltransferase able to methylate lysine 9 of the histone H3
EM	endothelial medium
ESC	embryonic stem cells
F8	Factor VIII, role in blood clotting
FACS	fluorescence-activated cell sorter
FFPE tissue	formaldehyde fixed paraffin embedded tissue
FITC	Fluorescein isothiocyanate
G9a	methyltransferase able to methylate lysine 9 of the histone H3
GAPDH	housekeeping gene, Glyceraldehyde-3-Phosphate Dehydrogenase
H&E staining	Haematoxylin - eosin staining
HATs	histone acetyltransferases
HDAC	histone deacetylases
HIER	heat induced epitope retrieval
HMTs	histone methyltrasferases
ICC	immunocytochemistry
IHC	immunohistochemistry
iPSCs	induced pluripotent stem cells
KLF4	transcription factor essential for achieving pluripotency
LINE1	long interspersed nuclear element 1, repetitive sequence
LSAB	Labeled Streptavidin-Biotin
MLL1	methyltransferase able to methylate lysine 4 of the histone H3
MSCs	mesenchymal stem cells
NAD+	nicotinamide adenin dinucleotide
NANOG	transcription factor essential for achieving pluripotency
NBT	nitroblue tatrazolinum
NCDs	non communicable diseases
OCT4A	transcription factor essential for achieving pluripotency
ox-LDL	oxidized low-density lipoprotein
PBS	phosphate buffer saline
PDGF	Platelet-Derived Growth Factor
PE	phycoerytrin
PECAM-1	Platelet Endothelial Cell Adhesion Molecule 1
PIER	proteolytic enzyme induced epitope retrieval
PKMTs	protein lysine methyltransferases

PMTs	protein methyltransferases
PRMTs	protein arginine methyltransferases
PTFE	polytetrafluoroethylene
PVDF memrane	polyvinylidene difluoride membrane
qPCR	quantitative PCR
RT	room temperature
RT-PCR	reverse transcriptase polymerase chain reaction
SAH	S-adenosyl-L-homocysteine
SAM	S-adenosyl-methionine
SATα	repetitive sequence
SDS	sodium dodecyl sulphate
SETD1A	methyltransferase able to methylate lysine 4 of the histone H3
SETD1B	methyltransferase able to methylate lysine 4, and 9 of the histone H3
SMCs	smooth muscle cells
SOX2	transcription factor essential for achieving pluripotency
TET	enzyme with demethylating function
TF	transcription factor
VCAM-1	Vascular Cell Adhesion Molecule 1
VEGF	Vascular Endothelial Growth Factor
VEGFR-2	Vascular Endothelial Growth Factor Receptor-2
VPA	valproic acid
VSMCs	vascular smooth muscle cells
WAT	white adipose tissue
WHO	World Health Organization

7.2 Publications

7.2.1 Original articles

Glanemann M, Knobeloch D, Ehnert S, Culmes M, Seeliger C, Seehofer D, Nussler AK. Hepatotropic growth factors protect hepatocytes during inflammation by upregulation of antioxidative systems. World J Gastroenterol. 2011 May 7;17(17):2199-205. PubMed PMID: 21633529; PubMed Central PMCID: PMC3092871.

Pelisek J, Well G, Reeps C, Rudelius M, Kuehnl A, Culmes M, Poppert H,vZimmermann A, Berger H, Eckstein HH. Neovascularization and angiogenic factors in advanced human carotid artery stenosis. Circ J. 2012 Apr 25;76(5):1274-82. Epub 2012 Mar 3. PubMed PMID: 22447000.

Seeliger C, Culmes M, Schyschka L, Yan X, Damm G, Wang Z, Kleeff J, Thasler WE, Hengstler J, Stöckle U, Ehnert S, Nussler AK. Decrease of global Methylation improves significantly hepatic Differentiation of Ad-MSCs: Possible future Application for Urea Detoxification. Cell Transplant. 2012 Apr 10. [Epub ahead ofprint] PubMed PMID: 22507189.

Bruckmeier M, Kuehnl A, Culmes M, Pelisek J, Eckstein HH. Impact of oxLDL and LPS on C-type natriuretic peptide system is different between THP-1 cells and human peripheral blood monocytic cells. Cell Physiol Biochem. 2012;30(1):199-209.Epub 2012 Jun 15. PubMed PMID: 22759967.

Culmes M., Pelisek J., Burgkart R., Nüssler AK., Wagner E., Eckstein HH. - Endothelial differentiation of adipose-derived mesenchymal stem cells is improved by epigenetic modifying drug BIX-01294, Eur J Cell Biol, *resubmitted.*

Culmes M., Dushenalieva S., Napieralski R., Rudelius M., Wagner E., Eckstein HH., Pelisek J. - DNA methylation in carotid plaques is associated with severity of atherosclerosis and reduced expression of methyltransferases, Atherosclerosis, *submitted.*

Culmes M., Pelisek J., Burgkart R., Wagner E., Eckstein HH. - Histone methylation in advanced carotid atherosclerotic lesions, *in preparation.*

7.2.2 Oral presentations

Culmes M., Pelisek J., Schyschka L., Schmitt M., Wagner E., Nüssler AK., Eckstein HH. (2011), Chromatin remodeling drug BIX-01294 increases expression of endothelial markers in adipose–derived mesenchymal stem cells, 15. Chirurgishe Forschungstage, Dresden Germany.

Culmes M., Grabher-Meier V., Hegenloh R., Eckstein HH., , Napieralski R., Schmitt M., Pelisek J. (2012), Analysis of DNA Methylation, DNA Methyltranferases, and Histone Modifications in Human Atherosclerotic Lesions, INTERACT Symposium, Munich, Germany.

Culmes M., Grabher-Meier V., Hegenloh R., Wagner E., Schmitt M., Eckstein HH., Pelisek J. (2012), Epigenetische Veränderungen in atherosklerotischen Läsionen bei Patienten mit fortgeschrittenen Carotisstenosis, 41. Jahrestagung der Deutschen Gesellschaft für Angiologie Gesellschaft für Gefäßmedizin e.V., Mainz, Germany.

7.2.3 Poster presentations

Seeliger C., Culmes M., Schyschka L., Ehnert S., Kleeff J., Stöckle U., Pelisek J., Nussler AK. (2010) Epigenetic Changes Improve Differentiation of Adipose-derived Mesenchymal Stem Cells (Ad-MSCs) to Hepatocyte-like Cells: Possible Use as an In Vitro Toxicity Test System, 16th International Congress on In Vitro Toxicology - ESTIV 2010 & 13th Annual Congress of EUSAAT - EUSAAT 2010 & 16th Congress on Alternatives to Animal Testing, Linz, Austria.

Seeliger C., Culmes M., Römer M., Ehnert S., Kleeff J., Stöckle U., Nussler AK. (2010) Epigenetic Changes improve Differentiation of Hepatocyte-like Cells from adipose Tissue: possible Application for Cell Therapies in Surgery, 26th Meeting of the German Association for the Study of the Liver (GASL), Bonn, Germany.

Nüssler AK., Seeliger C., Culmes M., Schyschka L., Stöckle U., Nüssler N., Schoenberg M., Ehnert S. (2010) Adipose tissue-derived MSCs are an eligible option to human hepatocytes, Gut and Liver - Falk Symposium, Beijing, China.

Culmes M., Pelisek J., Schyschka L., Tron A., Seelinger C., Napieralski R., Günther M., Wagner E., Kleeff J., Stöckle U., Ehnert S., Nüssler AK. (2010) Chemical approach to modify expression of pluripotency genes in adipose- derived mesenchymal stem cells, Epigenetics and Stem Cells Conference, Copenhagen, Denmark.

Culmes M., Pelisek J., Schyschka L., Tron A., Seeliger C., Napieralski R., Kleeff J., Stöckle U., Günther M., Wagner E., Ehnert S., Nüssler AK. (2010) Epigenetic-Modifying Drugs can Increase the Expression of Pluripotency Related Genes, ESNATS Summer School, Tallinn, Estonia.

Pelisek J., Culmes M., Napieralski R., Eckstein HH. (2011) Epigenetic changes in human advanced carotid artery lesions, The 79th European Atherosclerosis Society Congress Gothenburg, Sweden.

Culmes M, Pelisek J., Schmitt M., Wagner E., Nüssler AK., Eckstein HH. (2011) Inhibition of G9a Methyltransferase is positively influencing the reprogramming capacity of adipose derived mesenchymal stem cells into cells with endothelial features, Rediscovering pluripotency: from teratocarcinomas to embryonic stem cells, Cardiff, UK.

Yan X., Culmes M., Seeliger C., Schyschka L., Wang Z., Stöckle U., Ehnert S., Nüssler AK., (2011) Chemical Modification Of The Epigenetic Pattern Improved The Differentiation Potential Into Hepatocyte-like And Osteoblast-like Cells Of Human Ad-MSCs From Old Donors, World Conference on Regenerative Medicine, Leipzig, Germany.

Culmes M., Grabher-Meier V., Hegenloh R., Wagner E., Eckstein HH., Pelisek J. (2012) Targeted epigenetic changes induce a higher reprogramming capacity of adipose derived mesenchymal stem cells to differentiate into cells of endothelial features, INTERACT Symposium, Munich, Germany.

Culmes M., Pelisek J., Wagner E., Nüssler AK., Eckstein HH. (2012) Zielgerichtete epigenetische Modifikationen als neue therapeutische Option in vaskulärer Medizin, 28. Jahrestagung der Deutschen Gesellschaft für Gefäßchirurgie und Gefäßmedizin e. V., Wiesbaden, Germany.

7.3 Acknowledgments

It is with the sincerest gratitude that I acknowledge the contribution of many wonderful people to my education and my research experience gathered during the work for the present thesis.

Without the support of PD Dr. rer. nat. Jaroslav Pelisek my doctoral work would not have been possible at all. His patience and judgment guided me during the entire time. To him goes my gratitude for being a wonderful teacher, for always showing much interest in my work and for his professional guidance. I owe him special thanks for all the encouragement, supporting my ideas and for making it possible to perform all these experiments under his supervision.

Further I want to thank Prof. Dr. Hans-Henning Eckstein for allowing me to join his research team, for his guidance and encouragement, and for the constructive feed-back.

I am also very thankful to Prof. Dr. Ernst Wagner for giving me the opportunity to conduct my doctoral studies under his supervision at LMU – Faculty of Pharmacy.

I am thanking Prof. Dr. Andreas Nüssler for his support from the very beginning. Without him and Dr. Sabrina Ehnert, I would have never been able to achieve all this. I would like to acknowledge the wonderful laboratory staff where I began my project – the Research Laboratory of Traumatology Department from Klinkum rechts der Isar. Together with Prof. Nüssler, they taught and trained me in the basic methods of cell culture and laboratory methods. I am also thankful to Dr. rer. nat. Lilianna Shyschka for introducing me to the FACS analysis and for her technical support during these experiments.

To my colleagues and friends Renate and Verena: it was a great pleasure to work with you during my PhD-time, especially for improving my German language skills, thank you very much for listening, for your genuine enthusiasm, experience and encouragement.

An equally important person was Jutta Tübel, from the Research Laboratory of the Orthopedics Department, Klinikum rechts der Isar. I would like to thank her first of all for her kindness to provide technical support for both the qPCR device and microscope. Nevertheless, I am sure that the lunch breaks and discussions had a great impact on my German skills.

For their never-ending support in tackling the scientific and 'post-scientific' problems, I give my thanks to my friends Rudi, Karin, Camelia, and Angelica.

Finally, this thesis would not have been possible without the help of my family and my friends, foremost Alex: thank you very much for your support, your patience and continuous encouragements.